Physiological Chemistry and Physics and Medical NMR Volume 38, Number 1, 2006

Addresses of Chief Editor and Editorial College

Toshihiko Ubuka
Department of Clinical Nutrition
Kawasaki University of Medical Welfare
Kurashiki, Okayama, 701-0193, Japan

Denys Wheatley
Department of Cell Pathology
University of Aberdeen
Aberdeen AB24 4FA, Scotland
United Kingdom

EDITORIAL AND BUSINESS OFFICE

Physiological Chemistry and Physics
and Medical NMR
P.O. Box 1452
Melville, New York 11747

Editor In Chief, Dr. Gilbert N. Ling
Managing Editor, Margaret M. Ochsenfeld

SCOPE: PCP provides a forum for the review and publication of reports of original research in a broad range of subjects in biophysics, biochemistry and cellular physiology. Reports of direct applications of basic knowledge to human studies are invited; examples would include the measurements of relaxation times as part of NMR imaging. Single experiments, conclusions based on inadequate statistics, purely speculative papers, and clinical case reports are not accepted.

POLICY: The pages of PCP are accessible to competing viewpoints, interpretations, theories and opinions. Debate is invited via Editorial Comments and Letters to the Editor. Criteria for evaluating submissions include soundness of the study and clarity of presentation, and papers are not rejected on the basis of interpretation or theory, however controversial. PCP believes that scientific issues should be settled by investigation and open debate, not by an appeal to anonymous authority.

PCP attempts to achieve a balance between freedom of expression and constructive peer review. All papers are refereed by reviewers who may remain anonymous, but the Chief Editors make all final decisions, and will handle appeals from authors who feel their papers are unfairly reviewed.

The Editors endeavor to make decisions regarding acceptance or rejection of manuscripts quickly, and have set self-imposed deadlines for doing so. Referees also are given deadlines.

TYPES OF PAPERS: *Regular papers* may be experimental or theoretical. *Short notes, Priority notes* and *Letters* in response to published papers are invited. *Reviews* are desired, but authors are urged to contact an Editor before sending a finished review manuscript. *Symposia* may be published as regular or supplemental issues.

SUBSCRIPTIONS: Price is US$80.00 per volume in the United States and US$87.00 outside the United States. *Physiological Chemistry and Physics and Medical NMR* is published biannually, 2 issues per year, the volume numbered yearly. New subscriptions will start with the first issue of the volume in progress, unless the subscriber directs otherwise. Most back issues are available

Instructions to Authors

SUBMISSIONS: An original and two copies of all material are requested. The original must be typewritten on one side only. Papers should be sent to Dr. Gilbert N. Ling, Editor, P.O. Box 1452, Melville, New York 11747 U.S.A. Manuscripts should be submitted only to this journal and not have been published in part or whole in another publication, except as short preliminary notes, abstracts, or as unpublished work in reviews or symposia. Be sure to keep a copy of your manuscript.

NOTE: Referees will be instructed to destroy their copies of the manuscript after reviewing them. We will return only the original manuscript to you for revision or if rejected.

MANUSCRIPTS: All material should be typed double-spaced with margins at least one inch wide and pages numbered consecutively beginning with the title page. In addition to a paper copy, send an IBM- or Macintosh-compatible file on a floppy disk or CD, in Word or Wordperfect. *Title Page* should include title (of at most 100 characters and spaces), full names of authors as you wish them to be published, names and cities of institutional affiliation(s) of authors and of institution(s) where the studies were performed, and name, full address, telephone number, fax number and e-mail address of the person to whom correspondence, proofs, and reprint requests are to be sent. Four to six *key words* should be listed on the title page. These words will assist indexers. Also, at bottom of title page include a short running title of 40 characters or less.

Abstract should be concise and no longer than 225 words. *Body* may or may not be divided into Introduction, Materials and Methods, Results and Discussion, depending on the length and nature of the paper. Introductory remarks should indicate clearly the significance of the work presented. *References* may be indicated in the text and listed in the reference list in whatever style the author prefers, but we prefer that titles of articles be omitted.

TABLES: Tables should be typewritten on separate sheets and identified by roman numerals (eg. Table III) and titles. Table notes should be keyed by superscript italic lower-case letters (eg. [a]Control). The approximate locations of *tables* and *figures* should be indicated in the margins of the manuscript.

ILLUSTRATIONS: Original artwork or glossy photostatic prints, together with two photocopies (like Xerox copies) should be provided. Each illustration should be numbered on the back in pencil, along with the authors' names. It is preferred that line drawings be made on paper that is not larger than 8 1/2 by 13 inches, and that the drawing be its intended size in the printed paper. Most figures will occupy 1/2 to full column, that is 5 inches wide. Lines and lettering should be thick enough to allow reduction. A drawing of overall dimension of 8 by 10 inches that will be reduced to 1/4 of its original size should be lettered with 18-point (capitals 6 mm high, lower-case 4 mm high) or larger lettering. Glossy photostatic prints are acceptable, and should be attached firmly to a sheet of paper the same size as the manuscript. Postacceptance: If possible send figures as an image file using TIFF or JPEG formatting scanned at a resolution of 600 dpi.

PHOTOGRAPHS: High-quality black and white glossy prints should be provided in triplicate, and may be provided as one print plus two photocopies if the photocopies are sufficiently clear to portray the original to referees. Photographs should be attached firmly to a sheet of paper the same size as the manuscript. Photographs that have been scanned and stored as a TIFF file with a resolution of 300 dpi may also be submitted.

REFEREES: Two anonymous referees will be sought for each paper. Authors are encouraged to suggest names and addresses of suitable referees. Referees will be given deadlines for mailing manuscripts back or phoning reviews in, and will be invited to provide editorial statements or Letters that deal with issues raised by submitted papers.

REPRINTS: An order form is enclosed with proofs sent to authors.

PAGE CHARGES: Page charge is $20.00 per published page. It may be waived in the case of severe international exchange difficulties. An additional charge of $15.00 will be levied for photographs that require screening (eg., E.M's, chromatograms, scans).

Physiol. Chem. Phys. & Med. NMR (2006) *38*: 1–20

Stimulation of Membrane Permeability Transition by α-Lipoic Acid and its Biochemical Characteristics

Sanae Aoyama[1,2], Yuya Okimura[1,3], Hirofumi Fujita[1*], Eisuke F. Sato[4], Teruo Umegaki[1], Koichi Abe[5], Masayasu Inoue[4], Kozo Utsumi[1] and Junzo Sasaki[1]

[1]*Department of Cytology and Histology, Okayama University Graduate School of Medicine, Dentistry and Pharmaceutical Sciences, Okayama 700-8558, Japan,* [2]*Department of Integrated Medicine and Informatics, Ehime University Graduate School of Medicine, Toon, Ehime 791-0295, Japan,* [3]*Donan Institute of Medical Science, Akiyama Memorial Hospital, Hakodate 041-8502, Japan,* [4]*Department of Biochemistry and Molecular Pathology, Osaka City University Medical School, Abeno, Osaka 545-8585, Japan,* [5]*Vitamin E Information and Technology, Eisai Co., Ltd., Bunkyo-ku, Tokyo 112-8088, Japan.*
**Corresponding author, e-mail: Hirofumi Fujita, fujita00@md.okayama-u.ac.jp*

Abstract: Mitochondria play an important role in apoptosis by generating reactive oxygen species (ROS) and inducing membrane permeability transition (MPT). Recent studies on α-lipoic acid (LA) and its reduced form, dihydrolipoic acid, suggest that these agents (LAs) inhibit apoptosis of cells by means of their antioxidant activity. On the other hand, LAs also stimulate Ca^{2+}-dependent mitochondrial MPT and induce apoptosis of certain cells. Thus, the role of LAs in apoptotic cell death remains obscure. We investigated the mechanism of LA-induced MPT of mitochondria. Biochemical analysis revealed, in the presence of Ca^{2+}, inorganic phosphate and succinate, LA induced uncoupling of oxidative phosphorylation, stimulated oxidation of pyridine nucleotides and enhanced Ca^{2+}-induced MPT, as characterized by decrease in Ca^{2+} loading, ROS generation, oxidation of thiol groups of adenine nucleotide translocator, membrane depolarization, swelling, and cytochrome c release in an incubation time and concentration dependent manner. LA also stimulated hydroxyl radical-induced MPT in a α-tocopherol-inhibitable manner. Cyclosporine A, a potent inhibitor of mitochondrial MPT, inhibited all these events induced by LA.

These results indicate that, under certain conditions, LA stimulates Ca^{2+}- induced MPT through the decrease in loading capacity of Ca^{2+} and that MPT is involved in LA-induced apoptotic cell death. Since fairly high doses of LA have been used as a dietary supplement, the possible occurrence of such side effects, including mitochondrial dysfunction and induction of apoptosis in normal tissues, should be studied.

KEY WORDS: antioxidant; apoptosis; α-lipoic acid; membrane permeability transition; mitochondria; reactive oxygen species

α-LIPOIC ACID (LA) and its reduced form, dihydrolipoic acid (DHLA), are synthesized in prokaryotic and eukaryotic cells, including human cells (1). LA is a component of the multi-enzyme complex that catalyzes the decarboxylation of α-ketoacids (1, 2) and is involved in the regulation of carbohydrate and lipid metabolism (3). Both LA and DHLA exhibit antioxidant activity (1, 4, 5) and function as metal chelaters to prevent the precipitation of calcium oxalate in the kidney (6, 7). DHLA regenerates other antioxidants, including vitamin C and vitamin E (8). LA is absorbed from the gastrointestinal tract (9) and mobilized across the blood-brain barrier (10). LA decreases oxidative stress and restores reduced forms of other antioxidants *in vivo* (11). Thus, LA has been used therapeutically for the prevention of free radical injury of tissues.

Recent studies revealed that mitochondria play an important role in apoptotic cell death by modulating membrane permeability transition (MPT) (4). MPT opens a large pore in the inner membrane that causes the uncoupling and swelling of mitochondria and releases proapoptotic factors into the cytosol (12, 13). Ca^{2+} induces typical MPT characterized by depolarization and swelling of mitochondria, thereby releasing cytochrome c by the mechanism, which is sensitive to cyclosporine A, a potent inhibitor of mitochondrial MPT (14, 15). MPT is induced by Ca^{2+} accumulation and oxidative stress that modulates the redox state of mitochondria (16). Ca^{2+} enhances the generation of reactive oxygen species (ROS) coupled with MPT (16, 17). MPT and pore opening are induced by many factors, including prooxidants that oxidize the critical thiol groups of adenine nucleotide translocator (ANT) (18). Because LA undergoes redox cycling, it increases the GSH pool both in the cytosol and mitochondria (19). Hence, this compound has been postulated to inhibit the induction of MPT. However, several investigators reported that LA and DHLA (LAs) actually induced MPT by increasing ROS generation in mitochondria (20, 21, 22, 23). Thus, the cellular role of the action of LAs in the regulation of MPT remains unclear. The present work also describes the effect of LAs on Ca^{2+}- and Fe^{2+}/H_2O_2-induced MPT in rat liver mitochondria.

Materials and Methods

Chemicals

Cyclosporine A, horseradish peroxide, DHLA and antipyrylazo III were obtained from Sigma Co. Ltd. (St. Louis, MO, USA). Amplex Red and 2',7'-dichlorodihydrofluorescein diacetate (H_2DCF-DA) were purchased from Molecular Probes (Eugene, Oregon, USA). Monoclonal antibody against cytochrome c was purchased from PharMingen (San Jose, CA, USA). Rabbit antiserum against ANT was a gift from Dr. Hiroshi Terada (Tokyo Uni-

Abbreviations: ANT, adenine nucleotide translocator; CHL, chemiluminescence; CMPT, classical membrane permeability transition; diS-C3-(5), 3,3'-dipropyl-2,2'-thiodicarbocyanine iodide; DHLA, dihydrolipoic acid; H_2DCF-DA, 2',7'-dichlorodihydrofluorescein diacetate; L-012, 8-amino-5-chloro-7-phenylpyrido[3,4-d]pyridazine-1,4-(2H,3H)dione; LA, lipoic acid; MPT, membrane permeability transition; Pi, inorganic phosphate; PN, pyridine nucleotides; RCR, respiratory control ratio; ROS, reactive oxygen species; SOD, superoxide dismutase; ThioBond Resin, 4-aminophenylarsine oxide agarose.

versity of Science, Japan). LA (racemic LA), 4-aminophenylarsine oxide agarose (ThioBond Resin) and 3,3'dipropyl-2,2'-thiodicarbocyanine iodide (diS-C3-(5)), a cyanine dye, were obtained from Kanematsu Co. Ltd. (Tokyo, Japan), Invitrogen (Carlsbad, CA, USA) and Hayashibara Biochemical Laboratories (Okayama, Japan), respectively. 8-amino-5-chloro-7-phenylpyrido[3,4-d]pyridazine-1,4-(2H,3H)dione (L-012) was obtained from Wako Chemical Co. Ltd. (Osaka, Japan).

Isolation and biochemical analysis of mitochondria

Male Wistar rats, weighing 200 g, were used after overnight fasting. Mitochondria were isolated from rat livers by the method of Hogeboom as described previously (24). Mitochondria were incubated in 2 ml of a standard medium (230 mM mannitol, 70 mM sucrose, 1 μM EDTA and 3 mM HEPES, pH 7.4) at 25°C with continuous stirring and oxygenation.

The respiratory control ratio (RCR), state 4 respiration and ADP/O ratio of mitochondria used were 4.8, 30.4 μM /min /mg protein and 1.9, respectively, as measured in 10 mM Tris-HCl buffer (pH 7.4) containing 150 mM KCl, 5 mM $MgCl_2$, 2.5 mM succinate and 1 mM inorganic phosphate (Pi). The mitochondrial oxygen uptake was monitored polarographically using a Clark type oxygen electrode fitted to a 2 ml water-jacketed closed chamber at 25°C in the presence or absence of 20 μM Ca^{2+} and 100 μM LA as described previously (25).

The redox state of pyridine nucleotides (PN) in mitochondria was analyzed by measuring the fluorescence intensity at 460 nm during the excitation at 340 nm using a Hitachi 650-10LC fluorescence spectrophotometer equipped with a water-jacketed cell holder and magnetic stirrer. The mitochondrial concentration used was 0.1 mg protein /ml.

The mitochondrial uptake of Ca^{2+} was monitored using a metallochromic indicator, antipyrylazo III, at 720-790 nm using a dual-wavelength spectrophotometer (Hitachi 557) (17). Mitochondria (0.5 mg protein /ml) were incubated according to a standard medium in the presence of 5 μM rotenone, 1 mM Pi and 2.5 mM succinate. The reaction was started by adding 50 μM antipyrylazo III. The mitochondrial uptake and release of Ca^{2+} are accompanied proportionally by a respective decrease and increase in absorption. The amounts of mobilized Ca^{2+} were calibrated at the end of each experiment using authentic $CaCl_2$ solution.

Assay for mitochondrial ROS generation

The mitochondrial generation of H_2O_2 was evaluated using Amplex Red and horseradish peroxidase system and measured with a fluorescence spectrophotometer (26). The changes in fluorescence intensity were monitored at 590 nm using excitation at 550 nm. Mitochondria (0.1 mg protein /ml) were incubated in the standard medium at 25°C in the presence of 5 μM rotenone. The reaction was started by adding 20 μM Amplex Red, 1.1 mU /ml horseradish peroxidase, 2.5 mM succinate and 1 mM Pi. The mitochondrial generation of H_2O_2 was induced by 5 μM Ca^{2+} in the presence or absence of 20 μM LA or 1 μM cyclosporine A.

Because mitochondria have high Mn-superoxide dismutase (SOD) and glutathione peroxidase activities, the generation of ROS was analyzed using a highly sensitive chemiluminescence (CHL) probe, L-012 (27). Mitochondria were incubated in a standard medium (0.2 mg protein /2 ml) in the presence of 5 μM rotenone, 2.5 mM succinate, 1 mM Pi and

100 μM L-012 at 25°C for 1 min. Then, the reaction was started by adding $CaCl_2$. The CHL intensity was recorded continuously for 20 min and CHL was represented as an integrated value for 10 min.

The flow cytometric analysis of ROS generation in isolated mitochondria was also carried out using an H_2DCF-DA-fluoresence probe following the method of Mattiasson (28, 29). Mitochondria (0.1 mg protein /ml) were incubated in the standard medium containing 1 mM Pi and 2.5 mM succinate. The reaction was started by the addition of 10 μM H_2DCF-DA at 25°C.

Binding of ANT to a phenylarsine oxide-conjugated agarose

The amount of the reduced form of ANT was analyzed as described previously (30). After the incubation of mitochondria (2 mg protein /ml) in the presence of 5 μM rotenone, the reaction was started by adding 1 mM Pi and 2.5 mM succinate. Mitochondria were treated with 20 μM $CaCl_2$ for 10 min in the presence or absence of 5 ~ 50 μM LA followed by centrifugation at 12,000 x g and 4°C for 5 min. The proteins in the precipitate were soluble in 100 μl of a 50 μM HEPES buffer (pH 7.4) containing 0.15 M Na_2SO_4, 1 mM EDTA, 3% Triton X-100, 1 mM PMSF and 1 μM leupeptin. After centrifugation of the lysate at 15,000 x g and 4°C for 5 min, the supernatant fraction was incubated with ThioBond Resin equilibrated with 50 mM HEPES buffer (pH 7.4) containing 0.15 M Na_2SO_4, 1 mM EDTA, 0.25% Triton X-100, 1 mM PMSF and 1 μM leupeptin. After incubation at 4°C for 15 min, the resin was washed three times with 0.5 ml of the buffer by centrifugation for 1 min. Proteins bound to the resin were eluted with 50 μl of the buffer containing 10 mM dithiothreitol, and analyzed with SDS-PAGE and Western blotting using anti-ANT antiserum.

Assay for mitochondrial swelling and membrane potential

Mitochondrial swelling and depolarization were assessed by spectrophotometric and fluorometric methods, respectively. Mitochondria were incubated in the standard medium (0.1 mg protein /ml) at 25°C. Changes in the absorption at 540 nm were recorded using a Shimadzu UV-2400 equipped with a water-jacketed cell holder and magnetic stirrer. Mitochondrial swelling was also assayed by measuring the 90° light scattering at 540 nm using a fluorescence spectrophotometer (Hitachi 650-10LC).

Fluorescence analysis of the mitochondrial membrane potential was carried out in the standard medium (0.1 mg protein /ml) using 0.2 μg /ml of diS-C3-(5), 1 mM Pi and 2.5 mM succinate, respectively (31). Concentrations of other reagents added are indicated in each figure.

Western blot analysis

Mitochondrial lyses were prepared as described elsewhere (17). Briefly, 2 x 10^6 cells were dissolved in an SDS buffer (4% SDS, 10% 2-mercaptoethanol, 20% glycerol and 0.002% bromophenol blue, 125 mM Tris-HCl, pH 6.8) and boiled at 100˚C for 5 min. The boiled samples were subjected to SDS-polyacrylamide gel electrophoresis. Proteins in the gel were transferred to an Immobilon filter (Millipore Co. Ltd.), and then incubated with primary antibody (1:1000 dilution) and finally with horseradish peroxide-linked secondary antibody (1:2000 dilution) and analyzed using an ECL plus kit (Amersham). The protein

concentration was determined according to the method of Bradford using bovine serum albumin as a standard (17).

Assay of cytochrome c release

The release of cytochrome c from mitochondria was analyzed as described previously (17). Mitochondria were incubated according to the standard procedure (0.1 mg protein /ml) in the presence of 5 μM rotenone at 25°C. Mitochondrial swelling was induced by adding 2.5 mM succinate, 0.5 mM Pi and 7 μM $CaCl_2$ in the presence or absence of 50 μM LA or 1 μM cyclosporine A. Eight min after adding Ca^{2+}, mitochondria were centrifuged at 6,000 x g for 10 min. Mitochondria and supernatant fractions were added to a 0.5 volume of SDS-sample buffer and analyzed by Western blot with specific antibody.

Results

Effect of LA on mitochondrial oxidative phosphorylation

Since mitochondrial dysfunction often induces MPT, the effect of LA on its oxidative phosphorylation was examined in the presence or absence of Ca^{2+}. The presence of Ca^{2+} increased the state 4 respiration, and decreased the RCR and ADP/O ratio of mitochondria (Figure 1). LA also increased the state 4 respiration and decreased the RCR and ADP/O ratio. The presence of both LA and Ca^{2+} slightly increased the state 4 respiration and decreased the RCR and ADP/O. Cyclosporine A, a potent inhibitor of mitochondrial MPT, suppressed the uncoupled oxidative phosphorylation induced by LA and Ca^{2+} (data not shown). Similar results were also observed in the presence of 5 mM pyruvate as a respiratory substrate. However, the increasing effect of LA was stronger with pyruvate than with succinate.

Effect of LA on the redox state of PN

It has been known that the threshold of Ca^{2+} for the induction of MPT was low with pyruvate and high with succinate plus rotenone, and that the different sensitivity of MPT to LA with these substrates correlated with the redox state of PN (21). As shown in Figure 2A, PN was reduced by succinate-dependent respiration even in the presence of rotenone. These results suggest that LA-stimulated MPT might be correlated with the rotenone-insensitive NADH oxidation (''external pathway'') that is suppressed by cyclosporine A (32, 33). However, the time required for the occurrence of mitochondrial swelling induced by LA plus Ca^{2+} was shorter than that for the oxidation of PN (Figure 2B).

Effect of LA on the mitochondrial Ca^{2+} state

It has been known that, in the presence of rotenone and succinate, MPT occurred with the concomitant release of Ca^{2+} from mitochondria (17). In the presence of rotenone, Pi and succinate, the absorption intensity of Antipyrylazo III remained unchanged during the incubation of mitochondria for longer than 16 min (Figure 3A). However, exogenously added Ca^{2+} was rapidly taken up by mitochondria and then released when its concentration reached a high enough level to induce their uncoupling (Figure 3C). LA decreased the loading capacity of mitochondria, thereby stimulating the release of Ca^{2+} in a

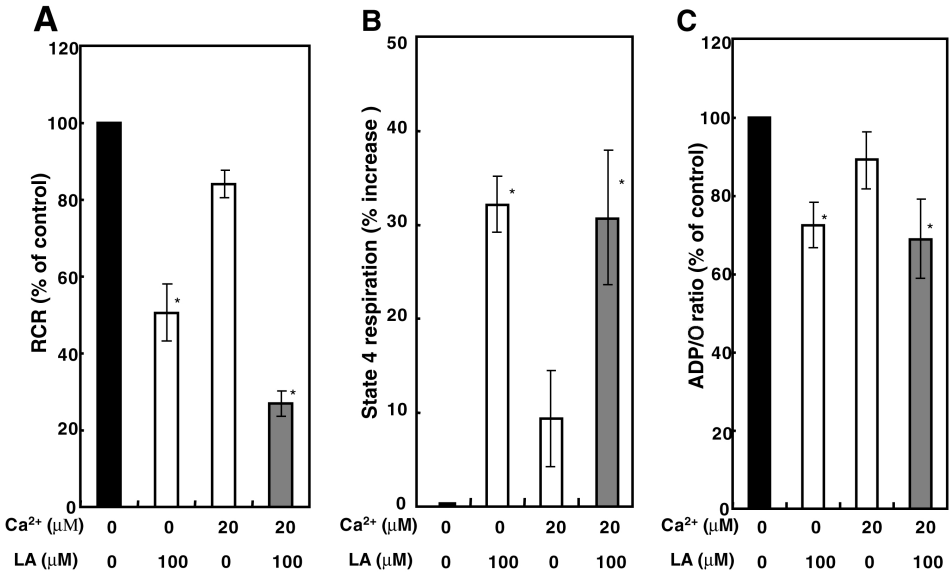

FIGURE 1. Effect of LA on succinate respiration and oxidative phosphorylation of mitochondria. Oxidative phosphorylation of isolated rat liver mitochondria was measured by oxygen electrode as described in a previous paper (17). A, B and C showed the respiratory control ratio (RCR), state 4 respiration and ADP/O ratio, respectively. In the medium of 10 mM Tris-HCl buffer (pH 7.4) containing 150 mM KCl, 5 mM $MgCl_2$, 1 mM Pi and 2.5 mM succinate, the RCR, state 4 respiration and ADP/O ratio of the mitochondria were 4.8, 30.4 mM /min /mg protein and 1.9, respectively. *Significant difference ($P < 0.05$). Similar results were obtained in three separate trials.

concentration dependent manner (Figure 3D and E). Cyclosporine A strongly suppressed the decrease in the loading capacity of mitochondria and stimulated the effect of LA (Figure 3B).

Effect of LA on Ca^{2+}-induced ROS generation

Since DHLA induces mitochondrial MPT by stimulating the generation of superoxide and related free radicals (20, 21), we examined the effect of LA on Ca^{2+}-dependent H_2O_2 generation. In the presence of rotenone, Pi and succinate, Ca^{2+} stimulated the mitochondrial generation of H_2O_2 *via* a cyclosporine A-sensitive mechanism (Figure 4A) (16, 17). Although 20 μM LA alone had no significant effect on the H_2O_2 generation by mitochondria, it enhanced the Ca^{2+}-induced H_2O_2 generation by a cyclosporine A-sensitive mechanism (data not shown).

In order to further investigate the effect of LA on ROS generation, we used a highly sensitive CHL probe, L-012, to analyze the Ca^{2+}-dependent ROS generation. Ca^{2+} stimulated mitochondrial chemiluminescence, suggesting the generation of ROS. LA further enhanced the chemiluminescence intensity *via* a cyclosporine A-sensitive mechanism (Figure 4B).

To obtain further insight into the mechanism of increased ROS generation by LA, FACScan analysis of ROS productions was examined using H_2DCF-DA dye assay. It has been

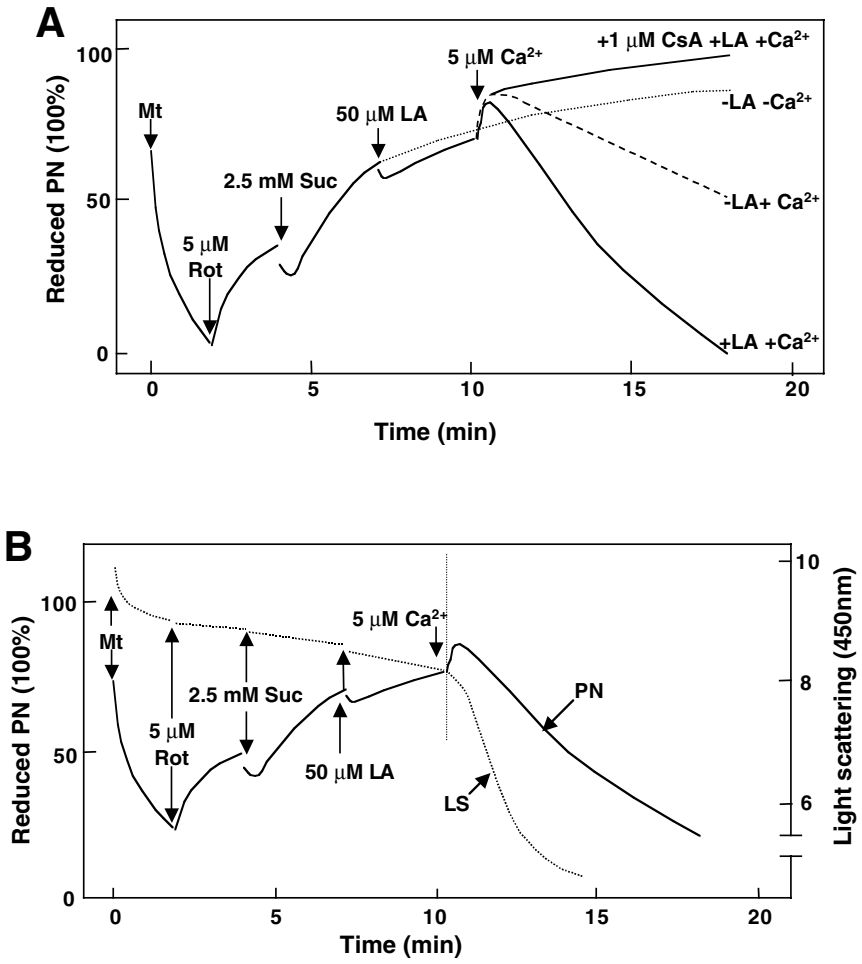

FIGURE 2. Effect of LA on the Ca^{2+}-induced redox state of PN in mitochondria. The redox state of PN was analyzed according to the fluorescence intensity at 460 nm during excitation with 340 nm using a fluorescence spectrophotometer. Mitochondria (0.1 mg protein /ml) were incubated according to the standard procedure in the presence of 1 mM Pi. Arrows indicate the point at which the following reagents were added: rotenone (Rot) = 5 μM, succinate (Suc) = 2.5 mM, LA = 50 μM, Ca^{2+} = 5 μM. A) Redox state of PN in mitochondria during incubation with various reagents. B) Relation between redox state of PN and light scattering properties of mitochondria during incubation with rotenone, succinate, LA and Ca^{2+}. LS, Light scattering; Similar results were obtained in three separate trials.

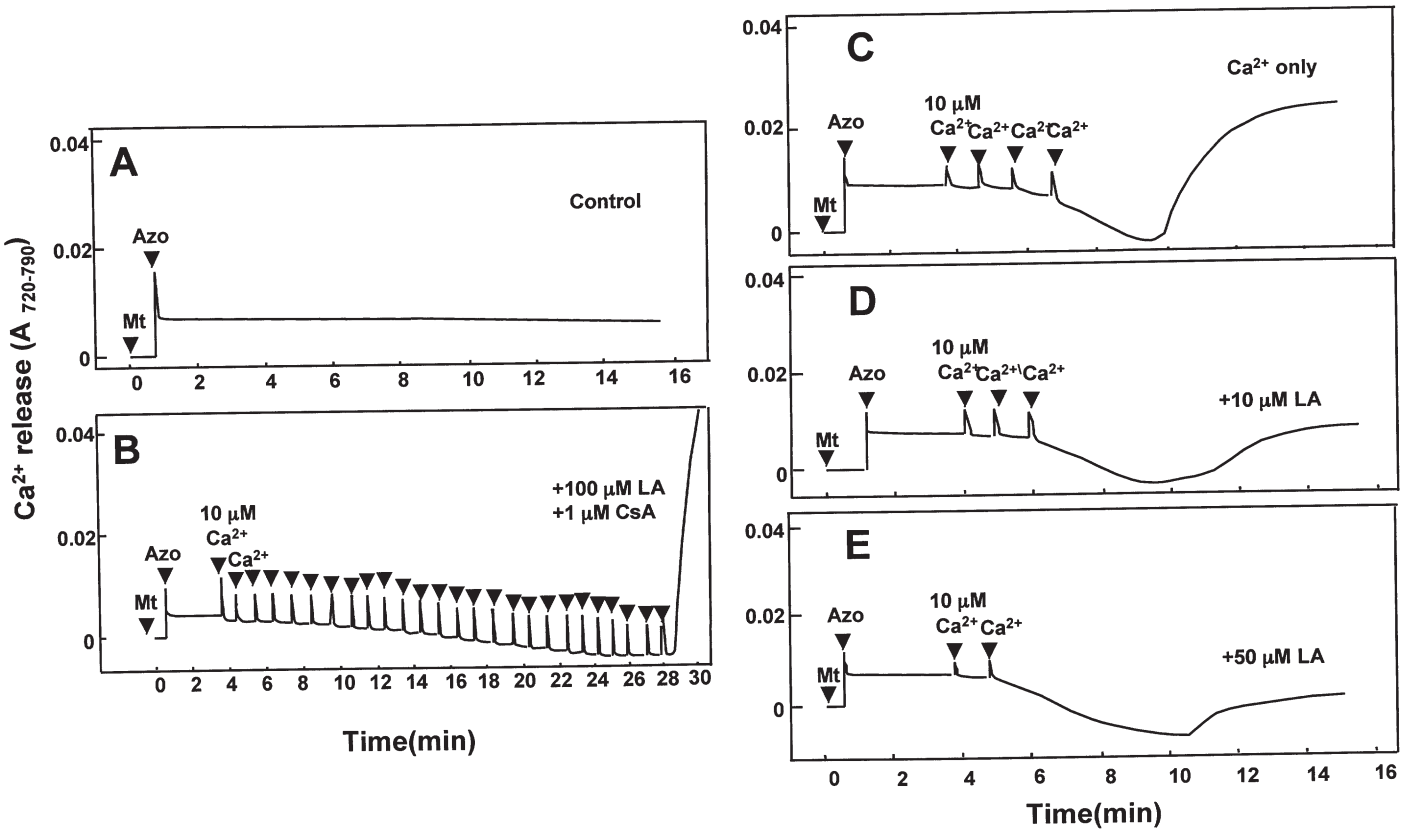

FIGURE 3. Effect of LA on Ca^{2+} loading and release in mitochondria. Mitochondria (0.5 mg protein /ml) were incubated according to the standard procedure at 25°C. After the addition of 1 mM Pi, 2.5 mM succinate and 50 μM antipyrylazo III, reaction was induced by 50 μM Ca^{2+} in the presence or absence of 10 ~ 100 μM LA or 1 μM cyclosporine A. A) Control experiment without Ca^{2+}. B) Effect of cyclosporine A on the Ca^{2+} loading in the presence of 100 μM LA. C) Effect of Ca^{2+} concentration. D and E) Effect of LA on Ca^{2+} loading in mitochondria. Upward deflection showed Ca^{2+} release. Arrows show the point where reagents were added. Similar results were obtained in three separate experiments.

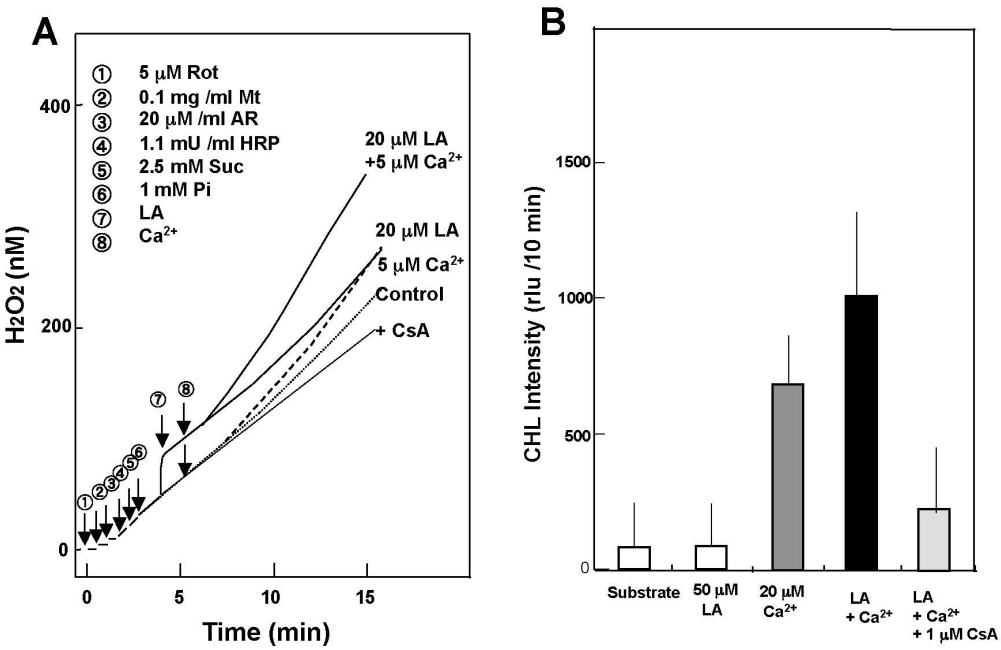

FIGURE 4. Enhancement of ROS generation in mitochondria by LA. A) Effect of LA on H_2O_2 generation induced by Ca^{2+}. Mitochondria (0.1 mg protein /ml) were incubated according to a standard procedure in the presence of 5 μM rotenone. Reaction was started as described in the text with or without 1 μM cyclosporine A. Changes in the fluorescence intensity were measured at 590 nm with excitation at 550 nm. B) Effect of LA on ROS generation induced by Ca^{2+}. Mitochondria (0.1 mg protein /ml) were incubated according to the standard procedure in the presence of 1 mM Pi, 2.5 mM succinate and 100 μM L-012. ROS generation was induced by adding 20 μM Ca^{2+}, and L-012 CHL was monitored using a Luminometer. Similar results were obtained in three separate experiments.

suggested that H_2DCF-DA crosses the cell membrane, subsequently undergoing deacetylation by intracellular esterases (34). The result of cytometric analysis using H_2DCF proposed to react with intramitochondrial hydrogen peroxide or other oxidizing ROS to give the fluorescent 2',7'-dichlorofluorescein (DCF). As shown in Figure 5, LA significantly increased the Ca^{2+} dependent ROS generation in mitochondria in a time dependent manner. This ROS generation was further suppressed in the presence of cyclosporine A (data not shown).

Effect of LA on the redox state of the critical thiol groups of ANT

ANT is an important component in ADP/ATP exchange across the inner membranes of mitochondria. ANT has three critical thiol groups; the cross linking between Cys160 and Cys257 increases the affinity of cyclophilin D to ANT, thereby inducing MPT (35). Since the presence of Ca^{2+} enhances the oxidation of these thiol groups (17), we examined the effect of LA on the redox state of ANT. ANT was prepared from intact mitochondria bound to phenylarsine oxide-conjugated agarose by a mechanism that was inhibited by

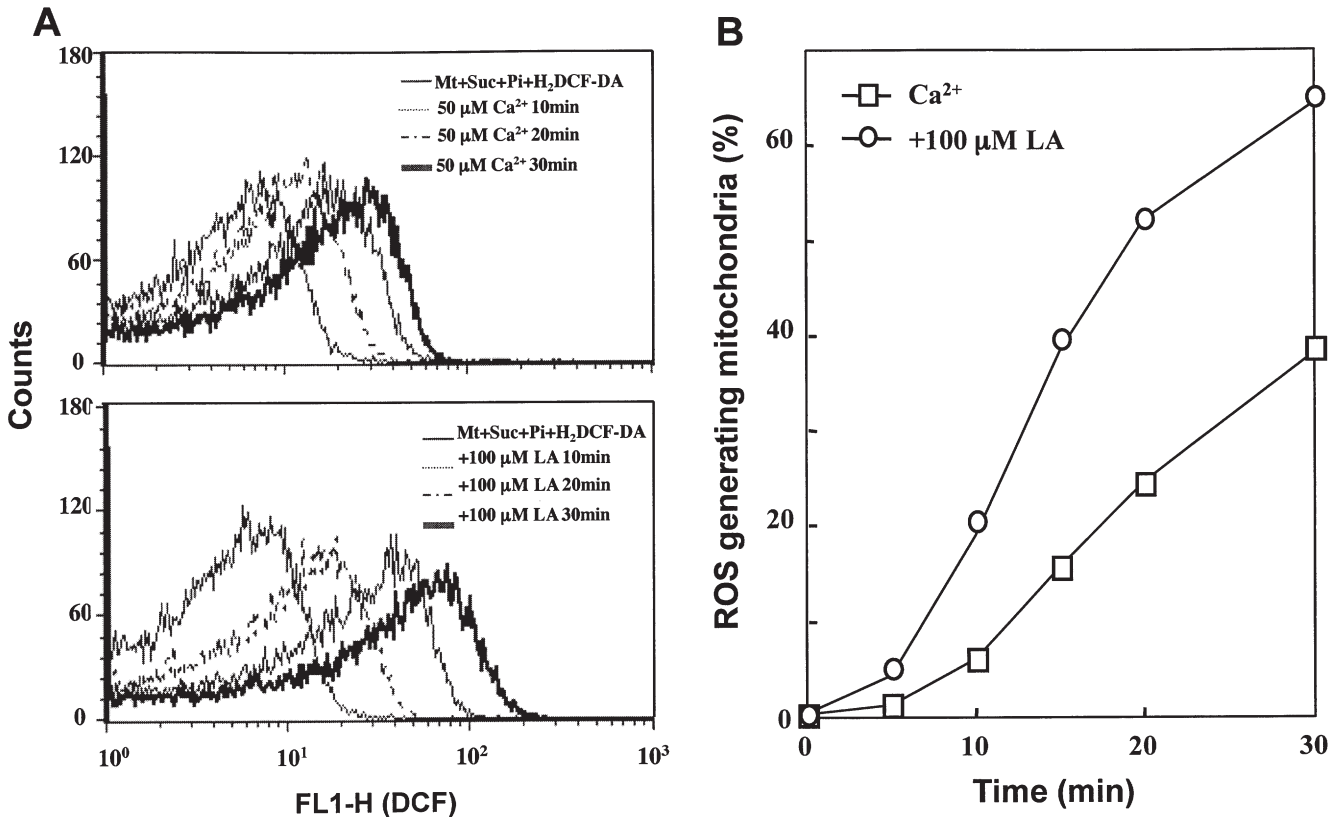

FIGURE 5. Flow cytometoric analysis of Ca^{2+}-induced ROS generation and its stimulation by LA. Experimental conditions were the same as those described in Figure 4. Mitochondria (0.1 mg protein /ml) were incubated in standard medium containing 1 mM Pi and 2.5 mM succinate at 25°C. After the addition of 10 μM H_2DCF-DA, 100 μM LA was added and ROS generation was stimulated by the addition of 50 μM Ca^{2+}. A) Time dependent increase in ROS generation by Ca^{2+} analyzed by FACScan (upper panel) and its enhancement with LA (lower panel). FL1-H (DCF) showed the fluorescence intensity of DCF. B) Percent increase in ROS generation during incubation with Ca^{2+} and LA. Similar results were obtained in three separate experiments.

pretreating mitochondria with Ca^{2+} (Figure 6A). High concentrations of LA inhibited the binding of ANT to the agarose (Figure 6B). The inhibitory effect of Ca^{2+} on the binding of ANT to the agarose was increased by LA but suppressed by cyclosporine A (Figure 6A and C).

Effect of LA on Ca^{2+}-induced membrane depolarization

Cyclosporine A-sensitive MPT, characterized by depolarization and swelling, requires Ca^{2+} and biological energy. In the presence of Pi and succinate, Ca^{2+} stimulated the depolarization of mitochondrial inner membranes (Figure 7A). LA enhanced the Ca^{2+}-induced depolarization in a concentration dependent manner (Figure 7B).

Effect of LA on Ca^{2+}-induced mitochondrial swelling

To get further insight into the mechanism of LA-stimulated MPT, the effect of LA on Ca^{2+}-induced mitochondrial swelling was examined. In the absence of Ca^{2+}, LA had no appreciable effect on mitochondria (Figure 8A). However, LA enhanced the Ca^{2+}-induced mitochondrial swelling in a concentration-dependent manner (Figure 8B). The enhancing effect of LA depended on the time of preincubation. It has been reported that DHLA enhances Ca^{2+}-induced mitochondrial swelling in the presence of pyruvate but not in the presence of rotenone plus succinate (20). However, preliminary experiments in this laboratory showed that the extent of LA enhancement was slightly lower in the presence of rotenone plus succinate than that of pyruvate (data not shown).

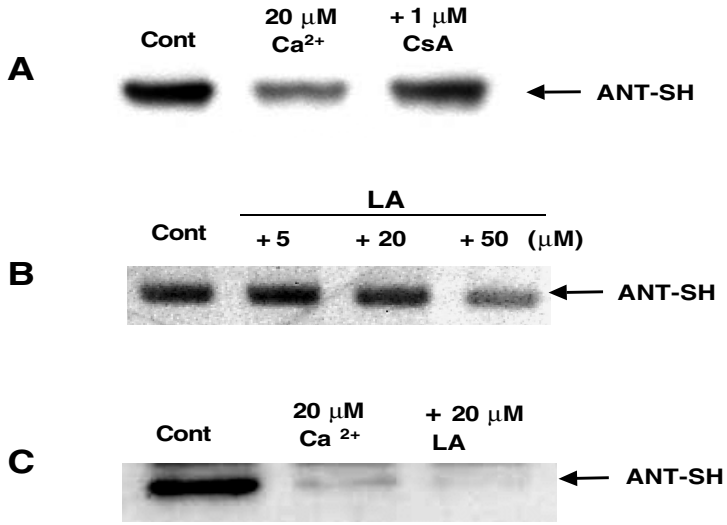

FIGURE 6. Effect of LA on oxidation of ANT thiol groups. Mitochondria (2 mg protein /ml) were incubated according to the standard procedure at 25°C for 10 min in the presence of 1 mM Pi and 2.5 mM succinate. The oxidation of ANT thiol groups was induced by 20 μM Ca^{2+} or 5 ~ 50 μM LA in the presence or absence of 1 μM cyclosporine A (CsA). ANT-SH band showed amount of reduced ANT thiol groups. A) Oxidation of ANT thiol groups by 20 μM Ca^{2+} and its sensitivity to cyclosporine A. B) Concentration dependent oxidation of ANT thiol groups by LA. C) Stimulation of ANT thiol group oxidation in the presence of Ca^{2+}. Similar results were obtained in three separate experiments.

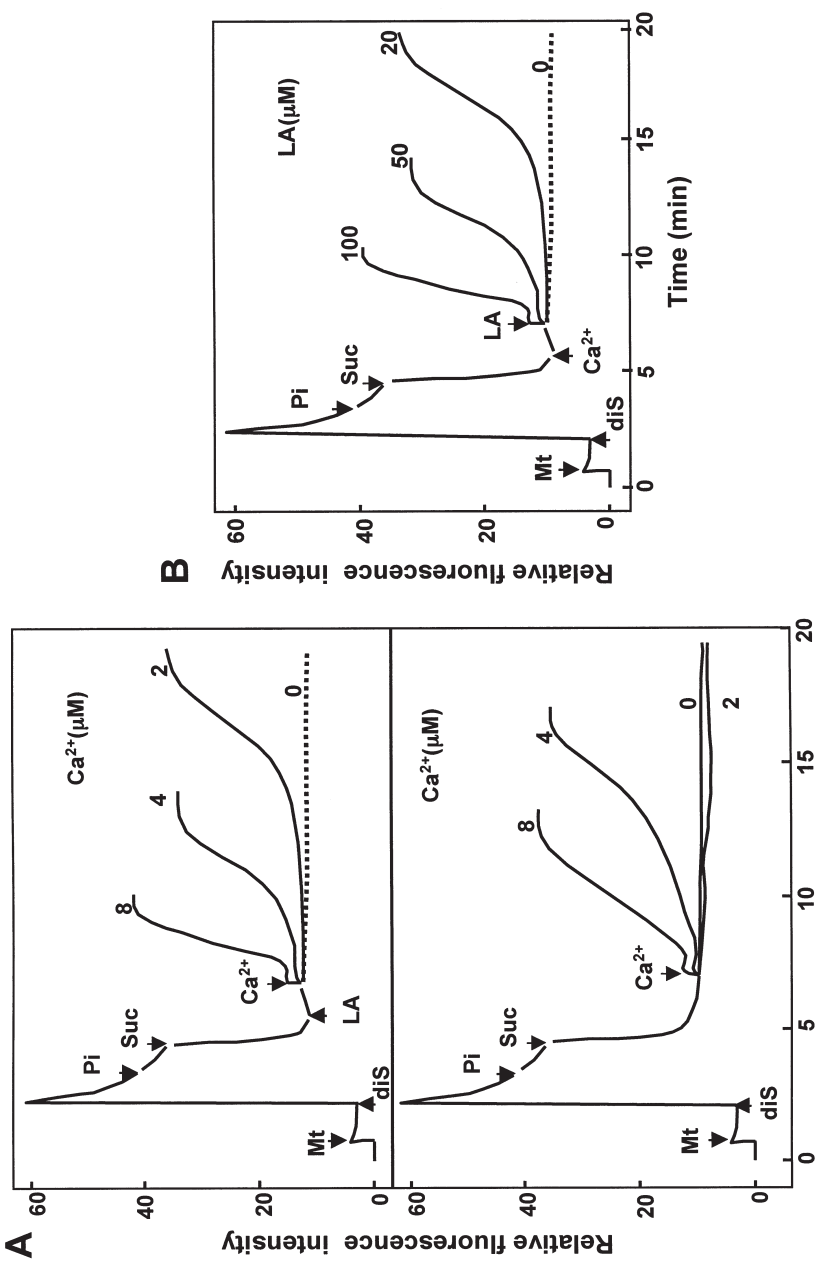

FIGURE 7. Effect of LA on Ca^{2+}-induced depolarization of mitochondria. The mitochondrial membrane potential was monitored using diS-C3-(5). Mitochondria (0.1 mg protein /ml) were incubated according to the standard procedure in the presence of 0.2 μg /ml diS-C3-(5) and 5 μM rotenone at 25°C. Membrane depolarization was induced by Ca^{2+} in the presence of succinate (Suc) and Pi. A) Ca^{2+}-induced depolarization in the presence or absence of 50 μM LA. B) Enhancement of Ca^{2+}-induced depolarization by LA in a concentration dependent manner. Arrows indicate the point where reagents were added. Similar results were obtained in three separate trials.

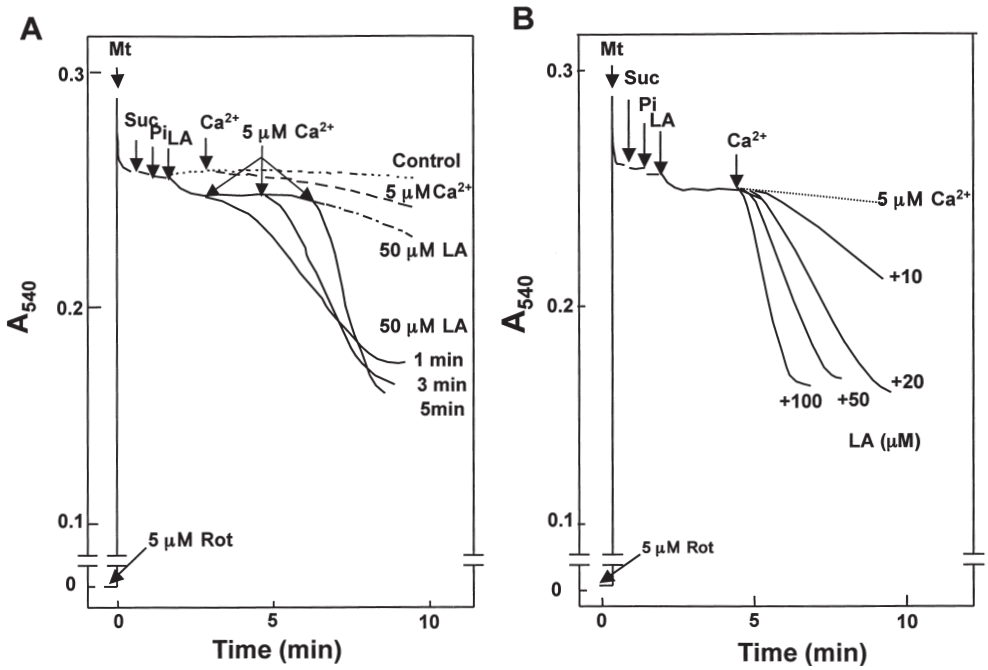

FIGURE 8. Effect of LA on Ca^{2+}-induced mitochondrial swelling. Mitochondria (0.1 mg protein /ml) were incubated according to the standard procedure and their swelling was monitored spectrophotometrically at 540 nm. Mitochondrial swelling was induced by adding Ca^{2+}. A) Effect of preincubation time with LA before the addition of 5 μM Ca^{2+}. B) Concentration dependent stimulation by LA of Ca^{2+}-induced swelling. Similar results were obtained in three separate trials.

Effect of LA on Ca^{2+}-induced cytochrome c release

It is well known that Ca^{2+}-induced swelling is accompanied by cytochrome c release by a cyclosporine A-sensitive mechanism (17). Mitochondrial swelling and cytochrome c release were induced by a low concentration of Ca^{2+} (~7 μM) but not by its high concentrations (>50 μM). LA also had no appreciable effect on the induction of mitochondrial swelling and cytochrome c release. However, LA stimulated Ca^{2+}-induced mitochondrial swelling with the concomitant release of cytochrome c by a cyclosporine A-sensitive mechanism (Figure 9A and B).

Effect of LA, cyclosporine A and α-tocopherol on hydroxyl radical-induced MPT

We previously reported that the hydroxyl radical induced the cyclosporine A-sensitive swelling of mitochondria (36). To test whether LA affected hydroxyl radical-induced MPT, its effect on mitochondrial swelling induced by Fe^{2+}/H_2O_2 was examined. LA enhanced the hydroxyl radical-induced swelling of the mitochondria in a concentration dependent- and cyclosporine A-sensitive mechanism (Figure 10A). Moreover, α-tocopherol suppressed the LA-enhanced and Fe^{2+}/H_2O_2-induced mitochondrial swelling in a concentration-dependent manner (Figure 10B). In this context, we previously

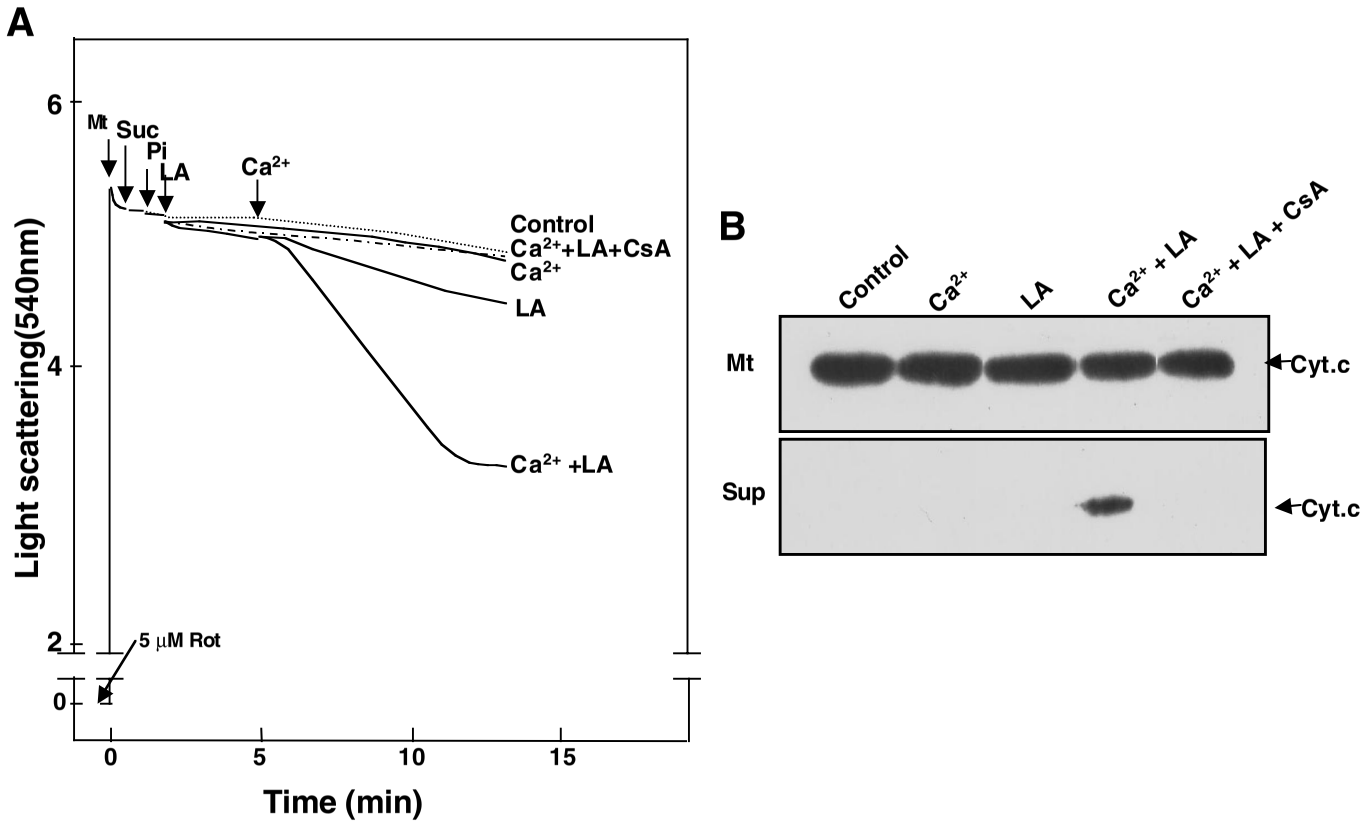

FIGURE 9. Stimulation of Ca^{2+}-induced cytochrome c release by LA. Experimental conditions were the same as described in Figure 7. After the incubation of mitochondria with 7 μM Ca^{2+} for 8 min according to the standard procedure, mitochondrial and supernatant fractions were separated and cytochrome c (Cyt. c) release was detected by an immunoblotting method using anti-cytochrome c antibody. A) Effect of 10 μM LA on the Ca^{2+}-induced swelling in the presence or absence of 1 μM cyclosporine A (CsA). B) Effect of 10 μM LA on the Ca^{2+}-induced cytochrome c release in the presence or absence of 1 μM cyclosporine A. Samples were obtained from the A) experiment. Similar results were obtained for three separate experiments.

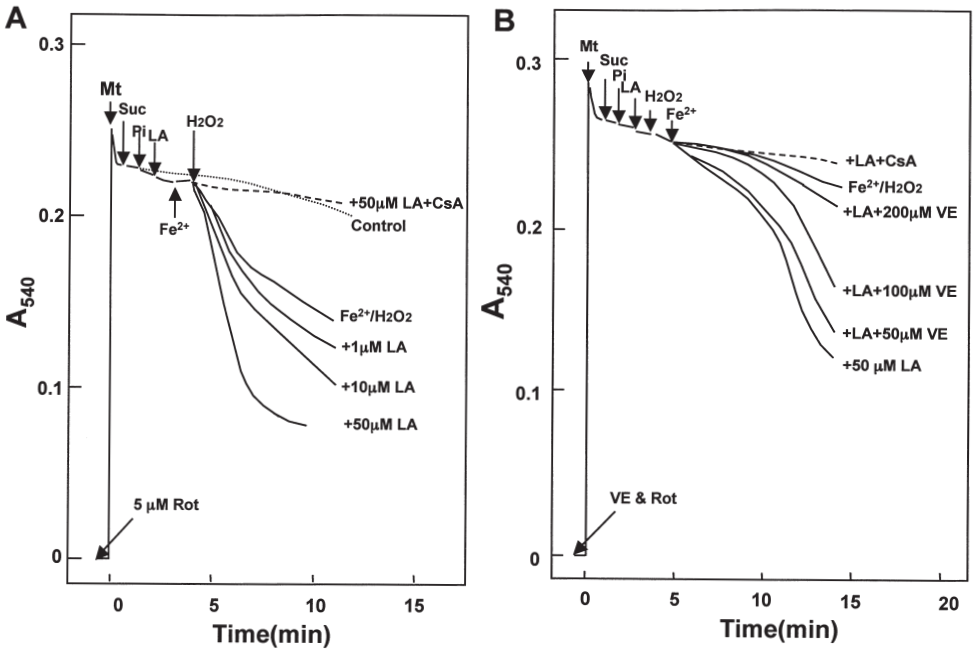

FIGURE 10. Effect of LA on the Fe^{2+}/H_2O_2ñinduced mitochondrial swelling and sensitivity to cyclosporine A and α-tocopherol. Mitochondria (0.1 mg protein /ml) were incubated according to the standard procedure in the presence of 1 mM Pi, 2.5 mM succinate and 2 μM rotenone at 25°C. Swelling was induced by 10 μM Fe^{2+}/100 μM H_2O_2 plus LA in the presence or absence of 1 μM cyclosporine A (CsA) or various concentrations of α-tocopherol (VE). LA was added before the addition of Fe^{2+}/H_2O_2. A) LA concentration dependent increase in Fe^{2+}/H_2O_2 induced mitochondrial swelling and its sensitivity to CsA. B) Concentration dependent suppression of Fe^{2+}/H_2O_2 plus LA-induced mitochondria swelling by VE and its sensitivity to CsA. Similar results were obtained in three separate experiments.

reported that 50 μM 17β-estradiol suppressed the Fe^{2+}/H_2O_2-induced MPT (37). Thus, we also examined the effect of 17β-estradiol on LA- and Fe^{2+}/H_2O_2-induced mitochondrial swelling and observed a similar suppressing effect of the steroid hormone (data not shown).

Discussion

Apoptosis triggered by dramatic changes of mitochondrial functions is important not only for embryonic development and the maintenance of tissue homeostasis, but also in the pathogenesis of various diseases (38, 39, 40, 41). The present work describes that LA enhanced the Ca^{2+}-induced classical MPT (CMPT) in isolated rat liver mitochondria, a prerequisite step to apoptosis, by activating the ''external pathway'' of NADH oxidase. CMPT is characterized by a dependency on energy metabolism, a decrease in mitochondrial capacity to accumulate Ca^{2+}, changes of inner membranes induced by binding of Ca^{2+} to cardiolipin, ROS generation, oxidation of critical thiol groups in ANT, and the

induction of swelling by a cyclosporine A-sensitive mechanism (42, 43). The opening of MPT releases cytochrome c and apoptosis-related proteins from mitochondria into cytosol and activates the caspase cascade, thereby inducing apoptosis of cells (42, 44). Thus, mitochondria play critical roles in determining both the survival and death of a wide variety of cells. The present work shows that LA enhanced all these events of CMPT induced by Ca^{2+}. LA also enhanced Fe^{2+}/H_2O_2-induced MPT by a Ca^{2+}-dependent and cyclosporine A-sensitive mechanism.

It should be noted that mitochondria are the potential site for ROS generation and ROS function as second messengers in cells that mediate signals from mitochondria to the cytoplasm and nucleus. Several studies have provided information concerning the antioxidant activity of LA (1, 4, 5), and LA supplementation was found to decrease oxidative stress and restore the reduced levels of other antioxidants *in vivo* (11). It has been known that Ca^{2+} loading in mitochondria modulates the electron transport system and enhances their generation of ROS (16, 17, 42). In the presence of Pi, succinate and a low concentration of Ca^{2+}, LA increased the state 4 respiration of mitochondria but decreased their RCR and ADP/O ratio. These uncoupling effects of LA were coupled with the enhanced generation of ROS in mitochondria (see Figure 4 and 5).

Recently, it has been reported that cells rapidly take up and reduce LA to DHLA by NADPH or NADP and release DHLA into the incubation medium (45). LA in mitochondria was also reduced to DHLA to enhance MPT through its prooxidant activity (23) and stimulate the Ca^{2+}-induced mitochondrial swelling in the presence of pyruvate but not succinate and rotenone, suggesting that LA might function as a cofactor for α-ketoacid decarboxylation (20). Furthermore, it has been reported that DHLA enhances MPT by DHLA-induced prooxidants, such as superoxide and related free radicals, *via* a mechanism that was inhibited by radical scavengers, including 2,2,6,6-tetramethylperidine-N-oxyl and 2,6-di-tert-butyl-4-methylphenol (20, 21). However, in a preliminary experiment in this laboratory, we observed the stimulated MPT by DHLA in the presence of succinate plus rotenone. We could not find evidence to support the hypothesis that these free radical scavengers suppressed the MPT induced by LA and Ca^{2+}, either. In this context, we found that LA stimulated the hydroxyl radical-induced MPT in α-tocopherol and 17β-estradiol sensitive mechanism. These antioxidants protected mitochondria from Fe^{2+}/H_2O_2-derived hydroxyl radicals but not MPT (36, 37). Therefore, these results indicate that both forms of LAs stimulated Ca^{2+}-induced MPT and ROS generation, and that their redox state is not important for the stimulation of MPT and ROS generation. However, the discrepancy of substrate dependency, such as pyruvate or rotenone plus succinate, between these experiments should be studied further.

It has been postulated that Ca^{2+}-induced CMPT is coupled with the activation of the ''external pathway'' of NADH oxidation (32, 33). The pathway of NADH oxidation includes NADH specific flavoprotein Fp5 and cytochrome b5 in the outer membranes, the inter-membranous electron transport, and cytochrome c oxidase in the inner membranes (46). The ''external pathway'' is not active in intact liver mitochondria, but is activated by rupture of the outer membranes (46). Since Ca^{2+}-induced and LA-enhanced mitochondrial swelling occurred before the oxidation of PN (see Figure 2B), nucleotide oxidation by the ''external pathway'' is not a cause of MPT. It has been reported that LA stimulated the release of Ca^{2+} strongly when PN are oxidized (47). In this context, we observed that the enhancement of Ca^{2+}-induced mitochondrial swelling required preincubation of mito-

chondria with LA. This observation seems to suggest the requirement of the reduction of LA in cells and/or the increase in intramitochondrial Ca^{2+} to induce effective swelling (see Figure 8). Thus, further study is necessary to understand the roles of LAs and the ''external pathway'' in the regulation of MPT.

MPT pore opening is stimulated by prooxidants that oxidize the critical thiol groups of ANT (17, 48), but inhibited by compounds that reduce the thiol groups (41, 48). Thus, disulfide LA and dithiol DHLA are expected to affect MPT. In fact, LA oxidized the thiol groups of ANT. However, DHLA also stimulated the Ca^{2+}-induced MPT (20, 21, 22, 23). Thus, both LA and DHLA seem to function as prooxidants. Since the two compounds undergo redox cycling between reduced and oxidized forms (45), they might exhibit activity as antioxidants as well as oxidants depending on the conditions in the cells (49). We previously showed that, in the presence of Pi and succinate, Ca^{2+} stimulated the oxidation of ANT thiol groups (17). The present work shows that LA stimulated the oxidation of ANT thiol groups at concentrations higher than 50 μM (see Figure 6). In this case, content of total ANT in mitochondria was not affected by the treatment with LA (data not shown). It has been reported that relatively high concentrations of LA (50~500 μM) preferentially oxidize vicinal thiol groups in various proteins, including NADPH-cytochrome P450 reductase (50). It was also reported that LA is readily absorbed from the diet, transported to cells and reduced to DHLA (51). Thus, LA and DHLA might affect the redox state of critical thiols of ANT, thereby modulating MPT.

Calcium status in cells plays important roles in the regulation of cell functions. Uptake of large amounts of cytosolic Ca^{2+} by mitochondria elicits MPT; loading and release of Ca^{2+} across mitochondrial membranes are early events of Ca^{2+} -induced MPT (42, 52). Since LA decreased mitochondrial capacity to load Ca^{2+} and enhanced their swelling, Ca^{2+} loading might trigger the LA-induced MPT. In the presence of rotenone and succinate, cyclosporine A inhibited the effect of LA to stimulate the Ca^{2+}- and hydroxyl radical-induced MPT. Thus, cyclosporine A seems to affect not only the opening of MPT pores by binding to cyclophilin D, but also the initial step of MPT including Ca^{2+} loading and release from mitochondria (35, 42, 47, 53). Thus, LA might affect the initial step of MPT including mitochondrial loading of Ca^{2+} rather than inhibiting the generation of ROS. A preliminary experiment in this laboratory revealed that rats died within 3 days after administration of 1.5 g LA/kg. The LA concentrations used in this experiment were fairly low as compared to its lethal dose. These results suggest that LA stimulates apoptosis of certain cells. In fact, the prooxidant activity of LA has been reported to induce apoptosis of human colon cancer cells by an increased uptake of oxidizable substrates into mitochondria (54). Furthermore, tumor cell lines but not non-transformed cell lines undergo apoptosis following exposure to LA (55). Thus, the specificity of proapoptotic effects of LA on the transformed cell lines supports the therapeutic potential of LA for the treatment of patients with cancer (55). Since fairly high doses of LA have been used as a dietary supplement, the possible occurrence of such side effects including mitochondrial dysfunction and induction of apoptosis in normal tissues should be studied further. The present findings indicate that LA stimulates an initial step of CMPT in mitochondria and that such properties should be taken into account in using LA and related compounds as dietary supplements.

The work was supported, in part, by grants from the Ministry of Education, Science and Literature, and funds of Tateyama Kasei Co. Ltd. and Eisai Co. Ltd.

References

1. Smith, A.R., Shenvi, S.V., Widlansky, M., Suh, J.H. and Hagen, T.M. (2004) Lipoic acid as a potential therapy for chronic diseases associated with oxidative stress. *Curr. Med. Chem. 11:* 1135–1146.
2. Perham, R.N., Borges, A., Dardel, F., Graham, L.D., Hawkins, C.F., Laue, E.D. and Packman, L.C. (1992) The lipoyl domain and its role in thiamin diphosphate-dependent oxidative decarboxylation. *J. Nutr. Sci. Vitaminol (Tokyo). Spe No:* 457–460.
3. Harris, J.B., Alonso, D., Park, O.H., Cornfield, D. and Chacin, J. (1975) Lipoate effect on carbohydrate and lipid metabolism and gastric H+ secretion. *Am. J. Physiol. 228:* 964–971.
4. Bast, A. and Haenen, G.R. (2003) Lipoic acid: a multifunctional antioxidant. *Biofactors. 17:* 207–213.
5. Packer, L. (1998) Alpha-Lipoic acid: a metabolic antioxidant which regulates NF-kappa B signal transduction and protects against oxidative injury. *Drug. Metab. Rev. 30:* 245–275.
6. Patrick, L. (2002) Mercury toxicity and antioxidants: Part 1: role of glutathione and alpha-lipoic acid in the treatment of mercury toxicity. *Altern. Med. Rev. 7:* 456–471.
7. Jayanthi, S. and Varalakshmi, P. (1992) Tissue lipids in experimental calcium oxalate lithiasis and the effect of DL alpha-lipoic acid. *Biochem. Int. 26:* 913–921.
8. Rezk, B.M., Haenen, G.R., van der Vijgh, W.J. and Bast, A. (2004) Lipoic acid protects efficiently only against a specific form of peroxynitrite-induced damage. *J. Biol. Chem. 279:* 9693–9697.
9. Peter, G. and Borbe, H.O. (1995) Absorption of [7,8-14C]rac-a-lipoic acid from in situ ligated segments of the gastrointestinal tract of the rat. *Arzneimittelforschung 45:* 293–299.
10. Farr, S.A., Poon, H.F., Dogrukol-Ak, D., Drake, J., Banks, W.A., Eyerman, E., Butterfield, D.A. and Morley, J.E. (2003) The antioxidants alpha-lipoic acid and N-acetylcysteine reverse memory impairment and brain oxidative stress in aged SAMP8 mice. *J. Neurochem. 84:* 1173–1183.
11. Hagen, T.M., Moreau, R., Suh, J.H. and Visioli, F. (2002) Mitochondrial decay in the aging rat heart: evidence for improvement by dietary supplementation with acetyl-L-carnitine and/or lipoic acid. *Ann. N. Y. Acad. Sci. 959:* 491–507.
12. Halestrap, A.P., McStay, G.P. and Clarke, S.J. (2002) The permeability transition pore complex: another view. *Biochimie. 84:* 153–166.
13. Tatton, W.G. and Olanow, C.W. (1999) Apoptosis in neurodegenerative diseases: the role of mitochondria. *Biochim. Biophys. Acta. 1410:* 195–213.
14. Brustovetsky, N., Brustovetsky, T., Jemmerson, R. and Dubinsky, J.M. (2002) Calcium-induced cytochrome c release from CNS mitochondria is associated with the permeability transition and rupture of the outer membrane. *J. Neurochem. 80:* 207–218.
15. Scorrano, L., Petronilli, V., Colonna, R., Di, Lisa, F. and Bernardi, P. (1999) Chloromethyltetramethylrosamine (Mitotracker Orange) induces the mitochondrial permeability transition and inhibits respiratory complex I. Implications for the mechanism of cytochrome c release. *J. Biol. Chem. 274:* 24657–24663.
16. Kowaltowski, A.J., Castilho, R.F. and Vercesi, A.E. (2001) Mitochondrial permeability transition and oxidative stress. *FEBS. Lett. 495:* 12–15.
17. Kanno, T., Sato, E.F., Muranaka, S., Fujita, H., Fujiwara, T., Utsumi, T., Inoue, M. and Utsumi, K. (2004) Oxidative stress underlies the mechanism for Ca(2+)-induced permeability transition of mitochondria. *Free. Radic. Res. 38:* 27–35.
18. Halestrap, A.P., Woodfield, K.Y. and Connern, C.P. (1997) Oxidative stress, reagents, and membrane potential modulate the mitochondrial permeability transition by affecting nucleotide binding to the adenine nucleotide translocase. *J. Biol. Chem. 272:* 3346–3354.
19. Han, D., Tritschler, H.J. and Packer, L. (1995) Alpha-lipoic acid increases intracellular glutathione in a human T-lymphocyte Jurkat cell line. *Biochem. Biophys. Res. Commun. 207:* 258–264.

20. Morkunaite-Haimi, S., Kruglov, A.G., Teplova, V.V., Stolze, K., Gille, L., Nohl, H. and Saris, N.E. (2003) Reactive oxygen species are involved in the stimulation of the mitochondrial permeability transition by dihydrolipoate. *Biochem. Pharmacol. 65:* 43–49.
21. Morkunaite, S., Teplova, V.V. and Saris, N.E. (2000) Mechanism of dihydrolipoate stimulation of the mitochondrial permeability transition: effect of different respiratory substrates. *IUBMB. Life 49:* 211–216.
22. Saris, N.E., Karjalainen, A., Teplova, V.V. and Lindros, K.O. (1998) The stimulation of the mitochondrial permeability transition by dihydrolipoate and alpha-lipoate. *Biochem. Mol. Biol. Int. 44:* 127–134.
23. Moini, H., Packer, L. and Saris, N.E. (2002) Antioxidant and prooxidant activities of alpha-lipoic acid and dihydrolipoic acid. *Toxicol. Appl. Pharmacol. 182:* 84–90.
24. Aono, K., Shiraishi, N., Arita, T., Inoue, B., Nakazawa, T. and Utsumi, K. (1981) Changes in mitochondrial function by lipid peroxidation and their inhibition by biscoclaurine alkaloid. *Physiol. Chem. Phys. 13:* 137–144.
25. Utsumi, T., Okuma, M., Kanno, T., Takehara, Y., Yoshioka, T., Fujita, Y., Horton, A.A. and Utsumi, K. (1995) Effect of the antiretroviral agent hypericin on rat liver mitochondria. *Biochem. Pharmacol. 50:* 655–662.
26. Mohanty, J.G., Jaffe, J.S., Schulman, E.S. and Raible, D.G. (1997) A highly sensitive fluorescencnt micro-assay of H_2O_2 release from activeated human leukocytes using a dihydroxyphenoxazine derivative. *J. Immuno. Methods. 202:* 133–141.
27. Imada, I., Sato, E. F., Miyamoto, M., Ichimori, Y., Minamiyama, Y., Konaka, R. and Inoue, M. (1999) Analysis of reactive oxygen species generated by neutrophils using a chemiluminescence prove L-012. *Anal. Biochem. 271:* 53–58.
28. Mattiasson, G. (2004) Flow cytometric analysis of isolated liver mitochondria to detect changes relevant to cell death. *Cytometry A.60:* 145–154.
29. Mattiasson, G. (2004) Analysis of mitochondrial generation and release of reactive oxygen-species. *Cytometry A.62:* 89–96.
30. Nishikimi, A., Kira, Y., Kasahara, E., Sato, E.F., Kanno, T., Utsumi, K. and Inoue, M. (2001) Tributyltin interacts with mitochondria and induces cytochrome c release. *Biochem. J. 356:* 621–626.
31. Furuno, T., Kanno, T., Arita, K., Asami, M., Utsumi, T., Doi, Y., Inoue, M. and Utsumi, K. (2001) Roles of long chain fatty acids and carnitine in mitochondrial membrane permeability transition. *Biochem. Pharmacol. 62:* 1037–1046.
32. Knorre, D.A., Dedukhova, V.I., Vyssokikh, M.Y. and Mokhova, E.N. (2003) Cyclosporin A-sensitive cytochrome c release and activation of external pathway of NADH oxidation in liver mitochondria due to pore opening by acidification of phosphate-containing incubation medium. *Biosci. Rep. 23:* 67–75.
33. Starkov, A.A., Markova, O.V., Mokhova, E.N., Arrigoni-Martelli, E. and Bobyleva, V.A. (1994) Fatty acid-induced Ca(2+)-dependent uncoupling and activation of external pathway of NADH oxidation are coupled to cyclosporin A-sensitive mitochondrial permeability transition. *Biochem. Mol. Biol. Int. 32:* 1147–1155.
34. Afri, M., Frimer, A.A. and Cohen, Y. (2004) Active oxygen chemistry within the liposomal bilayer. Part IV: Locating 2',7'-dichlorofluorescein (DCF), 2',7'-dichlorodihydrofluorescein (DCFH) and 2',7'-dichlorodihydrofluorescein diacetate (DCFH-DA) in the lipid bilayer. *Chem. Phys. Lipids. 131:* 123–133.
35. McStay, G.P., Clarke, S.J. and Halestrap, A.P. (2002) Role of critical groups on the matrix surface of the adenine nucleotide translocase in the mechanism of the mitochondrial permeability transition pore. *Biochem. J. 367(Pt2):* 541–548.
36. Yorimitsu, M., Muranaka, S., Sato, E.F., Fujita, H., Abe, K., Yasuda, T., Inoue, M. and Utsumi, K. (2004) Role of alpha-tocopherol in the regulation of mitochondrial permeability transition. *Physiol. Chem. Phys. & Med. NMR 36:* 95–107.
37. Miyaguchi, C., Muranaka, S., Kanno, T., Fujita, H., Akiyama, J., Yoshioka, T. and Yasuda, T. (2004) 17beta-estradiol suppresses ROS-induced apoptosis of CHO cells through inhibi-

tion of lipid peroxidation-coupled membrane permeability transition. *Physiol. Chem. Phys. Med. NMR. 36:* 21–35.
38. Shi, L., Kraut, R.P., Aebersold, R. and Greenberg, A.H. (1992) A natural killer cell granule protein that induces DNA fragmentation and apoptosis. *J. Exp. Med. 175:* 553–566.
39. Shi, L., Kam, C.M., Powers, J.C., Aebersold, R. and Greenberg, A.H. (1992) Purification of three cytotoxic lymphocyte granule serine proteases that induce apoptosis through distinct substrate and target cell interactions. *J. Exp. Med. 176:* 1521–1159.
40. Shi, L., Mai, S., Israels, S., Browne, K., Trapani, J.A. and Greenberg, A.H. (1997) Granzyme B (GraB) autonomously crosses the cell membrane and perforin initiates apoptosis and GraB nuclear localization. *J. Exp. Med. 185:* 855–866.
41. Zoratti, M. and Szabo, I. (1995) The mitochondrial permeability transition. *Biochim. Biophys. Acta. 1241:* 139–176.
42. Petrosillo, G., Ruggiero, F.M., Pistolese, M. and Paradies, G. (2004) Ca2+-induced reactive oxygen species production promotes cytochrome c release from rat liver mitochondria via mitochondrial permeability transition (MPT)-dependent and MPT-independent mechanisms: role of cardiolipin. *J. Biol. Chem. 279:* 53103–53108.
43. Fujita, H., Okimura, Y., Fujiwara, T., Utsumi, T., Kitamura, A., Kuroki, H., Kashiwagi, A. and Utsumi, K. (2006) 4-OH-3,5, 3',4'-Tetrchlorobihenyl induced membrane permeability transition in isolated mitochondria. *Clinical Biochemistry and Nutrition 38:* 167–175.
44. Kushnareva, Y.E., Haley, L.M. and Sokolove, P.M. (1999) The role of low (<or = 1 mM) phosphate concentrations in regulation of mitochondrial permeability: modulation of matrix free Ca^{2+} concentration. *Arch. Biochem. Biophys. J. 363:* 155–162.
45. Jones, W., Li, X., Qu, Z.C., Perriott, L., Whitesell, R.R. and May, J.M. (2002) Uptake, recycling, and antioxidant actions of alpha-lipoic acid in endothelial cells. *Free. Radi. Biol. Med. 33:* 83–93.
46. Lemeshko, V.V. (2002) Cytochrome c sorption-desorption effects on the external NADH oxidation by mitochondria: experimental and computational study. *J. Biol. Chem. 277:* 17751–17757.
47. Schweizer, M. and Richter, C. (1996) Stimulation of Ca2+ release from rat liver mitochondria by the dithiol reagent alpha-lipoic acid. *Biochem. Pharmacol. 52:* 1815–1820.
48. Chernyak, B.V. and Bernardi, P. (1996) The mitochondrial permeability transition pore is modulated by oxidative agents through both pyridine nucleotides and glutathione at two separate sites. *Eur. J. Biochem. 238:* 623–630.
49. Konrad, D. (2005) Utilization of the insulin-signaling network in the metabolic actions of alpha-lipoic acid-reduction or oxidation? *Antioxid. Redox. Signal 7:* 1032–1039.
50. Slepneva, I.A., Sergeeva, S.V. and Khramtsov, V.V. (1995) Reversible inhibition of NADPH-cytochrome P450 reductase by alpha-lipoic acid. *Biochem. Biophys. Res. Commun. 214:* 1246–1253.
51. Cakatay U. Pro-oxidant actions of alpha-lipoic acid and dihydrolipoic acid. (2006) *Med Hypotheses. 66:* 110–117.
52. Korge, P., Honda, H.M. and Weiss, J.N. (2001) Regulation of the mitochondrial permeability transition by matrix Ca(2+) and voltage during anoxia/reoxygenation. *Am. J. Physiol. Cell. Physiol. 280:* 517–526.
53. Waldmeier, P.C., Zimmermann, K., Qian, T., Tintelnot-Blomley, M. and Lemasters, J.J. (2003) Cyclophilin D as a drug target. *Curr. Med. Chem. 10:* 1485–1506.
54. Wenzel, U., Nickel, A., and Daniel, H. (2005) alpha-Lipoic acid induces apoptosis in human colon cancer cells by increasing mitochondrial respiration with a concomitant O2-*-generation. *Apoptosis. 10:* 359–368, 2005.
55. van de Mark, K., Chen, J.S., Steliou, K., Perrine, S.P. and Faller, D.V. (2003) Alpha-lipoic acid induces p27Kip-dependent cell cycle arrest in non-transformed cell lines and apoptosis in tumor cell lines. *J. Cell Physiol. 194:* 325–340.

Received August 23, 2006;
accepted September 12, 2006.

Physiol. Chem. Phys. & Med. NMR (2006) *38*: 21–29

Histological Changes in Spleens of Radio-sensitive and Radio-resistant Mice Exposed to Low-dose X-ray Irradiation

Takahiro Kataoka[1], Yuko Mizuguchi[1], Kenji Notohara[2], Takehito Taguchi[1] and Kiyonori Yamaoka[1*]

[1]*Graduate School of Health Sciences, Okayama University, 5-1 Shikata-cho, 2-chome, Okayama 700-8558, Japan,* [2]*Kurashiki Central Hospital, 1-1-1 Miwa, Kurashiki-shi, Okayama 710-8602, Japan.*
**Author for correspondence. E-mail; yamaoka @ md.okayama-u.ac.jp*

Abstract: We have previously determined by using immune-assay or bio-assay methods that low-dose irradiation enhances immune and anti-oxidation functions. In this study, we examined histological changes of lymphatic follicles at 4, 24, or 48 hrs after sham, 0.25, 0.5, or 15 Gy irradiation in the spleens of BALB/c mice, which are sensitive to radiation compared with other strains, and C57BL/6J mice, which are resistant to radiation, using hematoxylin-eosin staining for lymphatic follicles or methylgreen pyronin staining for plasma cells. Results show that the lymphatic follicles in the spleens of the two mouse strains decreased at 24 or 48 hrs after 15 Gy irradiation. The number of plasma cells in the spleens of sham irradiated BALB/c mice was greater than that of sham irradiated C57BL/6J mice. At 4 hrs after 0.25 Gy irradiation, plasma cells increased in the spleens of the two mouse strains. These findings suggest, by histology, that low-dose irradiation activates the plasma cells and enhances the immune function. Although those two mouse strains have different sensitivities to radiation, the above changes were similar in both time course and degree of response. Therefore, the phenomena observed may be common in mice.

KEY WORDS: low-dose X-irradiation, BALB/c mice, C57BL/6J mice, plasma cell, lymphatic follicle

Abbreviations: Con A - Concanavalin A; GPx - glutathione peroxidase; GSH - glutathione; IL - interleukin; INF γ - interferon-γ; LPS - lipopolysaccharide; MALP-2 - macrophage-activating lipopeptide-2; NF-κB - nuclear factor-κB; NK - natural killer; O_2^- - superoxide anion radicals; ·OH - hydroxyl radicals; ROS - Reactive oxygen species; SOD - superoxide dismutase; TNF-α - tumor necrosis factor-α.

REACTIVE OXYGEN species (ROS) are generated *in vivo* by ionizing radiation, stress or chemical agents. Most effects of the ionizing radiation are also mediated by reactive oxygen species such as superoxide anion radicals (O_2^-) or hydroxyl radicals (·OH). Low-dose irradiation, however, possesses different effects inducing radioadaptive responses (1) and activation of the antioxidant function (2–5). Yamaoka *et al.* (6,7) and Nomura *et al.* (8) reported that low-dose irradiation also reduced the carbon tetrachloride-induced or ferric-nitrilotriacetate-induced liver damage in mice. It is well known that low-dose irradiation induces activation of the immune function (9,10). Kojima (11–13) and Aneta (14) reported that the induction of endogenous glutathione or an antioxidative substance immediately after low-dose irradiation is at least partially responsible for the appearance of enhanced natural killer (NK) activity and that the suppression of experimental tumor metastases is primarily due to the stimulation of the cytolytic function of NK cells by irradiation. Mitogen-induced proliferative response of lymphocyte is inhibited by ROS through alteration of membrane thiol groups, and antioxidants such as glutathione (GSH) modulate the extent of these alterations (15–17). Immune function is generally lowered concomitantly with elevation of ROS formation and lipid peroxidation with aging (18).

The studies described above were performed primarily by immune assay or bio assay. There are little histological studies on the immune responses, especially the histological changes of lymphocytes, induced by low-dose irradiation in lymphoid tissues. Considering this background, we examined histological changes of splenic lymphatic follicles after X-irradiation in two strain mice with different sensitivities to radiation.

Materials and Methods

Animal models

The two strains of mice used were BALB/c, which is sensitive to radiation compared with other strains, and C57BL/6J, which is resistant to radiation. Animals were kept in a controlled environment (temperature: 20°C, humidity: 60%) at the Animal Center for Medical Research, Okayama University Medical School. They were fed on Oriental MF diet (Oriental Yeast Co., Tokyo) and tap water *ad libitum*. Approval from the affiliated bodies for animal experiments was received.

At seven to eight weeks of age (about 20 g of body weight), the mice received whole body X-ray irradiation of either 0.25, 0.5 (low-dose) or 15 Gy (high-dose) at a dose rate of 0.75 Gy/min of X-rays (voltage: 150 keV, ampere: 20 mA, filters: Cu:Al=0.2 mm:0.5 mm). Animals in control groups were irradiated falsely (sham irradiation) and treated similarly at the same time intervals (4, 24 or 48 hrs after sham irradiation) in order to examine the effect of stresses other than irradiation. Each mouse was sacrificed at 4, 24, or 48 hrs after irradiation by a cervical vertebra dislocation.

Assay

The spleen, a radio-sensitive organ, was excised, weighed, and divided into small blocks. These blocks were fixed in 10% neutral-buffered formalin, dehydrated by graded ethanol and xylene, and embedded in paraffin. Tissue paraffin sections of the spleens were prepared using a microtome (Department of Radiation Research, Shikata Laboratory Ad-

vanced Science Research Center, Okayama University) and stained conventionally with hematoxylin-eosin (HE) or especially with methylgreen pyronin for plasma cell detection. We calculated the ratio of the plasma cells.

Statistical analysis

The data values are presented as the mean ± the standard error of mean (SEM). The statistical significance of differences was determined with Student's *t*-test.

Results

Morphological changes after irradiation

In C57BL/6J mice, spleens became atrophied at 24 or 48 hrs after 15 Gy irradiation, while at 4 hrs after 15 Gy and at each time interval thereafter 0.25 or 0.5 Gy irradiation, morphological changes were not observed. We also compared the variously-irradiated spleen weight to the sham irradiated control weight at each time interval in the mice strain. The weight of spleens at 24 or 48 hrs after 15 Gy irradiation decreased by 49% and 52%, respectively (Figure 1).

Histological changes caused by 0.25, 0.5, or 15 Gy irradiation (HE staining)

No significant changes were observed in the lymphatic follicles of the spleens in either BALB/c mice or C57BL/6J mice at 4, 24, or 48 hrs after 0.25 or 0.5 Gy irradiation. The splenic lymphatic follicles, however, were sharply decreased at 24 or 48 hrs after 15 Gy irradiation in the two mouse strains (Figure 2-1, 2-2).

Histological changes caused by 0.25, 0.5, or 15 Gy irradiation (Methylgreen pyronin staining)

Plasma cells in the spleens were observed more in the sham irradiated BALB/c mice spleens than in the sham irradiated C57BL/6J mice. Although the plasma cells in the spleen increased at 4 hrs after 0.25 Gy irradiation in the two mouse strains, little difference of the cell population was observed between the two mouse strains. Also no significant changes of the cell population in the spleens were observed at 24 or 48 hrs after 0.25 Gy irradiation in either strain of mice. At 24 or 48 hrs after 15 Gy irradiation, plasma cells were sharply decreased in the spleens of BALB/c mice and C57BL/6J mice. There were no changes of the plasma cell population in either strain mice at 4, 24, or 48 hrs after 0.5 Gy irradiation (Figure 3-1, 3-2).

Discussion

We have reported that low-dose X-irradiation or low level radon inhalation reduced the lipid peroxide of adult animals to levels similar to those of juvenile animals (2–5). These mechanisms involve the induction of superoxide dismutase (SOD) which dismutated O_2^- to hydrogen peroxide (H_2O_2), catalase and glutathione peroxidase (GPx) which also detoxicated H_2O_2 into H_2O and O_2. These anti-oxide enzymes increase after low-dose irradiation. Low-dose irradiation causes the production of a small amount of O_2^- *in vivo*;

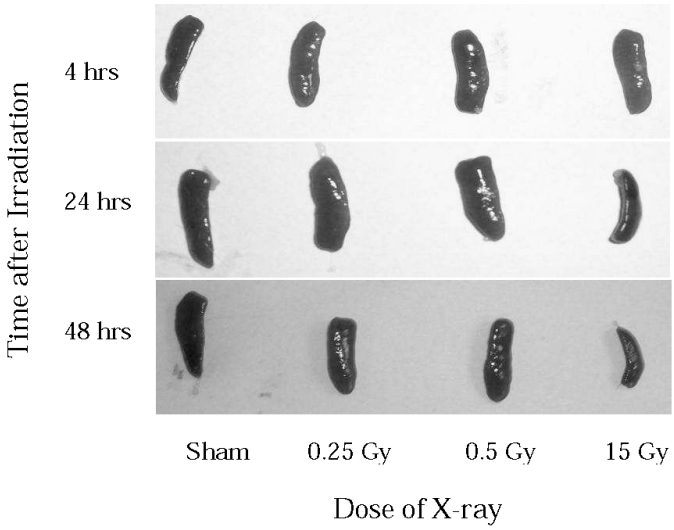

A) Morphological Changes after Irradiation

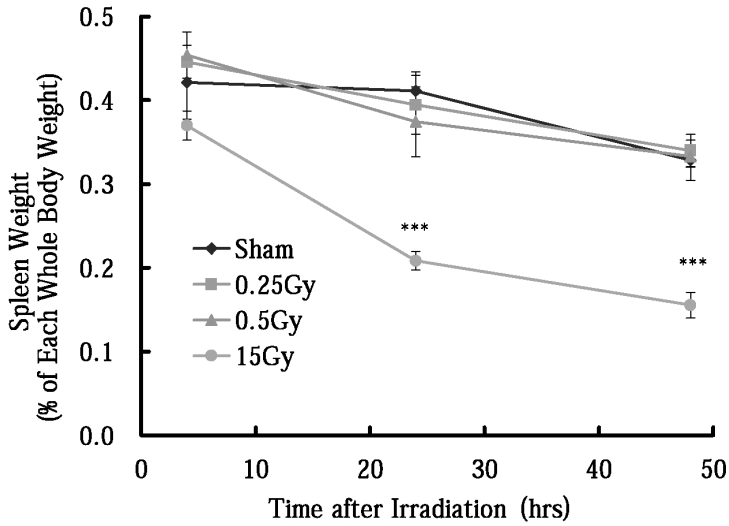

B) Weight Changes after Irradiation

FIGURE 1. Temporal changes of morphology (A) and weights (B) in C57BL/6J mice spleens after sham, 0.25 Gy, 0.5 Gy, or 15 Gy irradiation. Percentage of spleen weight to whole body weight at each time interval. Each value indicates the mean ± SEM. N = 3 – 4. ***Significantly different from the sham irradiated control group at $P < 0.001$.

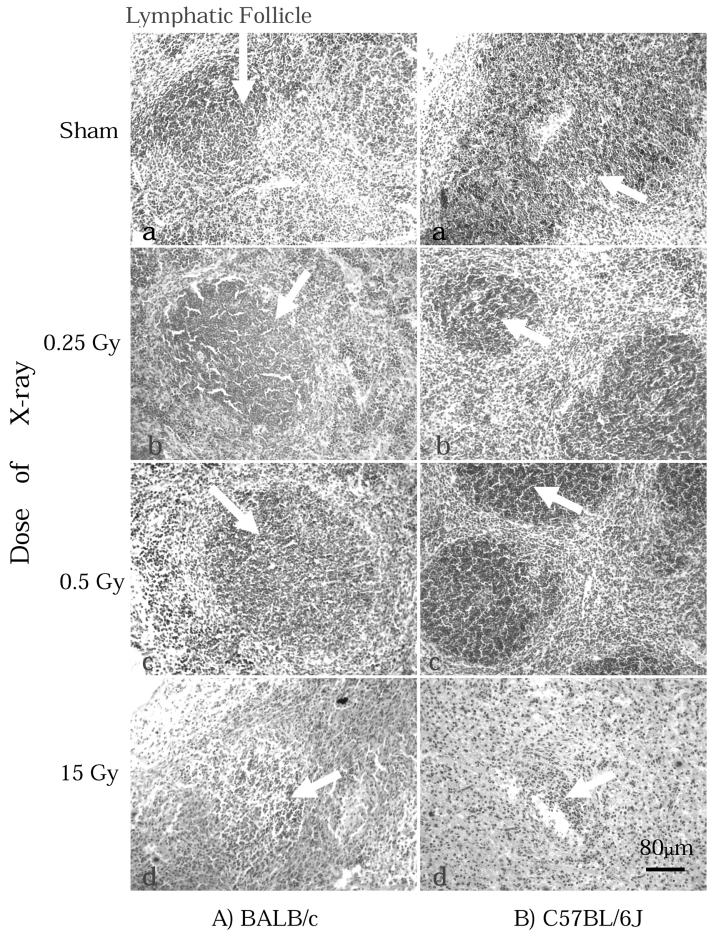

FIGURE 2-1. Differences in lymphatic follicles of spleens in BALB/c mice (A) and C57BL/6J mice (B) under sham irradiation (a), 4 hrs after 0.25 Gy irradiation (b), 4 hrs after 0.5 Gy irradiation (c), or 24 hrs after 15 Gy Irradiation (d). The length of scale bar is 80 μm. HE staining was used for the detection of lymphatic follicles.

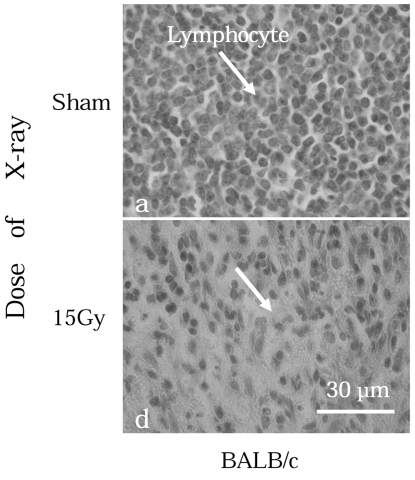

FIGURE 2-2. Differences in lymphocytes of spleens in BALB/c mice under sham irradiation (a) or 24 hrs after 15 Gy Irradiation (d). The length of scale bar is 30 μm. HE staining was used for the detection of lymphocytes.

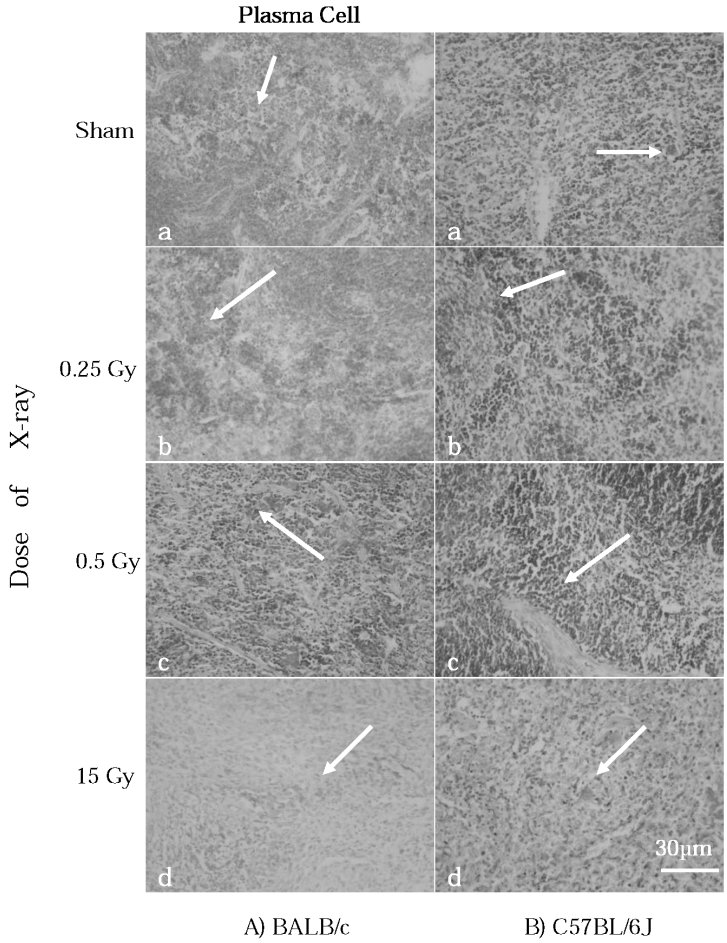

FIGURE 3-1. Differences in plasma cells of spleens in BALB/c mice (A) and C57BL/6J mice (B) under sham irradiation (a), 4 hrs after 0.25 Gy irradiation (b), 4 hrs after 0.5 Gy irradiation (c), or 24 hrs after 15 Gy irradiation (d). The length of scale bar is 30 μm. Methylgreen pyronin staining was used for the detection of plasma cells.

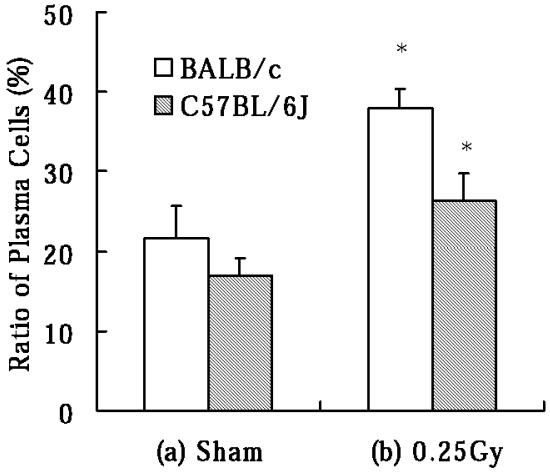

FIGURE 3-2. Ratio of plasma cells in spleens of BALB/c mice and C57BL/6J nice under sham irradiation (a) or 0.25 Gy irradiation (b). Each value indicates the mean ± SEM. N = 3 . *Significantly different from sham irradiated control group at $P<0.05$.

therefore, anti-oxidizing substances are induced. Therefore, activities of both SOD and GPx in the spleens of BALB/c mice and C57BL/6NJcl mice were found to be enhanced after low-dose X-irradiation. On the other hand, in the case of 4 Gy irradiation, activities of both SOD and GPx significantly decreased (19). A large quantity of the reactive oxygen in living bodies produced by high-dose irradiation seems to have deactivated the two species of enzymes.

There have been many reports concerning the effects of ionizing radiation on the enhancement of immune function (9,10) namely, Concanavalin A (Con A)-induced mitogen response of splenocytes 4 hrs after low-dose irradiation (9). However, there is no histological study on immune responses to low-dose irradiation. In the present study, we examined histological changes of lymphatic follicles after low-dose irradiation in the spleens of BALB/c mice and C57BL/6J mice. The lymphatic follicles decreased at 24 or 48 hrs after 15 Gy irradiation. On the other hand, there were no changes in lymphatic follicles of the spleens in BALB/c and C57BL/6J mice after 0.25 or 0.5 Gy irradiation. These findings suggest that proliferation of lymphocytes was not enhanced by low-dose X-irradiation, while high-dose irradiation suppressed the immune function. It may indicate that low-dose irradiation enhances the immune activities of individual lymphocyte.

The present study shows that the number of plasma cells in the spleens of sham-irradiated C57BL/6J mice was greater than that of sham-irradiated BALB/c mice. Genetic background is important in the Th1/Th2 balance in mice (20,21). Macrophages from C57BL/6 mice produced higher levels of tumor necrosis factor-α (TNF-α) and interleukin (IL)-12 than those from BALB/c mice after stimulation with macrophage-activating lipopeptide-2 (MALP-2, asynthetic TLR-2 ligand) or lipopolysaccharide (LPS, a TLR-4 ligand) (22). T cells from C57BL/6 mice preferentially produce Th1 cytokine with high interferon-γ (IN$F\gamma$) and low IL-4 which enhance the cellular immunity, while those from BALB/c mice favored Th2 cytokine production with low IN$F\gamma$ and high IL-4 which enhanced the humoral immunity. Similar T cell responses were observed when these strains mice were infected with *Leishmania major* (23,24).

Low-dose irradiation induced cytokine in macrophages (25). IL-6 expression was increased by low-dose irradiation, but IL-1β expression was not affected. Transcriptional activation of IL-6 and IL-1β is due to the enhanced binding of these cytokines to nuclear factor-κB (NF-κB) (26,27). NF-κB is induced and activated by ionizing radiation (27–30). On the other hand, 0.075 Gy irradiation induced the synthesis of IL-10 in splenocytes and the secretion of IL-12 in peritoneal macrophages (31). This report suggests that low-dose X-irradiation with 0.075 Gy may suppress IL-10 at the mRNA level and the protein level, and stimulate IL-12 expression simultaneously, which might contribute to a shift of the immune response in favor of Th1 differentiation leading this cellular immunity. Plasma cells are cellular factories devoted entirely to the manufacture and export of a single product: soluble immunoglobulin. As the final mediators of a humoral immune response, plasma cells play a critical role in adaptive immunity.

The present study, by histological method, showed that plasma cells in the spleens of BALB/c mice and C57BL/6J mice increased at 4 hrs after 0.25 Gy irradiation and decreased at 24 or 48 hrs after 15 Gy irradiation. These findings may indicate that the increase of plasma cells induced by 0.25 Gy, or low-dose irradiation, contribute to a shift of the immune response in favour of Th2 differentiation, leading to the humoral immunity. On the other hand, although those two mouse strains have different sensitivities to radiation,

the above changes were similar in both time course and degree of response. Therefore, the phenomena observed may be common in mice. We need further study to assess the thymus, one of the most sensitive lymphoid organs, with immunostaining for the main cellular constituents such as B cells.

The authors are indebted to Dr. Ichiro Naito for his valuable advice and technical assistance.

References

1. Ikushima, T., Aritomi, H. and Morishita, J. (1996) Radioadaptive: Efficient repair of radiation induced DNA damage in adapted cells. *Mutat. Res. 358:* 193–198.
2. Yamaoka, K., Edamatsu, R. and Mori, A. (1991) Increased SOD activities and decreased lipid peroxide levels in rat organs induced by low does X-irradiation. *Free Radic. Biol. Med. 11:* 299–306.
3. Yamaoka, K., Komoto, Y., Suzuka, I., Edamatsu, R. and Mori, A. (1993) Effect of radon inhalation on biological function, lipid peroxide, SOD activity and membrane fluidity. *Arch. Biochem. Biophys. 302:* 37–41.
4. Kojima, S., Matsumori, S., Ono, H. and Yamaoka, K. (1999) Elevation of glutathione in RAW 264.7 cell by low-dose γ-ray irradiation and its responsibility for the appearance of radioresistane. *Anticancer Res. 19:* 5271–5276.
5. Kojima, S., Teshima, K. and Yamaoka, K. (2000) Mechanisms involved in the elevation of glutathione in RAW 264.7 cells exposed low doses of γ-rays. *Anticancer Res. 20:* 1589–1594.
6. Yamaoka, K., Nomura, T., Iriyama, K. and Kojima, S. (1998) Inhibitory effects of prior low dose X-ray irradiation on Fe^{3+}-NTA-induced hepatopathy in rats. *Physiol. Chem. Phys. & Med. NMR 30:* 15–23.
7. Yamaoka, K., Kataoka, T., Nomura, T., Taguchi, T., Wang, D-H., Mori, S., Hanamoto, K. and Kira, S. (2004) Inhibitory effects of prior low-dose irradiation on carbon tetrachloride-induced hepatopathy in acatalasemic mice. *J. Radiat. Res. 45:* 89–95.
8. Nomura, T. and Yamaoka, K. (1999) Low-dose γ-ray irradiation reduces oxidative damage induced by CCl_4 in mouse liver. *Free Radical Biol. & Med. 27:* 1324–1333.
9. Nogami, M., Huang, J.T., James, S.J., Lubinski, J.M. and Makinodan, T. (1993) Mice chronically exposed to low dose ionizing radiation possess splenocytes with enhanced proliferation capacity and elevated levels of HSP-70 mRNA and protein. *Int. J. Radiat. Res. 63:* 775–786.
10. Ishii, K., Yamaoka, K., Hosoi, Y., Ono, T. and Sakamoto, K. (1995) Enhanced mitogen-induced proloferation of rat splenocytes by low-dose whole-body X-irradiation. *Physiol. Chem. Phys. & Med. NMR 27:* 17–23.
11. Kojima, S., Matsumori, S., Ishida, H. and Yamaoka, K. (2000) Possible role of elevation of glutathione in the acquisition of enhanced proliferation of mouse splenocytes exposed to small-dose γ-rays. *Int. J. Radiat. Biol. 76:* 1641–1647.
12. Kojima, S., Ishida, H., Takahashi, M. and Yamaoka, K. (2002) Elevation of glutathione induced by low-dose gamma rays and its involvement increased natural killer activity. *Radiat. Res. 157:* 275–280.
13. Kojima, S., Nakayama, K. and Ishida, H. (2004) Low dose γ-rays activate immune functions via induction of glutathione and delay tumor growth. J. *Radiat. Res. 45:* 33–39.
14. Cheda, A., Wrembel-Wargocka, J., Lisiak, E., Nowosielska, E.M., Marciniak, M, Janiak, M.K. (2004) Single low dose of X rays inhibit the development of experimental tumor metastases and trigger the activites of NK cells in mice. *Radiat. Res. 161:* 335–340.
15. Gougerot-Pocidalo, M.A., Fay, M., Roche, Y., Lacombe, P. and Marquetty, C. (1985) Immune oxidative injury induced in mice exposed to normobaric O_2: Effects of thiol compounds

on the splenic cell sulfhydryl content and Con A proliferative response. *J. Immunol. 135:* 2045–2051.
16. Pieri, C., Moroni, M. and Recchioni, R. (1992) Glutathione influences the proliferation as well as the extent of mitochondrial activation in rat splenocytes. *Cell Immunol. 145:* 210–217.
17. Pahlavani, M.A. and Harris, M.D. (1998) Effect of in vitro generation of oxygen free radicals on T cell function in young and old rats. *Free Radical Biol. Med. 25:* 903–913.
18. Miller, R.A. (1996) Aging and immune response. In: *Handbook of Biology of Aging*. Eds. E. Schneider, J Rowe. Academic Press, San Diego, CA. pp. 355–392.
19. Yamaoka, K., Obata, T., Iriyama, K., Iwasaki, T. and Hoshi, Y. (1998) Simultaneous quantitative analysis of prostaglandins and thromboxane after low-dose X-irradiation. *Radiat. Res. 149:* 103–106.
20. Stewart, D., Fulton, W.B., Wilson, C., Monitto, C.L., Paidas, C.N., Reeves, R.H. and Maio, A. (2002) Geneic contribution to the septic response in a mouse model. *Shock 18:* 342–347.
21. Hsieh, C.S., Macatonia, S.E., O'Garra, A. and Murphy, K.M. (1995) T cell genetic background determines default T helper phenotype development in vivo. *J. Exp. Med. 181:* 713–721.
22. Watanabe, H., Numata, K., Ito, T., Takagi, K. and Matsukawa, A. (2004) Innate immune response in Th1- and Th2- dominant mouse stains. *Shock 22:* 460–466.
23. Scott, P., Natovitz, P., Coffman, R.L., Pearce, E. and Sher, A. (1988) Immunoregulation of cutaneous leishmaniasis. T cell lines that transfer protective immunity or exacerbation belong to different T helper subsets and respond to distinct parasite antigens. *J. Exp. Med. 168:* 1675–1684.
24. Heinzel, F.P., Sadick, M.D., Holaday, B.J., Coffman, R.L. and Locksley, R.M. (1989) Reciprocal expression of interferon gamma or interleukin 4 during the resolution or progression of murine leishmaniasis. Evidence for expansion of distinct helper T cell subsets. *J. Exp. Med. 169:* 59–72.
25. Hosoi, Y., Miyachi, H., Matsumoto, Y., Enomoto, A., Nakagawa, K., Suzuki, N. and Ono, T. (2001) Induction of interleukin-1β and interleukin-6 mRNA by low doses of ionizing radiation in macrophages. *Int. J. Cancer (Radiat Oncolo Invest) 96:* 270–276.
26. Branch, M.A., Gruss, H.J., Kaisho, T., Asano, Y., Hirano, T. and Herrmann, F. (1993) Ionizing radiation induces expression of interleukin 6 by human fibroblasts involving activation of nuclear factor-kappa *B. J. Biol. Chem. 268:* 8466–8472.
27. Raju, U., Gumin, G.T. and Tofilon, P.J. (1999) NF kappa B activity and target gene expression in the rat brain after one and two exposures to ionizing radiation. *Radiat Oncol Investig 7:* 145–152.
28. Mohan, N. and Meltz, M.L. (1994) Induction of nuclear factor kappa B after low-dose ionizing radiation involves a reactive oxgen intermediate signaling pathway. *Radiat. Res. 140:* 97–104.
29. Abeyama, K., Kawano, K., Nakajima, T., Takasaki, I., Kitajima, I. and Maruyama, I. (1995) Interleukin 6 mediated differentiation and rescue of cell redox in PC12 cells exposed to ionizing radiation. *FEBS Lett. 364:* 298–300.
30. Basu, S., Rosenzweig, K.R., Youmell M. and Price, B.D. (1998) The DNA-dependent protein kinase participates in the activation of NK kappa B following DNA damage. *Biochem. Biophys. Res. Commun. 247:* 79–83.
31. Xiao-Dung, Liu, Shu-Mei, Ma and Shu-Zhen, Liu, (2003) Effect of 0.075 Gy X-ray irradiation on expression of IL-10 and IL-12 in mice. *Phys. Med. Biol. 48:* 2014–2049.

Received August 8, 2006;
accepted October 5, 2006.

Physiol. Chem. Phys. & Med. NMR (2006) *38*: 31–42

Diazepam Inhibits Reproduction and Reproductive Behavior of Oriental Hornet. A Possible Role for the Peripheral-Type Benzodiazepine Receptor

Jacob S. Ishay*, Elena Fuksman, Natalya Y. Ermakov and Marian Plotkin

Department of Physiology and Pharmacology, Sackler Faculty of Medicine,
Tel - Aviv University, Ramat - Aviv, 69978 Israel
**Author for correspondence. E-mail: physio7@post.tau.ac.il*

Abstract: Feeding of diazepam to young hornets completely inhibits or delays development of their ovaries for a relatively long period. In control hornets, the ovaries usually develop within a day or two post eclosion and comb building commences on the second day of life. The hornets then oviposit into the comb cells and the deposited ova give rise to larvae. Trials were performed on parallel groups of hornets of various ages. When the sedative diazepam was administered to hornets aged 0–24 hours the ovaries of these young hornets failed to show any development, so that no oocytes ripened and consequently there was no oviposition whatsoever. Neither were any comb cells built or, at best, only a few were built. When the diazepam was administered to hornet's being the age of 48 hours, it exerted no change, that is, the eggs developed normally and comb building was the same as in the control group. Longevity of hornets was uniform in all the test groups and similar to that in the control.

KEY WORDS: diazepam in hornets; diazepam inhibits fertility; social insects; hymenoptera; peripheral benzodiazepine receptor.

OUR LABORATORY has been engaged for many years in the study of social insects, specifically with social wasps and hornets, — that pose a danger to humans. Both bees and hornets sting, whereas some ants spray venom rather than sting. The mentioned social insects are highly sensitive to changes in their environment and are usually rendered aggressive upon such change. Consequently, we searched for a pharmacological material that would render the hornets with which we work more relaxed so that they could be more easily handled.

The Oriental hornet is widespread throughout Israel and is prevalent in the Mediterranean basin as well as in the near East, extending as far as India (Bodenheimer, 1933).

In the summer, the active season of this hornet, each hornet colony is comprised of a single queen, numerous workers and a brood within combs. The queens of hornets normally found a nest underneath the ground, which renders difficult the viewing of its interior. Details of nest activity have been collected mostly from laboratory observations on hornets maintained in breeding boxes, one wall of which is intentionally transparent. When hornet nests are collected from the field and brought to the laboratory, the brood combs from different nests are placed together in an artificial breeding box (ABB), whence there is daily eclosion of the young, be they workers in the months of July–September, or drones and queens during September–November. These newly ecloded hornets served in our experiments. Hornets from different colonies which eclode in the same ABB ordinarily are not aggressive toward one another (Ishay 1973). Our previous experience (Ishay and Sadeh 1975) has shown that groups of workers can be maintained on a diet of sugars, animal proteins (e.g., morsels of meat or fish) and drinking water, thus enabling a study of their development and social behavior.

Under the specified conditions, immediately after introduction into the ABB of young hornets aged 0–24 hours, one observed a typical pattern of behavior comprised of the following (Ishay 1975a,b; 1976): photophobia, wherein the hornets shun the illuminated area and congregate in shaded or dark areas; positive thigmotaxis, with the hornets congregating in group of 5–40 individuals; negative geotropism, the hornets seeking the highest point in the box. Thus the young hornets tend to remain upon the ceiling of the box for a day or two, during which time one of them occasionally descends to bring food for itself and the others as the need arises (Wheeler 1928; Duncan 1939; Ishay and Ikan 1968 a,b).

At the point beneath the roof of the box, where the hornets reside initially, the foundation for a pedicle is laid and subsequently a pedicle is built in the direction of the gravitational force. At the bottom of this pedicle cells are constructed which within a few days come to comprise a comb within each cell of which an egg is deposited and fastened to one of the cell walls so as to face down. The rate and quality of this comb construction can serve as criteria or markers in the various experimental groups. In the present study, we examined the influence of diazepam on the central receptor (CBR) associated with GABA (Abalis and Eldefrawi 1986) as well as on the peripheral benzodiazepin type receptor (PBR), (Snyder *et al*. 1987). The central receptors are among the most prevalent in the animal kingdom (Abalis *et al*. 1983; Eldefrawi and Eldefrawi 1987; Murphy and Wann 1988; Pinnock *et al.* 1988). These are the primary inhibitory receptors in the brain of vertebrates, exerting an effect on the Cl^- channels. Additionally there is the PBR of importance in the steroidogenesis (Besman *et al*. 1989; Weizman *et al*. 1989; Paradopoulus *et al*. 1991) and a variety of other functions (Gavish *et al*. 1999, Veeman and Gavish, 2006). High concentrations of this PBR, known as the mitochondrial benzodiazepine receptor (MBR), are encountered mostly in steroidogenic tissues.

The points which the present study set out to ascertain or explore were the following:

- Motor activity — do the test hornets fly, walk or congregate in a manner, speed and localization different than those of control hornets?
- Comb building — knowing that hornets build a comb within a day or two of their introduction into the ABB, does diazepam alter this activity, possibly in the direction of fewer cells or slower rate of building?

- Orientation (directionality) — since hornets seek the apex of the ABB (negative geotropism) and prefer shaded or dark areas (photophobia), does diazepampossibly alter this traits?
- Social activity — inasmuch as hornets initially exhibit gregariousness (positive thigmotaxis) lasting several days, is this changeable by diazepam?
- Fecundity — as is known, worker hornets lay an egg (unfertilized) in each cell of the comb which they build under laboratory conditions in the absence of the queen. After 5 days, each egg hatches a larva, which ultimately develops into a drone. Does diazepam exert any qualitative or quantitative changes in this pattern of activity?
- Aggressiveness — hornets are predatory organisms and this trait is assessable by the introduction into the ABB of bees, which in the field are preyed upon by them. How is this aggression affected by the administration of diazepam?
- Longevity — are there any changes in the life expectancy of hornets receiving diazepam as compared to control hornets?
- Effect of Age — is age of hornets an important determinant in trials with diazepam?

Materials and Methods

Diazepam (Assival, Teva Co., Israel) was available in ampoules 10 mg/2 ml. The material is miscible in water. The basic daily dose of diazepam was 17μg per hornet, but we also tested an one and a half of 35μg as well as half a dose comprising 8.5μg.

As the Test Animal for laboratory trials, we used the Oriental hornet *Vespa orientalis* (Vespidae, Hymenoptera). Hornet nests were sought in fields in the Tel - Aviv area as well as at Ein - Gedi, during the active season of this insect which is the summer months of June-July-August. Collections were made in 1993 and 1994. The nests were slightly anesthetized at various hours of the day by the use of diethyl ether, and then dug out of the ground, and the adult hornets extracted from the combs. These brood containing combs (larvae and pupae) were then transported to the laboratory. From the enclosing brood, groups of 10 workers each were placed in the special hornet breeding boxes devised in our laboratory and long in use in our experiments. We named these boxes artificial breeding boxes (ABBs) and each has a volume of approximately 13600 cm^3 and one transparent glass wall. The hornets placed in each ABB were of a uniform age. The diazepam solution was absorbed into a sugar cube and was then given to the hornets from the first day of their stay in the ABB, together with tap drinking water and bits of fish or meat.

Vespine response to external stimuli was assessed separately for acoustic stimuli (e.g., tapping on the ABB), optic stimuli (e.g., waving of the hand in front of the glass panel of the ABB), light stimuli (e.g., shining a light into the ABB) and a gravitational stimulus (e.g., altering the vector of the gravitational direction in static fashion).

Fertility of the hornets was assessed in view of the likelihood that administration of diazepam to the hornets might result in partial or complete delay in the development of their ovaries. We suspected that in hornets more than 24 hours past eclosion, whose ovaries had already commenced functioning the drug administration, might cause ovarian regression or delay in development. This possibility was investigated in two ways: a) by

observing the ovipositing by hornets and looking out for any changes in the rate or amount of this ovipositing (versus the control groups); and b) by studying the ovaries of the hornet, that is, by dissecting the abdomen of test hornets so as to ascertain the presence of ovaries and their degree of development. The dissection was carried out with standard surgical instruments and the observations proper were made under stereoscopic dissecting microscope at x10 - x40 magnification.

Statistics: the life expectancy was calculated using the Log Rank method. Analysis of survival Log Rank and Wilcoxon (Sun *et al*. 2005; Hasegawa Eng and Kosorok 2005). By this method 6 control groups longevity is compared to 6 test groups longevity. Using the following formula if χ^2 is 3.85 or larger only then there is a significant difference between the two groups.

Results

The present study entailed initially two series of experiments using diazepam, namely, experiments with juvenile hornets, whose results were significant and are given herein, and experiments with adult hornets, which yielded the same results in test and control hornets and were therefore omitted from this paper.

The juvenile hornets, aged 0–24 hours, were given diazepam while kept in ABBs.

Regular hornet behavior within an ABB has been reported previously in numerous publications and is characterized by typical behavioral traits. Following, however, is a description of the behavior of hornets that had been given diazepam, as broken down to specifics:

1. ***Food consumption*** — each hornet was free to eat *ad libitum.* The amount of protein (fish or meat) consumed was apparently equal for diazepam-administered hornets and control hornets. Likewise, also, the amount of water imbibed by the test and control hornets. There was, however, a significant difference in the amount of sugar consumed, in that control hornets each consumed about 37 mg of sugar per day, whereas the sugar uptake of test hornets was only 18 mg per day. The statistical data showed a mean daily uptake of 37±1.07 mg by control hornets versus 17.8±0.7 mg for test hornets, with n=8, t=4.18, DF=14, p value<0.001. The difference here is statistically significant.
2. ***Motor activity*** — this was assessed by the following criteria:
   a. **Walking ability** and approach to food, regarding which we found that test hornets receiving diazepam from eclosion freely approach the food, their walking ability seemingly unimpaired, but they tended to rest for longer periods than did control hornets, were generally less mobile and mostly came to rest on *the walls of the ABB* rather than on the ceiling, as customary;
   b. **Flight capability** — an important feature affecting also the building capacity – regarding which we did not find diazepam to alter either the capacity proper or the speed of flight;
   c. **Hornet orientation**, which was adjudged by the following sub-criteria: photophobia – hornets normally seeking shaded or dark areas, and this trait was unal-

tered by diazepam administration; negative geotropism – hornets normally settling at the zenith of the ABB, but after diazepam administration we found some hornets settling on the walls of the ABB rather than at the zenith underneath the roof of the ABB, which means that some hornets exhibited also *positive geotropism* in the wake of diazepam treatment;

d. **Hornet social activity** — here we observed a change in the customary thigmotaxis, wherein after their introduction into the ABB they no longer congregated at one spot but rather "sat" quite apart from one another, so that there was clearly a change in their social behavior following diazepam treatment, leading to *negative thigmotaxis*;

e. **Comb building** — this is one of the important criteria of hornet behavior. This trait also renders hornets suitable for experimentation in that other species of social wasps (Vespinae) refrain from building, usually, under laboratory conditions. Our observation of comb building conveyed several aspects of the building, and these are briefly summarized below:

Onset of building – the building in an ABB usually commences 24 hours after introduction of the hornets into the ABB, these we found that for control hornets the mean building commencement was 1.8±0.6 days for n=7, versus a mean of 8.2±4.3 days for test hornets, the difference being statistically significant, at t=4.56, DF=18, p value <0.001. Our results indicated that onset of building was considerably delayed in the test groups compared to the control.

Rate of building – here, too, the rate of comb building was markedly different between the test and control groups. Control hornets started with the comb pedicle and immediately after proceeded to build cells as usual till a complete comb was obtained. Test hornets, as already mentioned, commenced building much later, *if at all*, and even then built only a limited number of cells. Moreover, the rate of building was slow and in most instances only a single cell was built (Figure 1).

(A) **(B)**

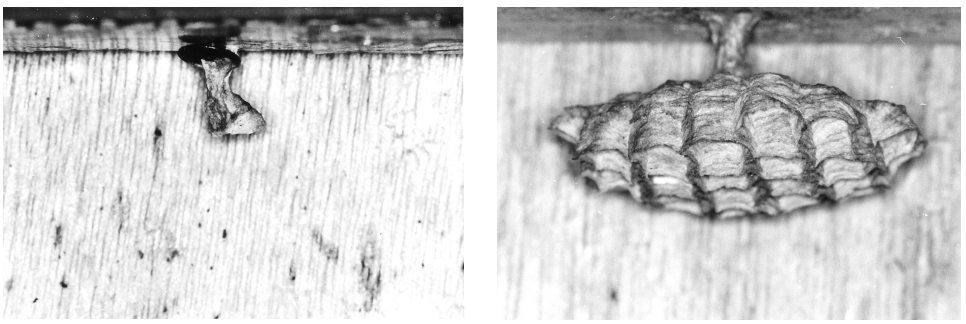

FIGURE 1. Total number of cells built by juvenile hornets receiving Diazepam (A), as compared to control hornets (B). As can be seen the test group has built only one cell while in the same time the control group has built a comb comprising about 28 cells, and in each cell an egg or a larva can be seen.

The number of cells and their shape – the quality of cells built by test hornets throughout their life span was statistically different from that by control hornets (Figure 2). The same number of ABBs (10) was used for test hornets and the population of hornets in both cases was randomly collected as eclosing juveniles.

The mean overall number of cells built by test hornets was 4.8±4.1 whereas the control group built an overall mean of 22.8±5.5 cells. In both cases n=10 and the difference was statistically significant at t=8.20, DF=18, p value<0.001.

The shape of cells built was identical in both cases being a well-developed hexagon and, in both, the direction of building was towards the gravitational force.

f. **Hornet fertility** — this was assessed following prolonged diazepam treatment lasting 2–4 weeks. At the end of this period, the test and control hornets were etherized and dissected to reveal presence of eggs inside the abdomen and the extent of development of the ovaries and ovarioles. The selection of hornets for dissection was random and the results of this experiment are given in Figure 3, which shows significant difference in ovarian development between test and control hornets. In fact, control hornets displayed considerable ovarian development whereas the ovaries of hornets receiving diazepam for two or four weeks were

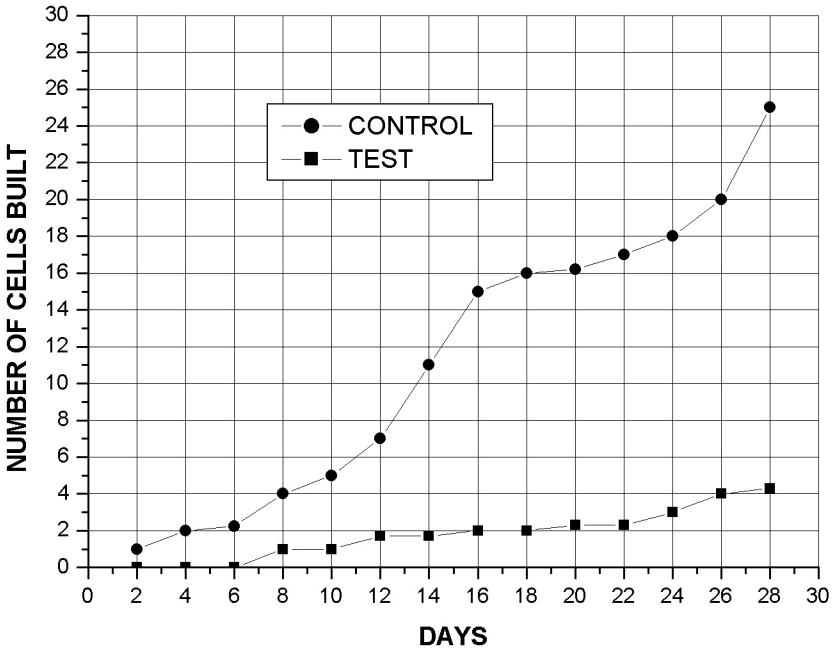

FIGURE 2. Number of cells built per day by test hornets (test), versus control hornets (control). As can be seen control hornets build 25 cells in 28 days, whereas test hornets only built 4 cells in 28 days.

not developed at all. Further comparison between the test and control hornets revealed the following differences:

a) the ovaries and ovarioles in control hornets were easily detectable because they were filled with eggs, some of which measuring 2 mm in length, were already suitable for ovipositing. Contrariwise, in test hornets receiving diazepam for 2 weeks, the ovaries were not discernible to the naked eye and only with the aid of a dissecting microscope at x40 magnification could the ovaries be identified as very minute structures not at all developed compared to their contemporary control hornets.

   Hornets receiving diazepam for a full month yielded the same results, namely, their ovaries could only be seen with a 2.5x10 or 4x10 magnification. In fact, their ovaries were undeveloped, and only in few instances could any onset of development be discerned;

b) in the control hornets, the number of eggs in the ovaries ready for ovipositing was 8–10 per hornet, whereas in test hornets no such ready eggs were detectable and only at x25 or x40 magnification could a single egg be discerned in a few of the hornets.

g. **Aggression** — aggressive behavior is natural in hornets and they are known to attack spontaneously other insects, particularly honey bees at the hive entrance or in the open field (Ishay *et al*. 1967). This aggressive behavior is observable

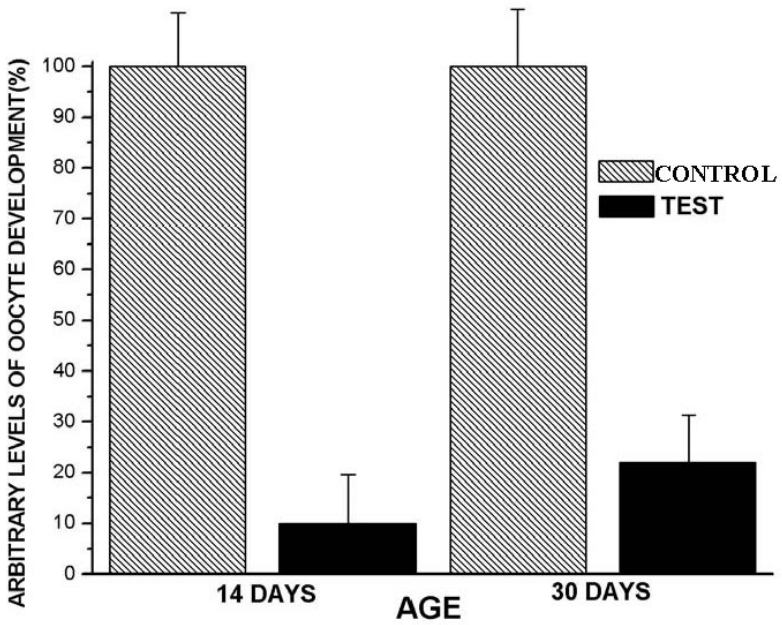

FIGURE 3. Extent of ovarial development in juvenile hornets receiving Diazepam (test), versus control hornets (control). Test hornets showed 10% and 20% of the number of oocytes of the control hornets after 14 days and 30 days of age, respectively.

under laboratory conditions by the introduction of bees into the hornets ABBs, and one can immediately see whether diazepam affects, this aggressive behavior towards bees. As it turned out, diazepam exerted no effect on aggression of the Oriental hornet, so that the introduced bees were set upon within 5 seconds of their introduction, being consumed to the same extent by test hornets as by the control hornets.

h. **Life span** — the life expectancy of the test and control hornets was computed by the Log rank method, basing on mean mortalities within six control and six test groups. Using the appropriate equation we obtained the following result:

$$\chi^2 \ (7–5.09)^2 / 5.09 + (2–5.09)^2 / 5.09 \ ]$$
$$\chi^2 = 2.58$$

by this Log rank method, the difference in longevity is significant when $\chi^2>3.85$, which means that in our case there was no significant difference between test and control hornets.

i. **After-effect of diazepam treatment** — we attempted to ascertain whether there were after-effects in hornets upon cessation of a prolonged treatment with diazepam. To this end, test hornets ceased getting diazepam after 10 days of continuous administration. We found that while on diazepam, these hornets failed to build cells or oviposit, much the same as all the test hornets receiving diazepam throughout their existence. However, one day after the withdrawal of diazepam, the hornets commenced building a comb pedicle and subsequently built a complete comb comprised of 10–14 cells, that is a comb fully consistent in terms of number and shape of cells to the comb built by control hornets.

j. **Effect of diazepam dosage** — most groups of juvenile test hornets received diazepam at a mean daily dosage of 17 mg per hornet. To assess the effect of dosage, three-test groups were placed on half this dosage (8.5 mg/ hornet / day) and three more groups on x1.5 the usual dose (25 mg/ hornet / day). The results showed that at a dose of 8.5 mg the hornets delayed their comb building activities, commencing to build only on the 9th day and building only on average 12 cells, throughout life, whereas "their" control hornets commenced building on the second day after their introduction into the ABB and built, on the average, a total of 30 cells throughout life. Apart from that, the test hornets built and oviposited similarly to the control hornets. In test hornets receiving 1.5 times the usual dose, however, the results were more dramatic, in that they failed to build altogether, they did not oviposit and apparently, also, this dosage was toxic to the hornets, because they started dying off between the third and tenth day after receiving this high dose and most of them succumbed to the drug.

k. **Gravity discernment** by test hornets in ABBs tilted 15° from the vertical orientation — an experiment was set up to investigate the ability of diazepam — treated hornets to recognize the zenith within the ABB and build in the direction of the gravitational force (i.e., vertically) even when their ABB is tilted by 15° from the gravitational direction. In the control ABB, the building of a comb ultimately comprised of many (17–30 cells approx.) cells commences on the second day of life of control hornets and this comb is usually built in the direction of earth's gravitational pull. On the other hand, the test hornets in the tilted ABB commenced building only on the 10th day of their stay in the ABB, and their

comb, which was built on the glass test tube (that provides drinking tap water in every ABB), was comprised of 2 cells only, albeit the orientation of these two cells was in the direction of gravity, just as in the control ABB. This latter result seems to indicate that the gravitational sense of the hornets is not impaired by diazepam. In a final experiment, we found that adult (more than 48 hours of age) hornets receiving diazepam, were not significantly affected either in behavior or in fecundity.

Discussion

The present study examined various properties typical of Oriental hornet behavior and development and their response to prolonged administration of diazepam, which is an agonist to both the central and peripheral benzodiazepinic receptor(s). Interestingly, this study was undertaken in the hope that diazepam might render hornets less aggressive or at least tranquilizing. In fact, our finding that hornets consume less sugar under the influence of diazepam reaffirmed our belief that diazepam should have a tranquilizing effect on hornets. Much to our surprise this seemingly did not transpire as was shown by the hornets response to the honeybees. In the final analysis, the most significant finding of the present study is the inhibitory effect of diazepam on the ovarian development, ovulation and fecundity of hornets subjected to this drug from their first hours of life. As we have shown the ovaries of the treated hornets were not as developed as they should have been for their age and treated hornets for the most part failed to oviposit altogether. Our findings suggested that diazepam exert an effect on the PBR (Gavish *et al*. 1992). As we deal with a benzodiazepine receptor we have the fact that the delaying effects of diazepam on the fecundity and ovulation were reversible, in that test hornets commenced ovipositing upon cessation of diazepam administration.

A few tissues in insect are recognized to be responsible for the synthesis of hormones (Rockstein 1973; Warren *et al*. 1988). One of these hormones, known to affect insect fecundity is the juvenile hormone, which is gonadotropic in its effect, as provable by transplantation of the corpora allata from one insect to that of another. Other agents are the prothoracic glands, which secrete ecdysone that apparently mediates the suppression of ovulation in insects (Whitehead *et al*. 1986). This ecdysone, which is steroidal in structure is produced from cholesterol and, *inter alia*, enhances the synthesis of RNA. As known, RNA synthesis is periodic, in accordance with the biotic requirements of the insect (Raabe 1989). Furthermore, cerebral hormones (secreted by neurosecretory cells) are known to stimulate the synthesis of ecdysone, as the need arises. A possible explanation for this could be that in queenless hornets there is *ab initio* stimulation of the various tissues that secrete ecdysone by cerebral hormones (e.g., ovaries), (Adams and Filipi 1988; Raabe 1989). Our results suggest that at this stage diazepam, apparently, binds onto the external membrane of mitochondria in enhanced amount thereby effecting, upon prolonged administration, a desensitization of these receptors. Consequently, cholesterol fails to enter the mitochondria in the needed level so that insufficient or no ecdysone is produced, such as required for the synthesis of DNA and RNA or the development of the eggs. Regrettably, we were unable to determine the level of this hormone in hornets. The question arises as to why hornets of more advanced age are not thus affected. We suggest that at a later stage in hornet life, the level of ecdysone in the hemolymph is sufficiently high to abrogate or markedly curtail the influence of diazepam.

A further finding with juvenile hornets was that under diazepam treatment they were late in starting to build a comb or failed to do so altogether. This finding is explainable in two ways. First, that in juvenile hornets one of the triggers to building is the need to oviposit, and as we have seen, in hornets not subjected to diazepam ovarial development commences right after eclosion from the puparium, so that on the second or third day of life, normal hornets start building a pedicle and first cells, with the trigger to this provided by the need to oviposit owing to rapid ovarial development and the accumulation of eggs inside them. Contrariwise, the suppression of ovulation by diazepam delays the stimulus to comb building and this effect is apparently exerted on the peripheral receptor. A second explanation for the delay in or absence of building by diazepam-treated juvenile hornets could be the detrimental changes in their motor activity. Yet these changes can provide only a partial explanation in that they account for the delay in building but not for the total absence of building activity. Here we suspect that there is influence of diazepam on the central receptors.

As pointed out, test hornets received diazepam (liquid) absorbed into a sugar cube, and our observations on food consumption by test hornets showed a reduction in sugar intake, apparently owing to the drug exerting a repelling effect on the hornets. Our choice of sugar for purpose of drug administration resided in the high absorbability of liquid diazepam upon it and the fact that it is sweet and thus masks the apparently repulsive taste of the diazepam. Another "substrate" for the diazepam which we considered using was the bits of fish / meat offered as protein food to the hornets. We discarded this possibility, however, on the grounds that the presence of diazepam on this foodstuff could deter the hornets from consuming protein and thereby impair their fecundity (having found that protein was essential during hornet ovarian development and ovulation).

To the best of our knowledge this is the first report on diazepam affecting ovulation and egg lying in insects. It is of interest to mention that this phenomenon discovered in hornets resembles in some way what happens some times in women where "menstrual irregularities have been noted, and women may fail to ovulate while taking benzodiazepines" (Baldesarini and Tarazi 2001). In rats it has been shown that PBR may be involved in ovulation and pregnancy (Bar Ami *et al*. 2006).

The results of diazepam treatment in hornets were reversible, so upon cessation of diazepam administration, the test hornets resumed normal building and oviposition. Interestingly, despite the influence of diazepam on various aspects of hornet behavior and fecundity, there was no evident effect on hornet longevity. This latter finding could be attributable to the fact that in the natural nest, hornet workers usually do not have a chance to oviposit. The presence on an egg-laying queen inhibits ovary development by workers excepting in cases of orphan nests (i.e., where the queen has died early in the season), so that the oviposition by workers is a phenomenon strictly associated with the end of the season — or life in captivity, and therefore there is no correlation between oviposition and hornet longevity.

References

Abalis, I.M., Eldefrawi, M.E. and Eldefrawi, A.T. (1983) Biochemical: Identification of putative GABA/benzodiazepine receptor in house fly thorax muscles. *Pestic. Biochem. Physiol. 20:* 39–48.

Abalis, I.M. and Eldefrawi, A.T. (1986) [-H] Muscimol binding to a putative GABA receptor in honey bee brain and its interaction with avermectin B. *Pestic. Biochem. Physiol. 25:* 279–287.

Adams, T.S. and Filipi, P.A. (1988) Interaction between juvenile hormone, 20-hydroxyecdysone, the corpus cardiacum-allatum complex, and the ovaries in regulating vitellogenin levels in the housefly, *Musca domestica*. *J. Insect Physiol. 34(1):* 11–19.

Baldesarini, R.J. and Tarazi, F.I., (2001) Drugs and the treatment of psychiatric disorders. Psichosis and mania. In: *Goodman & Gilman's. The Pharmacological Basis of Therapeutics*. 10th Ed., Hardman J.G., Limbird L.E., editors. New York: McGraw-Hill, p 507–511.

Bar-Ami, S., Bendel, N., Leschiner, S., Levin, E., Veenman, L. and Gavish, M. (2006). The effects of prostaglandin F2alpha treatment on peripheral-type benzodiazepine receptors in the ovary and uterus during pseudopregnancy of rats. *Biochem. Pharmacol. 71(4):* 472–478.

Besman, M.J., Yanagibashi, K., Lee, T.D., Kawamura, M., Hall, P.F. and Shively, J.E. (1989) Identification of des-(Glu-Ile)-endozepine as an effector of corticotropin-dependent adrenal steroidogenesis : stimulation of cholesterol delivery is mediated by the peripheral benzodiazepine receptor. *Proc. Natl. Acad. Sci. USA 86:* 4897–4901.

Bodenheimer, F.S., (1933) Uber die aktivitat von *Vespa orientalis* F. im Jahresverlauf in *Palaestina. Zool. Aus. 102(5–6):* 135–140.

Duncan, C. (1939) A contribution to the biology of North American Vespine Wasps. *Stanford Univ. Publ. Biol. Sci. VIII:* 1–272.

Eldefrawi, A.T. and Eldefrawi, M.E. (1987) Receptor for g-aminobutiric acid and voltage-dependent chloride channels as targets for drugs and toxicants. *FASEB J. 1(4):* 262–271.

Gavish, M., Bachman, I., Shoukrun, R., Katz, Y., Veenman, L., Weisinger, G. and Weizman, A. (1999) Enigma of the peripheral benzodiazepine receptor. *Pharmacol. Rev. 51(4):* 629–650.

Gavish, M., Kats, Y., Bar-Ami, S. and Weizman, R., (1992). Biochemical, physiological and pathological aspects of the peripheral benzodiazepine receptor. *J. Neurochem. 58(5):* 1589–1601.

Hasegawa Eng, K. and Kosorok, M.R. (2005) A sample size formula for the supremum log-rank statistic. *Biometrics 61:* 86–91.

Ishay, J. (1973) The influence of cooling and queen pheromone on cell building and nest architecture by *Vespa orientalis* (Vespinae, Hymenoptera). *Insectes Sociaux 70(3):* 243–252.

Ishay, J.(1975a) Caste determination by social wasps: Cell size and building behavior. *Anim. Behav. 23*: 425–431.

Ishay, J. (1975b) Hornet nest architecture. *Nature 253:* 41–42.

Ishay, J. (1976) Comb building by the Oriental hornet *Vespa orientalis. Anim. Behav. 24(1):* 72–83.

Ishay, J. and Ikan, R. (1968a) Food exchange between adults and larvae in *Vespa orientalis. Anim. Behav. 16(2–3):* 298–303.

Ishay, J. and Ikan, R. (1968b) Gluconeogenesis in the Oriental hornet (*Vespa orientalis*). *Ecology 49*(1): 169–171.

Ishay, J. and Sahed, D. (1975) Direction finding of hornets under gravitational and centrifugal forces. *Science 190(4216):* 802–804.

Ishay, J., Bytinski-Salts, H. and Shulov, A. (1967) Contributions to the bionomics of the Oriental hornets *Vespa orientalis. Israel J.Entomol. II:* 45–106.

Murphy, V.F. and Wann, K.T. (1988) The action of GABA receptor agonist and antagonist on muscle membrane conductance in *Schistocerca gregaria. Br. J. Pharmacol. 95(3):* 713–722.

Paradopoulos, V., Bercovich, A., Krueger, K.E., Costa, E. And Guidotti, A. (1991) Diazepam binding inhibitor and its processing product stimulate mitochondrial steroid biosynthesis via an interaction with mitochondrial benzodiazepine receptor. *Endocrinology 129(3):* 1481–1488.

Pinnock, R.D., David, J.A. and Sattelle, D.B. (1988) Ionic events following GABA receptor activation in an identified insect motor neuron. *Proc. R. Soc. London (Biol) 232(1269):* 457–470.

Raabe, M. (1989) R*ecent Development in Insect Neurohormones.* Plenum Press, New York.

Rockstein, M. (1973) *The Physiology of Insecta*, Chapter 1. Academic Press, New York, pp 271–274.

Snyder, S.H., Verma, A. and Trifiletti, R.R. (1987) The peripheral-type benzodiazepine receptor: a protein of mitochondrial outer membranes utilizing porphyrins as endogenous ligands. *FASEB J.1*: 282–288.

Sun, J., Zhao, Q. and Zhao, X. (2005) Generalized log-rank tests for interval-censored failure time data. *Scandinavian Journal of Statistics 32:* 49–57.

Veenman, L. and Gavish, M. (2006) The peripheral-type benzodiazepine receptor and the cardiovascular system. Implications for drug development. *Pharmacol. Ther. 110(3):* 503–524.

Warren, J.T., Sakurai, S., Rountree, D.B. and Gilbert, L.J. (1988) Synthesis and secretion of ecdysteroids by the prothoracic glands of *Manduca sexta. J. Insect Physiol. 34(7):* 571–576.

Weizman, R. and Gavish, M. (1989) Chronic diazepam treatment induces an increase in peripheral benzodiazepine binding sites. *Clin Neuropharmacology 12:* 346–351.

Wheeler, W.M. (1928) *The Social Insects: Their Origin and Evolution*. London: Kegan Paul, Trench, Trubner and Co LTD, 1–378.

Whitehead, D.L., Osir, E.W., Obenchain, F.D. and Thomas, L.S. (1986) Evidence for the presence of ecdysteroids and preliminary characterization of their carrier proteins in the eggs of the brown ear tick *Rhipicephalus appendiculatus* (Neumann). *Insect. Biochem. 16(1):* 121–133.

Received March 14, 2006;
accepted May 1, 2006.

Physiol. Chem. Phys. & Med. NMR (2006) *38*: 43–54

MRI of Oriental Hornet Head

Marian Plotkin[1], Arnon Neufeld[2,3], Natalya Y. Ermakov[1], Stanislav Volynchik[1], David J. Bergman[4], Gil Navon[2] and Jacob S. Ishay[1*]

[1]*Department of Physiology and Pharmacology, Sackler Faculty of Medicine,*
[2]*School of Chemistry (NMR) and* [3]*The Wohl Institute for Advanced Imaging.*
Tel Aviv Sourasky Medical Center, [4]*School of Physics and Astronomy,*
[2,4]*Raymond and Beverly Sackler Faculty of Exact Sciences,*
[1,2,3,4]*Tel Aviv University, Ramat Aviv, 69978, Israel.*
**Address for correspondence. E-mail: physio7@post.tau.ac.il*

Abstract: The head of the Oriental hornet *in situ*, detached from a live sample was imaged using Magnetic Resonance Imaging (MRI). This non-invasive method enabled us to visualize the three-dimensional structure of the hornet's brain and intracerebral organs, as based on cubic voxels of 23 μm^3. From these images, we could identify various cephalic structures in both supra-esophageal and sub-esophageal locations. In the former location, we identified and visualized the ocelli, ommatidia, mushroom body, lobula, medulla and the compound eyes in the protocerebrum, as well as the olfactory lobe and bases of the antenna in the deutocerebrum, while in the sub-esophageal region we visualized organs such as the mouthparts, the esophagus, the gnathal pouch and the salivary ducts that empty into the region. Additionally, we identified various muscles, the aorta, cuticular thickenings lending support to the interior of the head and also the cuticular skeleton providing support on the outside. All the mentioned structures and organs were visualized in their relative, normal proportions, without touching or dislocating them.

KEY WORDS: hornet brain, MRI, hornet cerebral structures, Vespinae Hymenoptera.

MAGNETIC RESONANCE IMAGING (MRI) has the advantage of being a non-destructive technique and enables one to obtain three dimensional images. Its main drawback relative to optical microscopy methods is its limited resolution. In the present work we minimized this limitation by equilibrating the sample with a solution containing the paramagnetic Cu^{2+} ions. The head of the Oriental hornet contains beneath the frons plate an organ that contains about 120 nervous strings (1). This organ with its strings is immersed in hemolymph and has been named the Ishay organ (Figure 1A–D). In another publication (2), we detected and described in vespan cephalic sections, uninterrupted

stretches of cilia also in the region behind the genal and vertex plates, and also focused on the structure of these cilia and their possible connection with gravity and the Ishay organ (Figure 1E). Under this area one can see transverse section through the hornet's head (Figure 1F). Descriptions of the head of the wasp and hornet from cephalic or caudal aspects exist in the literature, but are based on coarse sections (3–6) and consequently are not sufficiently detailed. There is, however, a recent study of the head of the honeybee *via* the NMR methodology (7). As we shall show later in the present paper, there are structural differences between the head of the honeybee and that of the hornet among others because the hornet is a relatively big predatory insect, while as known the bee is smaller and vegetarian. Additionally, we need mention an excellent study on the micro-anatomy of a mosquito (8).

In the present study, reliance was made on numerous earlier publications on the structure of the neural system in invertebrates (9–15).

When one sets out to identify head parts of the hornet from the outside (see legend to Figure 1) one can see (Figure 1A), the following: ocelli (1), compound eyes (2), the frons plate (3), and in the center of the latter — the sutura coronalis (4) with a pit that forms a deep indentation on the one side and a projection on the other (see large arrow in Figure 1B). To the frons plate are attached nerve fibers that also connect to the protocerebrum (Figures 1C, D) and this on the plate between the antennae and the compound eyes.

In the present study we shall describe step by step the anatomical details (relating to the hornet's head) that could be gleaned by use of MRI.

Materials and Methods

For purposes of the present study the heads of queens of the Oriental hornet *Vespa orientalis* (Vespinae, Hymenoptera) were used. The queens were collected from a natural nest by a method published earlier (16, 17). In total 11 queens were used. The head of a hornet queen is bigger (mean 8×6 mm) than that of the worker (mean 5×4 mm) and efficiently fills the inner volume of the MRI coil (designed to hold samples in 10 mm tubes). Thus, better sensitivity results. The heads were cut off from ether anesthetized hornets. (The hornet is alive during the process.) To avoid mass hemolymph loss the wound was sealed with melted wax. To enable minimal field of view (FOV), the antennae of each queen specimen were fastened by cyanoacrylate- glue to the side of the head rather than cut off, and this in order to prevent the loss of hemolymph incurred by excision. In the few instances where we failed to obtain complete images by MRI, supplementary images were obtained *via* scanning electron microscopy (SEM). See Figure 1(A–F); Figure 2(A); Figure 3(A1,A2).

The factor limiting the rate of imaging in MRI is the longitudinal relaxation, represented by the time constant T_1. In order to achieve a major reduction in the total experimental time, we chose to equilibrate our sample for two days in a solution of 40mM $CuSO_4$ that reduces T_1 from 1.5 sec to 0.2 sec (as measured by the inversion-recovery method), thus reducing the total experimental time by a factor of more than seven (18, 19). $CuSO_4$ is superior to Gadolinium complexes (such as Gd-DTPA) since it easily diffuses to all tissues and biological compartments. Due to its toxicological properties $CuSO_4$ prevents the hornet tissues from deterioration due to bacterial infection.

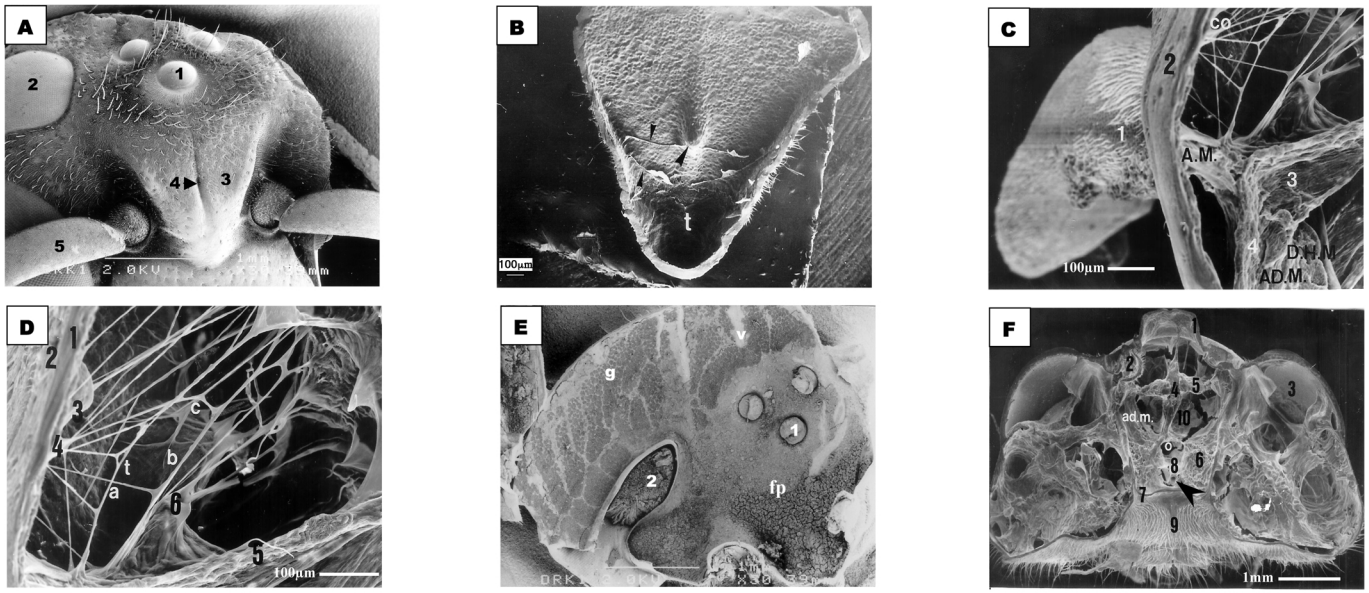

FIGURE 1. (A) (*via* SEM)-The head of a hornet worker: 1-ocelli, 2-compound eyes, 3-frons plate and 4-the sutura coronalis. At the center, one can see a pit that forms a deep indentation (arrow), 5-antenna. Bar = 1mm. (B) The frons plate viewed from the inside: large arrow - the pit, small arrows - membranes of "acoustic box", and t-trachea. Bar = 100µm. (C) A portion (1) of the "acoustic box" connected to the right antenna and showing: the base of the antenna connected to the juncture of the frons (2) - criss-crossing muscles that forms the center of the muscular structure in the area (3). A branch of the these muscles connecting to the lower mouthparts (4). A.M - the muscles of the antenna, D.H.M - dorsal hypopharyngeal muscle, and AD.M - adductor mandibularis. Bar = 100µm. (D) Dynamic fibers in the lower part of the "acoustic box" are shown: 1-external surface of the frons plate; 2-the sutura coronalis; 3-several fibers originating from the conus; 4-a central point from which 6 fibers emerge; 5-horizontal (transverse) fibers that attach both to the 6-masticatory muscles and the tritocerebrum; a, b-two horizontal fibers to which the six vertical fibers attach and form a unique hand-shaped complex; c-cross links between the fibers in the complex; t-a minute triangle formed by one of the horizontal fibers, and possibly intended to reinforce the complex. Bar = 100µm. (E) Details of the interior of the head showing frons plate area (fp) covered with hair cells, mostly arranged in circular groups. The ocelli (1) and part of a compound eye (2) are also observable. g = genae; v = vertex. Bar = 1mm. (F) Transverse section through the base of the "acoustic box" viewed from below. The brain capsule is supported by the tentorial bridge (7) and toward the bottom one sees the postocciput (9). Above the tentorial bridge, at center, there is a round aperture, which is the aorta (8 arrow head). Further upward there is the cerebral ganglion (6), an expended hollow which is the dilation of the esophagus within the occipital foramen (o). On both sides of the occipital foramen are located the adductor mandibularis (ad.m.) muscles, and above them are criss-crossing muscles which interconnect the pharyngeal muscles (4). In the space between the two bundle of muscle fibers, there are vestiges of a membrane (10) which 'seals' the "acoustic box" from below. In the upper part of the Figure, one sees the 'pocket' formed by broadening of the frons plate near its base (adjacent to the clypeus). On both sides of the frons there are vestiges of the antennal bases (5), and at upper margin of the Figure on both sides, are the plates of the compound eyes (3), the antennal base (2) and the frons plate (1). Bar = 1mm.

We chose to use a three-dimensional spin-echo sequence where, following each excitation of the entire sample, phase is encoded in two orthogonal directions and frequency is encoded along the third. This was found superior to exciting discrete slices whose width is of the desired resolution in one dimension (23 μm). The rationale here was that gradient strength is limited and one needs to use long slice-selecting pulses, resulting in a further increase in the echo time (TE) and hence in a major signal decay due to transverse relaxation (T_2). Due to this limitation (7), those who preferred to excite discrete slices could not reduce slice thickness to less than 100 μm which compromised the resolution in the slice plane (15.6 μm^2).

All spectroscopy and imaging experiments were performed on a Bruker AVANCE 360 WB spectrometer, using a micro-imaging probe equipped with a 180 gauss/cm gradient unit. The samples were immersed in Flourinert (FC-77, Sigma, USA) to improve static field homogeneity and placed in a 10 mm tube at approximately 22 °C. 90° (hard). Pulse was 16 μs long.

FOV = 6×12×12 mm^3, matrix = 256×512×512 pixels, resulting in a resolution of 23 μm in all three dimensions. TE = 2.593 ms. Time to return (TR) = 210 ms. Bandwidth = 166.666 Hz. A total of seven signal acquisitions were averaged over 107 hours.

Results

The current MRI resolution does not enable visualization of minute objects (under 23 μm) such as the nervous strings in the Ishay organ, but the use of sequential imaging may allow us to determine the orientation of this organ relative to the surrounding structures and organs. In Figure 2A, we see, on top left, a schema of the queen's head, wherein the following landmarks can be discerned. First, the anterior surface of the capsule of the Ishay organ (1), (the arrow pointing to the pit).

In inset on bottom right of Figure 2A, we show the aftermath of the injection of liquid acrylic into the cavity of the acoustic box (which houses the Ishay organ), namely filling up of the box with a rapidly hardening material. The pit (see arrow) is a continuation of the cone shown in Figure $1A_4$ or 1B (large arrow). The next 5 images (B to F) in Figure 2 are sequential in the coronal (frontal) plain. Thus Figure 2B shows the pit, which is a continuation of the conus (see arrow) and also the gnathal pouch, an antenna, and the Ishay organ. Figure 2C is the sequential section showing the Ishay organ and the gnathal pouch, an antenna while the triangular structure represents the tentorial arms. Figure 2D shows additionally the pharyngeal pegs, while in this picture as well as in Figures 2E, 2F we also see the pharyngeal diverticula. In the latter two pictures can also be seen the sectioned esophagus. Note that in all pictures pertaining to Figure 2, the Ishay organ is seen as a rough rectangle, while in plates E and F we can also see the compound eyes additionally to an antenna and the mandibles.

Turning now to Figure 3, which again presents pictures of a queen's head, we need to explain that due to insufficient resolution of images *via* MRI, we offer first (in Figure 3A) two views of the pertinent head organs taken *via* SEM. Now for the images attained via MRI: In Figure 3B can be seen an antenna in full length, compound eyes, mandible, gnathal pouch, mouth, esophagus and pharyngeal pegs. The two circles at top are α lobes and the two circles somewhat below them are olfactory lobes. At the center top there is the pars intercerebralis and at the top also the basis of the median ocellus.

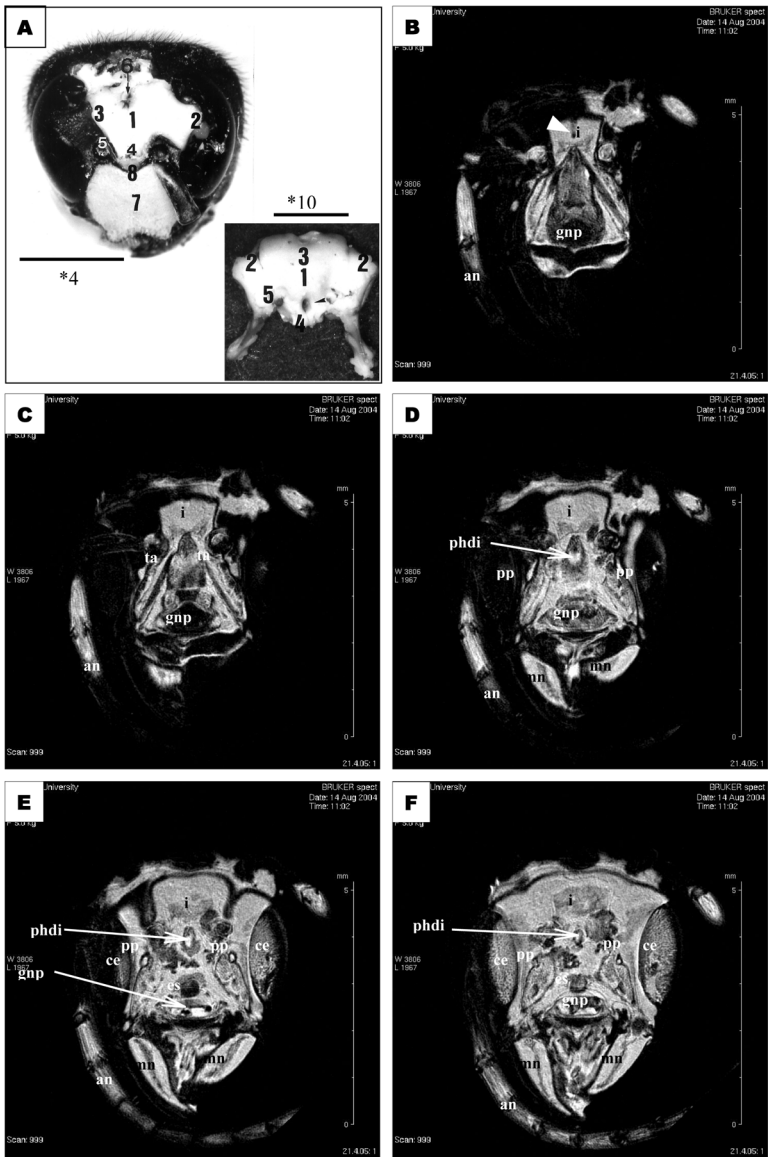

Key to MRI plates

αl, α lobes
an, antenna
ao, aorta
ar, antennal ridge
cb, central body
ce, compound eye
cp, corpora pedunculata
es, esophagus
gl glossa
gnp, gnathal pouch
i, Ishay organ
ic, inner calyx
l lobula
la labium
li linqua
lo, lateral ocelli
lp, lingual plate
m, medulla
mb, mushroom body
mmp, muscles of the mouth parts
mn, mandible
mo, median ocellus
mp, maxillary palp
mth, mouth
oc, outer calyx
ol, olfactory lobe
os, occipital suture
osl, opening of the salivarium
phdi, pharyngeal diverticula
pi, pars intercerebralis
plad, posterior labial adductors
pp, pharyngeal pegs
sd, salivary duct
ta, tentorial arms
tb tentorial bridge
ver, vertex

FIGURE 2. (A) (*via* SEM) We see, on top left, a schema of the queen's head, wherein the following landmarks can be discerned. First, the anterior surface of the capsule of the Ishay organ (1), (the arrow pointing to the pit) faces the frons plate and the ocular sinus plates (2), while its lateral parts face the compound eye (3). The dorsal part of the Ishay organ extends to the vertex and up to the ocelli. Ventrally the organ borders with the clypeus plate (4), and on both its sides borders with the antennal sockets (5). In the middle of its upper side there is a depression formed by the median ocellus (6). The upper side of the clypeus plate is visible (8) and also seen is the lower side (7). Bar×4. In inset of 2A (lower right corner) one can see the acrylic model of the Ishay organ. 1-behind the frons plate; 2-the border with the ocular sinus; 3-border with the median ocellus; 4-the lower border of the Ishay organ; 5-the two long arms that extend ventrally to terminate with the eyes at mid-clypeal level. The pit (see arrow) is a continuation of the cone shown in Figure $1A_4$ or 1B (large arrow). Bar×10. (B–F) MRI images of queen's head. See Key to MRI Plates.

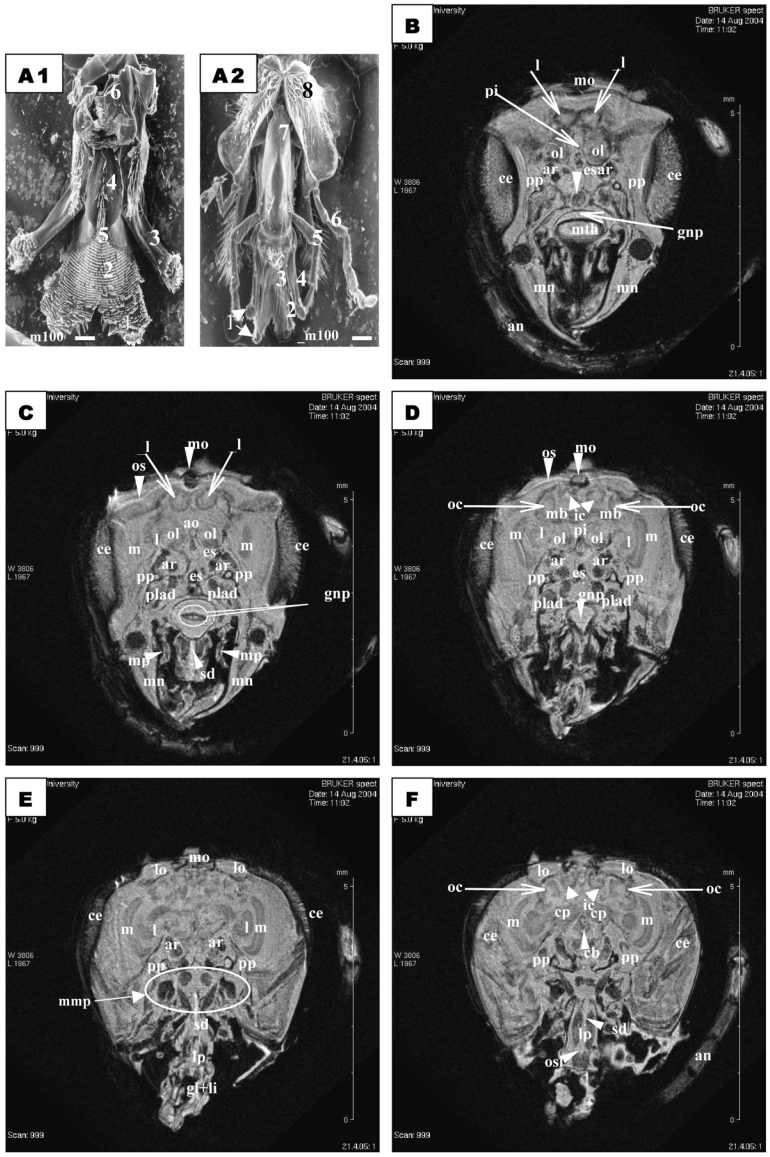

FIGURE 3. (A1) (via SEM) We can see the upper part of the labium of a queen and adjacent regions: 1-glossa, 2-lingua, 3-paraglossa, 4-lingual plate, 5-opening of the salivarium, 6-hypopharynx. Bar = 100µm; (A2) (*via* SEM) The adjacent regions from the underside of the labium showing the following landmarks: 1-acroglossal buttons, 2-glossa, 3-lingua, 4-paraglossa, 5-labial palp, 6-maxillary palp 7-prementum, 8-stipes. Bar = 100µm. (B–F) MRI images of queen's head. See Key to MRI Plates page 47.

Turning now to Figure 3C, we see two circles designating the α lobe. The region is supported also by the occipital suture. Between the two olfactory lobes there is the round opening of the aorta and beneath it is a secondary section through the esophaguses. To the right and left of the olfactory lobes and the antennal ridges we can discern the compound eye and between them first the medulla and more inwardly the lobula. Beneath the olfactory lobes, there are the two antennal ridges and below them the primary section through the esophagus. On both sides of the esophagus opening there are the pharyngeal pegs while on both sides of the gnathal pouch one can discern a mass of muscles which, as can be seen, cuts through the posterior labial adductors. At the center of the labium passes the salivary duct. Finally on both sides of the lingua there is a maxillary palp as well as a mandible.

In the middle of Figure 3D one can see the median ocellus and on each of its sides one can discern the occipital suture. Also visible is part of the mushroom body as well as the inner calyx and outer calyx. At the center between the two parts of the head is located the pars intercerebralis. On both sides of the head can be seen the compound eyes, the medulla, the lobula, the olfactory lobe, the two antennal ridges and beneath them the cavity of the esophagus, then the gnathal pouch, the pharyngeal pegs and on the sides the posterior labial adductor muscles.

In Figure 3E we see at the top center the median ocellus and on both its sides is the lateral ocelli, then parts of the compound eye, lobula and medulla. Also visible are the antennal ridges and below them the pharyngeal pegs as well as the muscles of the mouth parts, namely, the posterior labial adductor, the posterior dilator of the anterior pharynx, the extensor of the maxilla and the flexor of the stipes. One can also see the labial plate and the salivary duct, and less clearly the lower parts of the glossa and lingua.

In Figure 3F we see at the top the ocelli and beneath them the inner and outer calyxes. Further down there is the corpora pedunculata, which forms an axis between the two compound eyes. In the center of the corpora pedunculata is located the central body. Farther down on both sides, we have the pharyngeal pegs, the lingual plate with the salivary duct reaming down its center and finally the opening of the salivarium. On right side of the head there is one transversely cut antenna. Note: the images here (Figure 4 and Figure 5) are in the transversal plain.

Turning now to Figure 4, we note first in Figure 4A the compound eyes on both upper sides of the head, then the inner calyxes and outer calyxes at the middle of the head, and finally at the upper part is a portion of the vertex. In Figure 4B we can see the compound eyes at the two sides of the head and in the center we see the initial sections of the lobula and the medulla. In Figure 4C we again see the compound eyes, medulla and lobula but now also the olfactory lobe.

In Figure 4D, at center of image, we see the central body, on both sides the compound eyes, beneath them the lobula and the medulla, and in the upper center is the initial part of the gnathal pouch. In Figure 4E one can see the compound eyes the lobula end at the upper center the gnathal pouch. Finally in Figure 4F, we see the compound eyes, the pharyngeal pegs beneath them and at the upper center is the terminal part of the gnathal pouch (gnp).

Figure 5 offers further views of the queen's head. In Figure 5A can be seen the compound eyes on both lower sides and between them the tentorial bridge. In the upper center the esophagus (es) is visible and beneath it the gnathal pouch. In Figure 5B we again

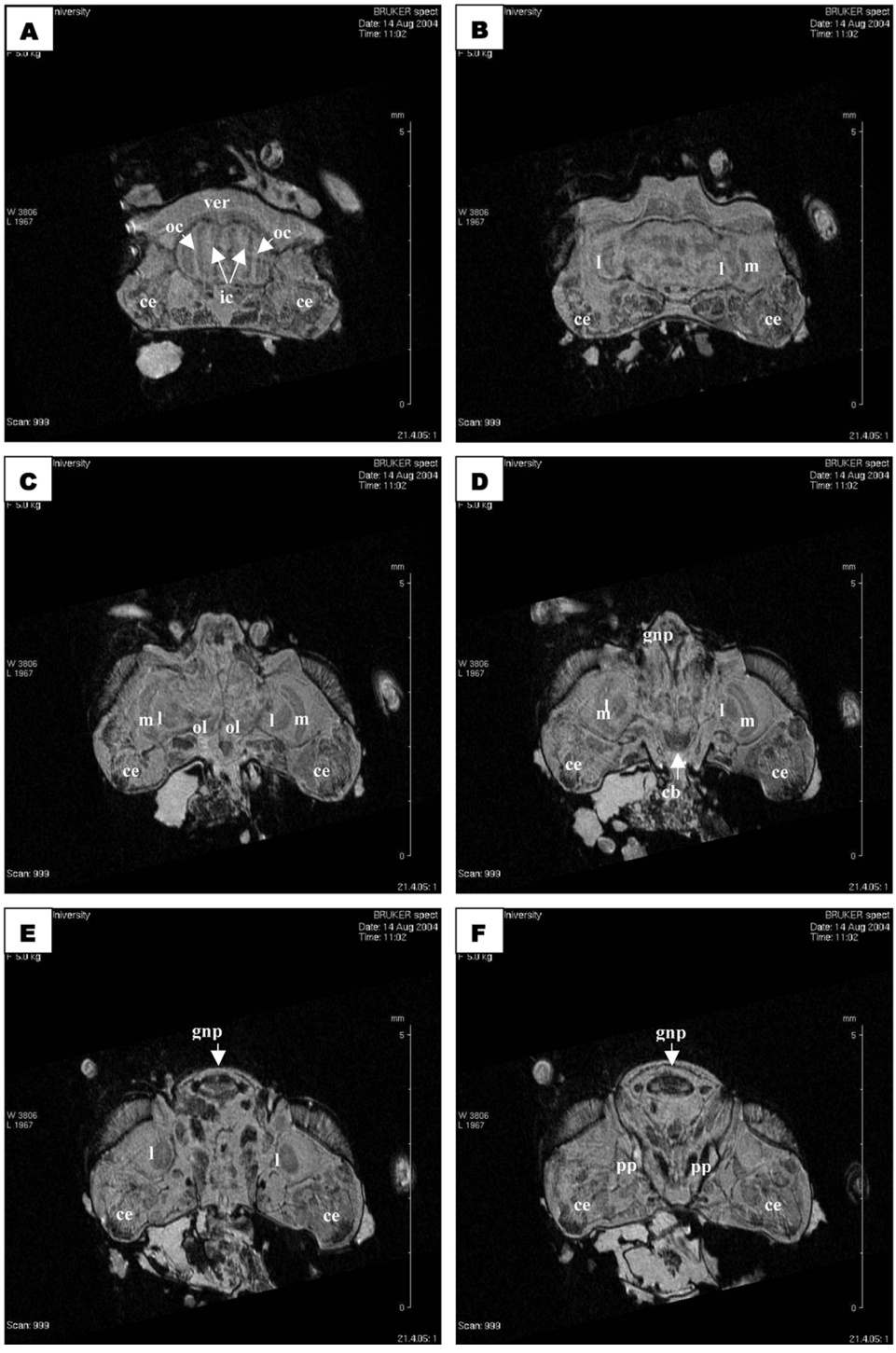

FIGURE 4. Views of queen's head. See Key to MRI Plates page 47 and text.

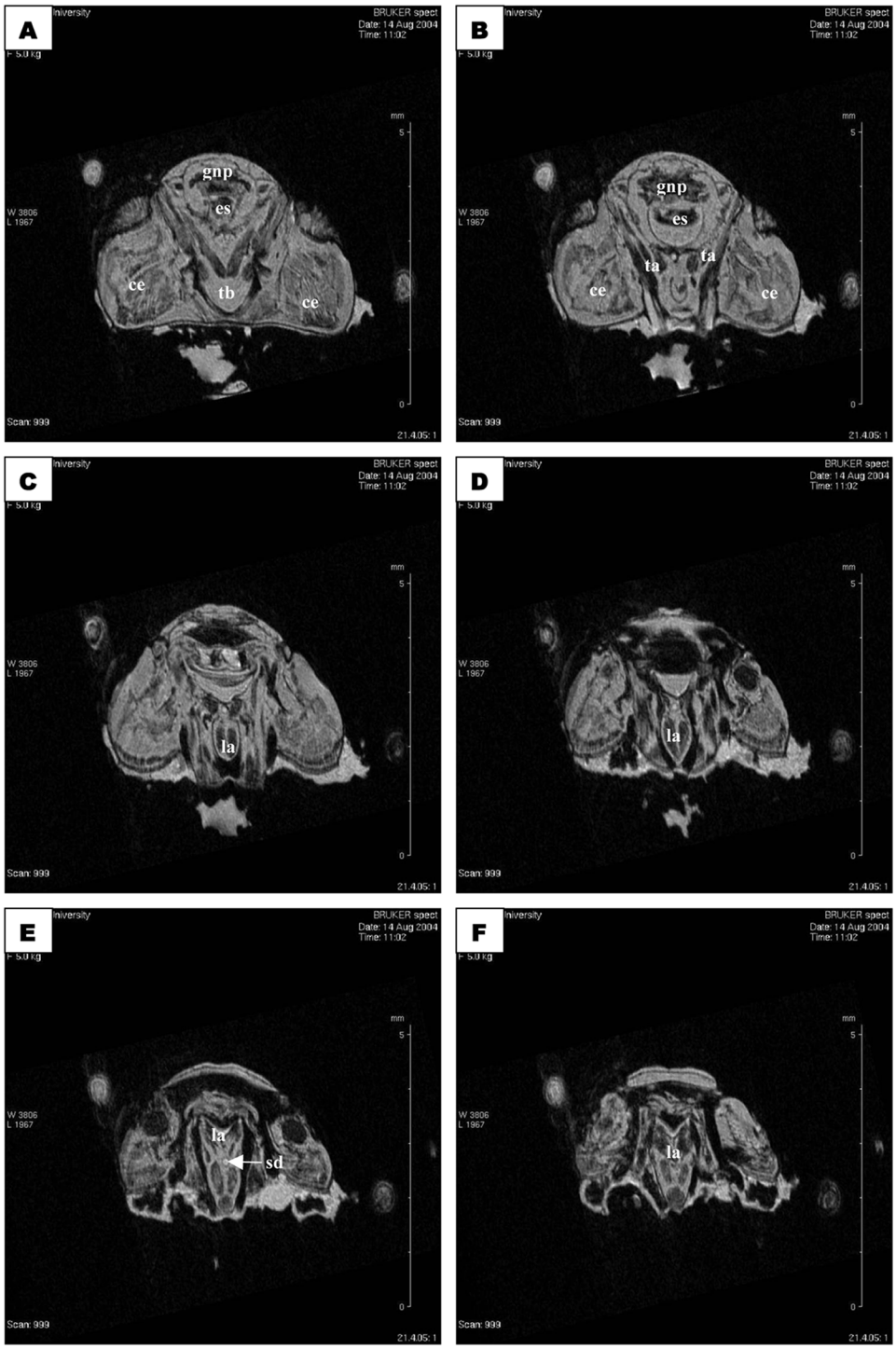

FIGURE 5. Views of queen's head. See Key to MRI Plates page 47 and text.

see the compound eyes on both sides, the tentorial arms between them, the esophagus farther up at center and beneath it the gnathal pouth. In the remaining pictures (5C to 5F), we offer segmental sections of the labium and in Figure 5E, additionally one can see a section through the salivary duct.

Discussion

In the present study, unlike in that of (7), our use of paramagnetic-ion solution to shorten T_1 and increase SNR in MRI microscopy has proved a success, and we have also demonstrated the superiority of three-dimensional sequencing over discrete-slice excitation. Where further enhancement of resolution is desired, designing a special coil for the imaged sample (7) is to be preferred, since coil sensitivity drops as the third power of the sample-coil distance.

The ratio of the volume of the calyx to that of the central body was calculated (20). It was found that there is an increase in ratio in *Vespula* and *Bombus* at the top of other Hymenoptera. It appears that an increase in the ratio of calyx/central body is correlated with high levels of complex behavior, memory storage and the coordination of sequential patterns of activity (12).

Till now, study of the Vespine brain has been achieved through surgery and the use of various techniques of microscopic observation. Our present employ of MRI obviates the use of surgery and enables viewing organs in their natural state and form, without altering dimensions and without deterioration of the tissues that results from various preparatory procedures that involve drying, coating, plating, warming and the like. In the present study, the head of the hornet has been examined from various angles, but of course necessarily conditional on the studied structures having a thickness of at least 23 μm. Thus, for instance, we were unable to properly observe in the Ishay organ the nerve fibers whose diameter is only about 10 μm (1). This can be due to insufficient resolution but also due to inadequate contrast method; it cannot be ruled out that all magnetization in the vicinity of the Ishay organ fibers decays very quickly. Neither could we observe clearly muscle fibers, nor ganglia. Strausfeld (8) was able to describe the diffuse end of the calyx in *Vespa.* The MRI technique did not of course enable us to identify the membranes that coat the hornet's brain (present in other insects as well), and selectively regulate the entry of substances into the brain by a quasi blood-brain barrier mechanism (21). In the case of the hornet, its brain does receive a supply of hemolymph from the aorta (as indicated by 'ao' in Figure 3C), but it lacks any small blood vessels, so that the sites of cerebral hemolymph flow remain undetectable. Earlier (22) the distribution of neurotransmitters in the insect brain was described and this by mapping the various cerebral regions with the aid of antibodies. We have herein shown that MRI, too, can contribute importantly to our understanding of the hornet brain.

In the present study we used the heads of young hornet queens whose age ranged from several weeks to several months. In future studies, it should prove worthwhile scanning the brain of a hornet queen throughout her lifespan of about a year, hopefully detecting any changes in brain structure that may occur during the season of maximal vespine activity (in the spring and summer) or during the senescence at the end the summer. When we compare the present MRI study of the hornet head with the NMR imaging study of the honeybee brain undertaken (7), we need mention two significant differences, namely,

that in honeybees only the supraganglionic part of the brain was investigated whereas in the present study subganglionic organs were also investigated, and secondly that honeybees do not possess an Ishay organ.

We wish to thank the Israeli Ministry of Immigrant Absorption for their generous support of Dr Stanislav Volynchik and Dr Natalya Y. Ermakov. Thanks are due also to the Y.H. Mirzoeff & Sons Foundation Inc. for financial support.

References

1. Ishay, J.S., Landsberg, A., Pelah, S. (1996) Micromorphology of the fibers behind the frons plate and its adjacent regions in the Oriental hornet (Hymenoptera, Vespinae). *Scan. Microsc. 10(1):* 187-208
2. Jongebloed, W.L., Rosenzweig, E., Kalicharan, D., van der Want, J.J.L.H., Ishay, J.S. (1999) Ciliary hair cells and cuticular photoreceptor of the hornet *Vespa orientalis* as components of a gravity detecting system: an SEM/TEM investigation. *J. Electron Microsc. 48(1):* 63-75
3. Snodgrass, R.E. (1935) *Principles of Insect Morphology*. McGraw-Hill. Book Co, New York
4. Duncan, C.D. (1939) *A Contribution to the Biology of North American Vespine Wasps.* Stanford University Press, California
5. Imms, A.D. (1960) *Entomology*. London, Methuen & Co LTD
6. Spradbery, J.P. (1973) *Wasps*. Sidgwick & Jackson. London
7. Haddad, D., Schaup, F., Brandt, R., Manzel, R., Haase, A. (2004) NMR Imaging of the honeybee brain. *J. Insect Sci. (JIS) 4:* 1-7
8. Strausfeld, N.J. (1976) *Atlas of an Insect Brain.* Springer-Verlag. Berlin Heidelberg. New-York
9. Kirmayer, R. (1909) Bau and Entwiklung der Mundteile bei *Vespa vulgaris. Morph. Jb. 39:* 11-30
10. Crampton, G.C. (1932) A phylogenetic study of the head capsule in certain orthopteroid, psocid, hemipteroid and holometabolous insects. *Bull. Brooklyn Ent. Soc. 27:* 19-49
11. Bullok, T.H., Horride, G.A. (1965) *Structure and Function in the Nervous System of Invertebrates*. Freeman, San Francisco
12. Howse, P.E. (1972) The insect brain in relation to behavior. *Proc. R. Ent. Soc. Lond. (C) 36:* 41, 37:2-4
13. Ishay, J.S., Shimony, (Benshalom) T., Arcan, L. (1986) The Biomineralization in Social Wasps (Vespinae): The presence of statoliths. *Scanning Electron Microscopy IV:* 1619-1634
14. Ishay, J.S., Ganor, E. (1992) External micromorphology of the frons plate and its adjacent areas in workers of the Oriental hornet. *J. Morph. 213 (1):* 1-13
15. Arcan, L., Ishay, J.S. (1993) Internal micromorphology of the frons plate in females of the Oriental hornet. *J. Morph. 217:* 147-159
16. Ishay, J. (1964) Observations sur la biologie de la Guêpe orientale *Vespa orientalis* en Israël. *Insectes Sociaux XI(3):* 193-206
17. Kirshboim, S., Ishay, J.S. (1998) Ether anesthesia of hornets: the development of tolerance and the influence exerted by various body parts on the duration of anesthesia. *Physiol. Chem. Phys. & Med. NMR 30:* 113-127
18. Johnson, G.A., Cofer, G.P., Gewalt, S.L., Hedlund, W. (2002) Morphologic phenotyping with MR microscopy: the visible mouse. *Radiology 222(3):* 789-793
19. Zhang, X., Yelbuz, T.M., Cofer, G.P., Choma, M.A., Kirby, M.L., Johnson, G.A. (2003) Improved preparation of chick embryonic samples for magnetic resonance microscopy. *Magnetic Resonance in Medicine 49:* 1192-1195

20. Howse, P.E., Williams, J.L.D. (1969) The brains of social insects in relation to behaviour. *Proc. VI Congr. IUSSI, Bern:* 59-64
21. Abbott, N.J., Lane, N.J., Bundgaard, M. (1986) The blood-brain interface in invertebrates. *Ann. NY Acad. Sci. 481:* 20-41
22. Homberg, U. (1994) *Distribution of Neurotransmitters in the Insect Brain*. G. Fischer, Stuttgart

Received May 25, 2006;
accepted September 5, 2006.

Physiol. Chem. Phys. & Med. NMR (2006) *38*: 55–76

In Response to an Open Invitation for Comments on AAAS Project 2061's Benchmark Books on Science

Part 1: Documentation of Serious Errors in Cell Biology

Gilbert Ling

Damadian Foundation for Basic and Cancer Research
Tim and Kim Ling Foundation for Basic and Cancer Research
110 Marcus Drive, Melville, NY 11747
Email: gilbertling@dobar.org

Abstract: Project 2061 was founded by the American Association for the Advancement of Science (AAAS) to improve secondary school science education. An in-depth study of ten 9 to 12th grade biology textbooks led to the verdict that none conveyed "Big Ideas" that would give coherence and meaning to the profusion of lavishly illustrated isolated details. However, neither the Project report itself nor the Benchmark books put out earlier by the Project carries what deserves the designation of "Big Ideas." Worse, in the two earliest-published Benchmark books, the basic unit of all life forms — the living cell — is described as a soup enclosed by a cell membrane, that determines what can enter or leave the cell. This is astonishing since extensive experimental evidence has unequivocally disproved this idea 60 years ago. A "new" version of the membrane theory brought in to replace the discredited (sieve) version is the pump model — currently taught as established truth in all high-school and college biology textbooks — was also unequivocally disproved 40 years ago. This comment is written partly in response to Bechmark's gracious open invitation for ideas to improve the books and through them, to improve US secondary school science education.

KEY WORDS: AAAS, AAAS Project 2061, association-induction hypothesis, cells, cell biology, cell membrane, membrane permeability, potassium ion, semipermeability, sieve membrane theory, sodium ion, sodium pump hypothesis, solute distribution in cell

IN THE EARLY 1980's, thoughtful Americans began to suspect something seriously remiss in the educational system, especially in science education. Books after books were written. It began with "*A Nation at Risk: The Imperative for Education Reform,*" published 1983 by the National Commission on Excellence in Education — in response to an

urgent request from the then Secretary of Education of the United States, T. H. Bell. The following is an excerpt from the Commission's report:

"In many other industrialized nations, courses in mathematics (other than arithmetic or general mathematics), biology, chemistry, physics and geography start in grade 6 and are required of *all* students. The time spent on these subjects, based on class hours is about three times that spent by even the most science-oriented students (in the US), i.e., those who select 4 years of science and mathematics in secondary school."

As years went by, the concern began to focus more and more on biology teaching. Thus in 1990*, Fulfilling the Promise: Biology Education in the Nation's Schools* was published conjointly by three organizations: the Board on Biology, Commission on Life Sciences and the National Research Council. The authors of this volume first pointed out that in the widely adopted high school curriculum in the US, biology holds a pivotal position. It is at the start of the sequence of science courses. At its best, an inspiring biology course may invoke the student's interest in not just biology but other sciences as well. In most cases, this goal has not been reached, as a 1988 survey showed.

Of the 1200 students tested for their knowledge on biology, 50% of those who never took a course in biology actually did better than 40% of those who did. As the (high school) students left the biology course, their typical reaction was "never to take another science course unless made to do so."

One major cause for the trouble, according to the authors of *Fulfilling the Promise*, is the poor quality of the biology textbooks. They de-emphasize the drama and excitement of discovery and "portray biology as the worst kind of literature — all characters and no story." Other studies reached a similar verdict.

On June 8, 2000 Anjetta MacQueen of the Associated Press made banner headlines in newspapers across the Nation with her article, "Group gives biology textbooks failing grade."

In brief, a study by Project 2061 of the American Association for the Advancement of Science (AAAS), revealed that 9th through 12th grade biology textbooks used in the United States, despite their enormous size and lavish illustrations, uniformly fail to convey "big ideas." Of all the ten most popular textbooks examined, none escaped the indictment.

Dr. George Nelson, the director of this arm of Project 2061, explains with a parable what the project meant by "big ideas". "*Providing bits of information about transmission, carburetors, fuel injectors, universal joints, and cooling systems doesn't convey a sense of a car as a mode of transformation*." What the parable suggests is that, like the disassembled auto parts, the biology textbooks also present the names, illustrations and other descriptions of bits and pieces of the living cell — to the exclusion of the "big ideas" how these parts work together to make a living cell living. Put it differently, what is completely missing in the high school textbooks is a valid coherent theory of living phenomena at the basic level.

The question now shifts to, Has Project 2061 itself uncovered these "Big Ideas? It seemed that Project 2061 was way ahead of me in asking this question.

Thus, Project 2061 did not begin and end with this survey of high school biology textbooks its ultimate goal. Much earlier, Project 2061 had involved several hundreds of scientists, mathematicians, engineers, physicians, historians and educators in producing a series of benchmark books on all sciences (Project 2061 1990, p. x.)

The first one of the series that came off the press in 1993 is entitled *Science for All American.* As pointed out by Project Director, Dr. F. James Rutherford in its Preface, the

purpose is to present what he regards as a valid expression of "the view of the scientific community on what constitutes literacy in science." Then on page 63 of the book, I found the following passage describing the basic unit of all life: the living cell:

> "*All living cells have similar types of complex molecules that were involved in these basic activities of life. These molecules interact in a soup, about 2/3 water surrounded by a membrane that controls what can enter or leave...*"

Four years later, Project 2061 published the second book of the series, entitled *Benchmarks for Science Literacy*. On page 113, it describes once more the living cell:

> "*Every cell is covered by a membrane that controls what can enter and leave the cells. . . .*"

However, neither in these passages nor elsewhere in the books could one find what Dr. George Nelson might call the "big ideas." That is, ideas that would give coherence to, and make sense out of the unconnected bits and pieces of the living cell.

Worse, the idea reiterated in both volumes that *a cell membrane determines what can enter or leave the cell* is wrong. The idea that chemicals in the biological environment can be sorted out into two kinds — those that can enter and leave the cell and others permanently and absolutely left out — is implicit in van't Hoff's theoretical concept of *semipermeabilit* (van't Hoff 1887, 1888*.)* It is more commonly known under the name of the Sieve Membrane Theory of the living cell. Unfortunately, this too has been unequivocally disproved well over half of a century ago. However, even that is not all that has gone wrong and calls for prompt recognition and remedy.

The discovery of the fallacy of the Sieve version of the membrane theory in the 1930–1940's led to the adoption of the sodium pump version of the membrane theory. And soon it was taught in virtually all high school as well as college biology textbooks, including the ten most prominent biology textbooks Project 2061 scrutinized as well as four of the most prominent college biology textbooks I examined (for names, see Endnote 1 of article.)

Figure 1 is a cartoon of the elaborate four-color renditions of the sodium pump found without fail in every one of the heavy biology textbooks that I have examined.

The trouble is, this pump version of the membrane theory too was disproved — not last year, or the year before that, but fully forty (40) years ago — a solid fact that was, as if by magic, made invisible to Project 2061 and its advisors.

There is little question in my mind that Dr. George Nelson and Dr. F. James Rutherford as well as their staffs are highly capable and dedicated people. Nonetheless, the inability to see and recognize the proven fallacy of the (later) pump version of the membrane theory in all the textbooks scrutinized was Mystery 1.

The recommendation as a guideline for future textbook improvements, another version of the membrane theory that was disproved even earlier, the sieve version, was Mystery 2. Taken together, these two mysteries have created a grave crisis.

For if allowed to continue uncorrected, it would undermine the high-minded and noble purpose of Project 2061. For inaction would create the false impression that no one really cares about the future of all high school students — which literally means the future America — as well as the rest of the world that follows in the footsteps of America.

It is almost an anticlimax to point out how allowing proven falsehood to be taught universally year after year as established truth would also demoralize the teachers and

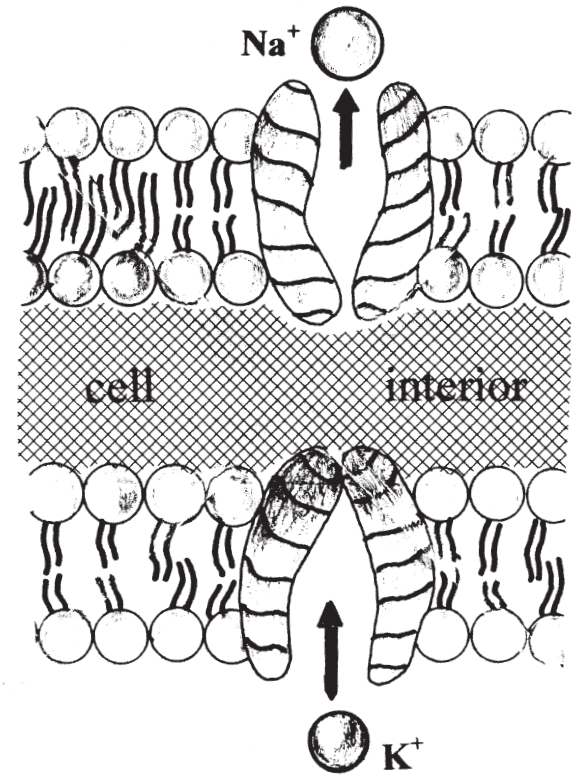

FIGURE 1. A diagrammatic illustration of what is given in most if not all current biology textbooks, representing of a phospholipid bilayer cell membrane traversed by one sodium (potassium) pump.

seriously tarnish the good name and credibility of Project 2961 in particular and AAAS in general.

However, like many other crises, it also brings with it an uncommon opportunity. For as the Chinese word for crisis (wei-chee) points to, it is a combination of the word for danger (wei) and that for opportunity (chee). Incidentally, former Vice-President Al Gore also called attention to this Chinese word combination in his immensely important book on global warming, *The Inconvenient Truth* — a title that, I think, may aptly be applied to what I am writing too.

This communication, the first installment of what I am writing on the crisis, was begun in the hope that Project 2061 was seriously looking for ways to improve their otherwise wonderful books when it offered at the end of Benchmark a gracious open invitation for comments.

This installment will concentrate on what has so far eluded Project 206: the disproof of both the sieve version and the pump version of the membrane theory. In a following installment, I shall examine how I can in other ways help Project 2061 in realizing its goal — by thinking aloud with my readers how major scientific progress had been achieved in the past and how learning science, especially the rapidly advancing life science, is not

only committing to memory some facts but in learning how to question and the mental skill to determine what is popular fallacy and what is truth.

In the end, I may be able to help by pointing out the direction where the "Big Idea" might be in existence all along but made invisible by the same magic factors that have blinded Project 2061 to part of the real-life history of sieve and pump.

The experimental unanimous disproof of the concept that the cell membrane determines what can enter or leave the cell

By the mid-19th century, it was already widely known that salts, like table salt, or sodium chloride (NaCl), do not exist as single entities but comprise two (or more) electric charge-bearing entities called ions. For sodium chloride, the two kinds of ions are the positively-charged *cation*, sodium ion, represented by the notation, Na^+ and the negatively-charged *anion*, chloride ion, represented by the symbol Cl^-. Similarly, the salt, potassium chloride (KCl) consists of the cation, K^+, and the anion, Cl^-.

When sodium chloride is dissolved in water, each ion goes its own way and in the process taking on a more or less permanent coat of water molecules. For that reason, the sodium cation in water or another aqueous medium is sometimes called *hydrated* sodium ion. Now, the force holding the Na^+ and water molecules together in the hydrated sodium ion is electrostatic in nature. As such, its strength depends on the "distance of the closest approach" separating the ion and water molecules. Now, a naked Na^+ has an atomic weight of 22.99; it is therefore smaller than an unadorned K^+ with an atomic weight of 39.10. As a result, the positive charge of the smaller Na^+ can come and stay closer to, and thus exercises a stronger attraction for, the surrounding water molecules than the larger K^+ and consequently the smaller Na^+ holds onto more water molecules around itself than around the larger K^+. The net result is that the hydrated Na^+ ends up being larger than the hydrated K^+. This difference in the hydrated ionic sizes is important for understanding the once popular theory on selective membrane permeability to be discussed below.

But before that, we must first turn our attention to two other salts: cupper sulfate ($CuSO_4$) and potassium ferrocyanide ($K_4Fe(CN)_6$). Like NaCl and KCl, when these salts dissolve in water, they too dissociate into their component ions, which include the copper cation, Cu^{++}, carrying two positive electric charges and the ferrocyanide anion, $Fe(CN)_6^{4-}$ carrying four negative electric charges. These two salts played a key role in a simple but fateful experiment carried out by a Berlin tradesman-scientist by the name of Moritz Traube some time before the year 1867.

In this experiment, Traube (1867) brought together one drop of a solution of copper sulfate and another drop of a solution of potassium ferrocyanide. He noted that at the surface of contact between the two drops, where the copper ion from one drop met the ferrocyanide ion from the other drop, a reddish-brown gelatinous precipitate of copper ferrocyanide was formed. And, once this precipitation membrane was formed, no further precipitate was formed beyond the membrane in either direction. The conclusion Traube reached was that this gel membrane is impermeable to the copper ion and the ferrocyanide ion.

So Traube had thus discovered the way to make a nearly perfect model of what the Dutch physical-chemist, J. H. van't Hoff (1887, 1888) envisaged theoretically as a *semi-permable membrane.* Namely, a membrane that permits the passage of water but not the substances or solutes dissolved in water.

By allowing the precipitation to take place not in open water as Traube did but in the fine pores of an unglazed porcelain thimble, Pfeffer succeeded in making a much sturdier copper ferrocyanide membrane that can be freely handled and manipulated (Pfeffer 1877, 1985.)

Now, if one immerses such a copper-forrocyanide membrane thimble in a vessel containing water and introduces a strong solution of cane sugar, or sucrose, inside the thimble, water outside the thimble will move to the inside of the thimble. However, this movement of water can be stopped or even reversed in direction if one applies a positive mechanical pressure to the inside of the thimble. The magnitude of the mechanical pressure required just to stop the water flow was referred to as the *osmotic pressure* produced by the sucrose solution used (Findlay 1919.) The demonstration of a positive osmotic pressure then becomes a way to determine whether or not a particular water-soluble substance like sucrose is able to permeate the copper ferrocyanide membrane. Soon a large number of solutes were tried, some pronounced as *permeant*, others *impermeant*.

Among the substances found unable to cross the copper ferrocyanide membrane are sucrose, potassium sulfate, calcium chloride, potassium ferrocyanide. In contrast, potassium chloride (KCl) was able to pass through the copper ferrocyanide membrane (Ostwald 1890.)

To explain the behavior of this nearly ideal semipermeable property, Traube introduced an "*atomic sieve theory*." In this theory, the copper ferrocyanide gel membrane has pores of such a diameter that only small molecules and ions can pass through the membrane. Larger molecules and ions are barred — indefinitely. (For the ultimate fate of this theory, see Ling 2001, p. 115, 133.)

Asymmetrical distribution of Na^+ and K^+ in living cells

Abderhalden was a talented and highly productive scientist. Once he studied under the great German chemist, Emil Fischer, to whom we owe much of the fundamental knowledge of proteins. In 1898 Abderhalden published the results of an analysis of the K^+ and Na^+ concentration in the blood plasma and in the red blood cells of rabbits. His data, reproduced here in Table 1, shows much more Na^+ than K^+ in the blood plasma. In sharp contrast, the red blood cells contain a high concentration of K^+ and no Na^+ at all (Abderhalden 1898.)

Other investigators went on to find out if this absence of Na^+ in (rabbit) red blood cell could be confirmed in other types of living cells that could also be isolated from the host animal in intact and healthy form. One type of cells they chose was the cell of the small voluntary muscles of frogs, notably the frog sartorius muscle, which can be easily isolated surgically in an intact form. In the 4th edition of his famous *Textbook of General Physiology*, which appeared in print in 1923, Sir William Bayliss noted that from all the evidence

TABLE 1. Abderhalden's historic data on the K^+ and Na^+ contents of the rabbit plasma and red blood corpuscles.

	plasma (mM)	Red blood cells (mmoles/kg)
Potassium	6.59	133
Sodium	193	0

The unit of concentration has been changed from parts per million in the original to milli-molarity or millimoles per gram. (data from Abderhalden 1898)

on hand, "it is almost certain that there is no sodium ion in frog muscle cells " (Bayliss 1927, p. 121.) From these historical "discoveries" many at the time believed that cells in general contain no sodium ion but at the same time an abundance of its chemically highly similar sister alkali metal ion, K^+.

In 1926 L. Michaelis, a very capable biologist, was aware of the difference in the sizes of the hydrated K^+ and hydrated Na^+. Thus armed, he introduced the idea that it was the smaller size of the hydrated K^+ that allows it to pass through the new kind of membrane model made of dried collodion (i.e., nitrocellulose or gun cotton.) And as he also observed experimentally, the larger hydrated Na^+ apparently could not do so. Two years later, a pair of German cell physiologists, R. Mond and K. Amson (1928) from Heidelberg adopted Michaelis's pore-size vs K^+/Na^+ selectivity idea and used it to explain the sustained high concentration of K^+ and absence of Na^+ (or low Na^+, see below) in frog muscle cells. Namely, the small K^+ can enter through small membrane pores and accumulates inside the cells while the larger Na^+ are kept out permanently.

In 1941 P.J. Boyle and E.J. Conway from Dublin published a landmark paper beginning on page 1 of Volume 100 of the (English) Journal of Physiology (Boyle and Conway 1941.) The paper bears the title, *Potassium Accumulation in Muscle and Associated Changes*. (Regrettably, these authors, who have in fact elaborated on the theme of Mond and Amson gave no credit to the prior authors for expressing the same idea earlier — even though they knew about Mond and Amson's relevant paper, which in fact was in the reference list of Boyle and Conway's paper, but noted only for a minor side issue.) However, Boyle and Conway did add something new. While Mond and Amson believed that the muscle cell membrane is impermeable to chloride ion (Cl^-) as many others also believed at that time, Boyle and Conway believed and showed evidence supporting the opposite. This is important for their theory.

Table 2, reproduced from Boyle and Conway's article shows their quantitative theory for the sieve membrane idea. Based on the known mobility data in the literature, they were able to divide a gathering of ions into two categories: those supposedly able to traverse the cell membrane and others unable to do so. Examples of *permeant* ions include

TABLE 2. Boyle and Conway's quantitative sieve membrane theory.

Velocities of ions under gradient of I V./cm. or 0·5 V./cm. for divalent ions				Relative ion diameters (diameter of potassium ion= 1·00)			
Cations		Anions		Cations		Anions	
H	315·2	OH	173·8	H	0·20	OH	0·37
Rb	67·5	Br	67·3	Rb	0·96	Br	0·96
Ca	64·2	I	66·2	Cs	1·00	I	0·97
NH_4	64·3	Cl	65·2	NH_4	1·00	Cl	0·98
K	64·2	NO_3	61·6	K	1·00	NO_3	1·04
Na	43·2	CH_3COO	35·0	Na	1·49	CH_3COO	1·84
Li	33·0	SO_4	34·0	Li	1·95	SO_4	1·89
Ca	25·5	HPO_4	28	Ca	2·51	HPO_4	2·29
Mg	22·5			Mg	2·84		

The mobility data were from the International Critical Table and Chemiker Kalender. The relative ionic diameters were calculated on the basis of their diverse mobilities and on the assumption that K^+ has a relative diameter of one. (from Boyle and Conway, by permission of the *Journal of Physiology*, London)

the K^+ and Cl^-, which, being smaller are able to traverse the muscle cell membrane and accumulate inside the cell. The larger hydrated Na^+ and sulfate (SO_4^-), like the other larger ions magnesium (Mg^{++}) and calcium (Ca^{++}), are unable to go through the pores and are left out permanently and absolutely.

Boyle and Conway's 1941 paper gained worldwide attention. Nonetheless, before it had appeared in print, evidence refuting the the underlying concept that the muscle cell membrane is impermeable to Na^+ (and other large ions) began to appear and with time became a torrent of mutually-supportive, and highly consistent revolutionary findings.

Disproof of the concept that membrane impermeability accounts for the (once-believed) absence of Na^+ in living cells

The following are six examples of experimental findings, which unanimously testified to the permeability of the cell membrane to ***the*** classic membrane-impermeable cation, Na^+:

1. Wu and Yang (1931) reported experiments in which they injected NaCl solution into the veins of dogs and found significantly higher concentration of Na^+ in the muscle cells. They conclude that the muscle cell membrane is permeable to Na^+.
2. Kaplanski and Boldyreva (1933, 1934) kept carps (a large fresh water Cyprinid fish) for one month in a 1.5% solution of NaCl. In consequence, the Na^+ concentration of the fish muscle nearly doubled while that in the blood remained unchanged (Table 3.) They too concluded that the muscle cell membrane is permeable to Na^+.
3. Cohn and Cohn (1939) injected intravenously radioactive isotope ^{24}Na into veins of dogs. After varying lengths of time, blood was withdrawn, the red blood cells separated from plasma by centrifugation and then washed twice before their radioactivity was assayed. Their figure reproduced here as Figure 2, demonstrates steady accumulation of radioactive ^{24}Na in the red blood cells with time, leading the authors to the conclusion that the the cell membrane of the canine red blood cells is also permeable to Na^+.
4. L. Heppel fed rats on a low-potassium diet for 34 to 44 days, sacrificed some of the rats and analyzed the K^+ and Na^+ contents of rat tissues and found a decrease of K^+ level and an increase of Na^+ level. Heppel concluded that the muscle cell membrane is permeable to Na^+(Heppel 1939.) When radioactive isotope ^{24}Na was injected into the K^+-depleted rats, the ratio of ^{24}Na in rat muscle over that in serum reached the ratio of *total* Na^+ in muscle over that in serum in about 60 minutes as shown in Heppel's data presented here as Table 4 (Heppel 1940.)
5. B. Steinbach (1940) demonstated that frog sartorius muscle when incubated in a solution containing no K^+ but the normal amount of Na^+, lost K^+ and gained Na^+. These changes were reversed when the depleted sartorius muscles were transferred to a Ringer's solution containing a normal concentration of both K^+ and Na^+. After another period of incubation, the muscles regained its lost K^+ and extruded the extra Na^+ accumulated. Steinbach's table is reproduced here as Table 5. The author also concluded that the frog muscle cell membrane is permeable to Na^+.
6. Several tenths of a 1 mm in diameter and one or more centimeters in length, the giant inter-nodal cell of fresh water alga Nitella is diagrammatically illustrated in Figure 3. S.C. Brooks (1940) exposed Nitella internodal cells to radioactive ^{24}Na-labeled Na^+ and $^{86}Br^-$-labeled Br^- for different lengths of time. He then determined the concentra-

TABLE 3. The concentration of Na^+ in the blood and muscle of carps kept in a 1.5% NaCl solution for 70 days.

Tissue	Control	Experimental
Blood	123	129
Muscles	40	111·4

Data represent averages of many experiments and are in units of mg. per cent. (data of Kaplanskii and Boldyreva, 1934)

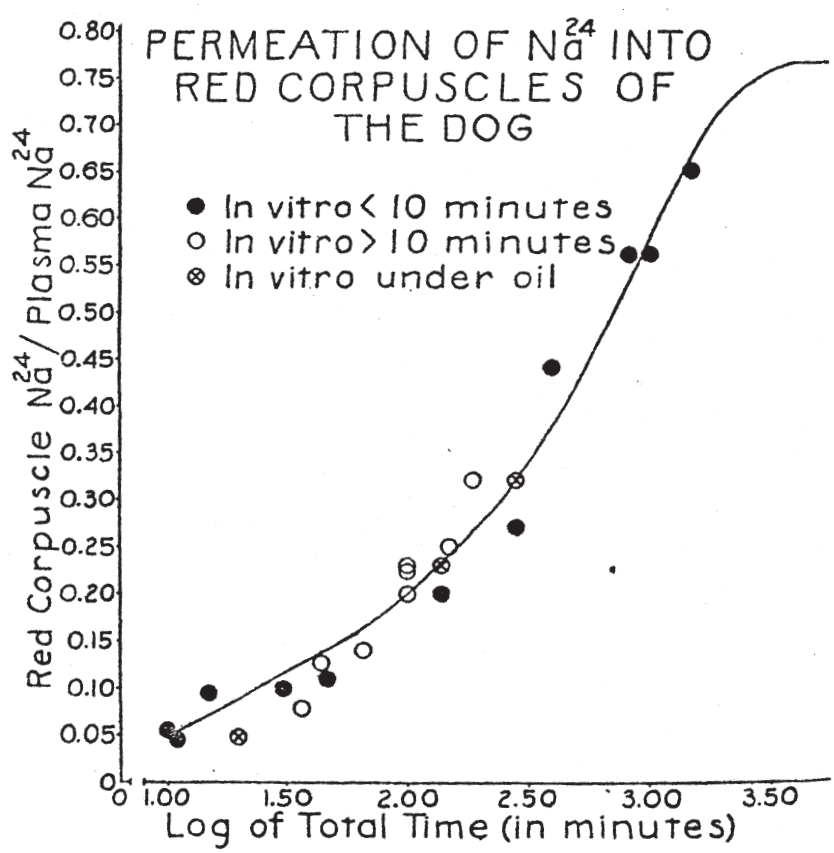

FIGURE 2. Radioactive ^{24}Na in isotonic saline was injected intravenously into normal healthy dogs. After varying lengths of time, blood samples were withdrawn, centrifuged and the red cells collected, washed and its radioactivity assayed. The red cell ^{24}Na contents expressed as a fraction of the plasma ^{24}Na concentration and shown on the ordinate and the total time after injection given as the abscissa. Different symbols refer to length of time between withdrawal of blood and radioactivity assay and whether or not the sample was kept under oil to prevent entry of CO_2. (from Cohn and Cohn, 1939 by permission of the Society of Experimental Biology and Medicine)

tions of these labeled ions in both the cytoplasm and the sap filling the large central vacuole. Figure 4 shows that labeled Na^+ entered the cytoplasm very rapidly while it took longer to reach the sap. Fast or slow, there is no question that both the cell membrane (*alias* plasma membrane) lining the outer surface of the cytoplasm and the vesicular membrane or tonoblast lining the inner surface of the cytoplasm are permeable to Na^+ (and Br^-.)

TABLE 4. Penetration and equilibration of ^{24}Na into K^+-depleted rats fed on a low K^+ diet for 34–44 days.

Time between injecting ^{24}Na solution and sacrifice of animal (min)	$\frac{^{24}Na \text{ in muscle}}{^{24}Na \text{ in serum}}$ $\left(\frac{cpm/g}{cpm/g}\times 100\right)$	$\frac{Na^+ \text{ in muscle}}{Na^+ \text{ serum}}$ $\left(\frac{mmoles/kg}{mmoles/kg}\times 100\right)$
5	14	39.2
10	17	23.5
10	15	26. 8
20	23	36.4
31	31	34.4
60	33	32.7
60	28	35.0
182	38	31.1
187	38	41.2
215	32	30.2
260	33	32.6

(Data from Heppel 1940)

TABLE 5. K^+ and Na^+ exchange in frog muscle

Frog No.	Muscle No.	Na	K	Cl	Change
1	1	5.95	3.60	2.82	Na –2.67, K +25, Cl none
	2	3.28	6.05	2.94	
2	1	5.35	3.75	2.97	Na –1.93, K +1.55,
	2	3.42	5.30	2.78	Cl none
Pooled analyses[†]	1	5.04	3.44	3.79	Na –1.00, K +1.55,
		(4)	(8)	(8)	Cl +0.31
	2	4.04	4.99	4.10	
		(4)	(8)	(8)	

Muscles were soaked for 17 hours in K^+-free Ringer solution. One muscle was taken out for analysis while a second muscle was returned to a Ringer solution containing 10 mM K^+ and 6 to 8 hours before analysis. The data are not corrected for ions in the extracellular space. (from Steinbach, by permission of the *Journal of Biological Chemistry*.)

[†]The figures in parentheses give the number of separate analyses making up the average figure. The figures are not corrected for extracellular space.

In summary, from 1931 to 1940 scientists using a variety of experimental methods and animal tissues — including mammalian red blood cells and isolated frog muscle — have unanimously demonstrated that the cell membrane in general is permeable to Na^+. Thus, the once-popular idea that there is no sodium in living cells and that this absence of Na^+ is due to an absolute impermeable cell membrane with pores too narrow for the large hydrated Na^+ to squeeze through are unequivocally disproved.

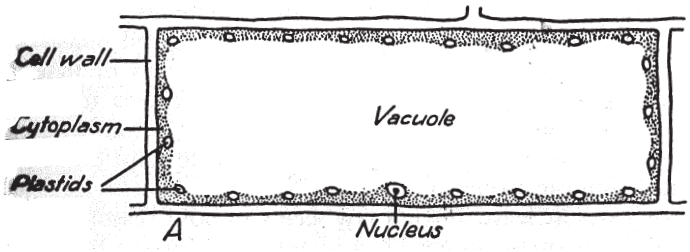

FIGURE 3. A diagrammatic illustration of a mature plant cell. (from Miller, 1936?)

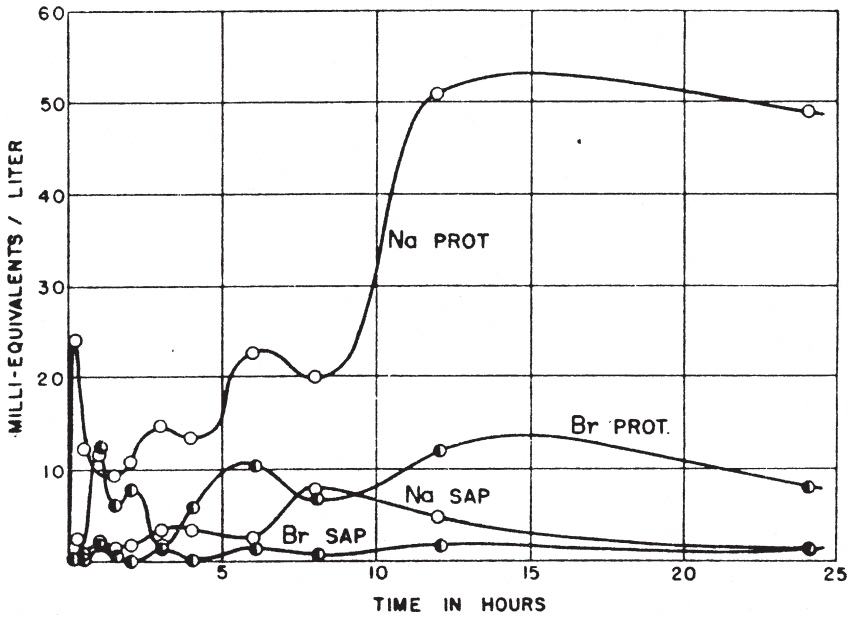

FIGURE 4. The time course of the changing concentrations of radioactively labeled Na^+ and Br^- in the cytoplasm and in the vacuolar sap of internodal cells of Nitella *clavata*. Cells were incubated in a solution containing 0.02 M labeled NaCl or 0.01 M labeled NaBr for up to 24 hours. Plants used in the Na^+ experiments had been pretreated by a prior incubation for 15 hours in a 0.01M non-labeled NaCl solution. pH of the media used about 6.0. Procedures of isolating the sap, the determination of the weight of cytoplasm (protoplasm), the intensity of illuminations etc. can be found in Brooks' original article. (from Brooks 1939, by permission of *Journal of Cellular and Comparative Physiology*.)

However, by itself, this set of evidence could not be seen as having disproved in general the (atomic) sieve membrane theory — which was introduced first by Traube, reaching its peak development in the work of Michaelis, Mond and Amson and Boyle and Conway. We will come back to this subject later.

I have reproduced in Table 1 Abderhalden's data on zero sodium concentration in rabbit red blood cells mostly for historical reason. Later work using more precise methods showed that there is Na^+ in rabbit red blood cells after all — though at a concentration much lower than either that of K^+ in the red blood cell or that of Na^+ in the bathing plasma. For example, Ponder's book, *Hemolysis and Related Phenomena* gave an intracellular K^+ concentration of 90 mmoles per liter of rabbit red blood cells and an intracellular Na^+ concentration of 16 mmoles per liter (Ponder 1948, p121.) This high intracellular/extracellular ratio of K^+ and low intracellular/extracellular ratio of Na^+ are by no means limited to rabbit and other red blood cells. Rather, they are the rules for K^+-Na^+ distribution in most living cells examined.

Thus, Table 6 taken from Ling (1962) shows that the rule holds for all 14 kinds of rat tissues listed. However, the data are given in micro-molarity per gram of fresh tissue. No correction was made for $Na^+$and other ions trapped in the extracellular space.

TABLE 6. The K^+ and Na^+ (as well as Rb^+ and Cs^+) concentration in the plasma and 14 rat organs fed a K^+-free diet containing Rb^+ and Cs^+ for a total of 14 days.

Animal No.		9070806		9070807		9071713		9071714	
Duration of feeding (days)		6		8		14		15	
Organ	Ion	Concentration, µM/g	[p] tissue / [p] plasma	Concentration, µM/g	[p] tissue / [p] plasma	Concentration, µM/g	[p] tissue / [p] plasma	Concentration, µM/g	[p] tissue / [p] plasma
Plasma	Na	142.84	-	128.89	-	150.98	-	151.00	-
	K	8.22	-	5.26	-	5.03	-	4.03	-
	Rb	0.22	-	0. 24	-	0.12	-	0.31	-
	Cs	0.56	-	0.30	-	0.30	-	0.67	-
Brain	Na	59.84	0.42	44.84	0.35	38.53	0.26	53.72	0.36
	K	90.42	11.00	85.41	16.24	63.86	12.70	72.29	17.00
	Rb	0.64	1.14	2.56	8.53	2.49	8.30	-	-
	Cs	-	-	0.64	2.67	0.71	5.92	-	-
Lens	Na	-	-	-	-	28.06	0.19	36.41	0.24
	K	-	-	-	-	32.50	6.46	59.71	14.80
	Rb	-	-	-	-	2.83	9.43	6.64	21.40
	Cs	-	-	-	-	0.71	5.92	3.67	5.48
Gastroeneimus	Na	30.74	0.22	23.52	0.18	41.90	0.28	30.32	0.20
	K	88.15	10.72	85.04	16.17	83.80	16.66	71.54	17.80
	Rb	1.79	6.27	4.34	14.47	7.29	24.30	8.80	13.20
	Cs	1.38	3.20	2.39	9.96	4.86	40.50	7.64	24.60
Diaphragm	Na	41.42	0.30	29.71	0.23	31.50	0.21	46.30	0.33
	K	93.75	12.41	78.63	14.95	31.49	6.26	69.44	17.20
	Rb	2.16	3.86	4.10	13.67	4.81	28.75	8.47	18.20
	Cs	1.70	7.72	2.65	11.04	3.45	16.03	12.22	27.30
Heart	Na	59.07	0.41	62.05	0.48	50.53	0.34	49.18	0.33
	K	72.80	8.86	54.29	10.32	30.85	6.14	158.24	14.47
	Rb	1.15	2.05	3.70	10.53	3.12	17.50	8.15	12.16
	Cs	1.48	6.59	1.39	8.92	2.11	10.40	3.57	11.50

TABLE 6. (continued)

Animal No.		9070806		9070807		9071713		9071714	
Duration of feeding (days)		6		8		14		15	
Organ	Ion	Concentration, µM/g	[p] tissue / [p] plasma	Concentration, µM/g	[p] tissue / [p] plasma	Concentration, µM/g	[p] tissue / [p] plasma	Concentration, µM/g	[p] tissue / [p] plasma
Spleen	Na	35.82	0.25	32.53	0.25	30.02	0.20	49.63	0.33
	K	95.56	11.63	84.86	16.13	62.99	12.52	70.59	17.50
	Rb	3.01	5.37	3.56	11.87	6.64	20.58	11.65	17.40
	Cs	1.12	5.09	2.04	8.50	2.47	22.13	3.97	12.80
Erythrocyte	Na	32.32	0.23	24.77	0.19	30.41	0.20	32.01	0.21
	K	70.41	8.57	68.96	13.11	67.70	13.45	61.96	15.40
	Rb	1.21	2.16	2.46	8.20	4.16	13.86	5.88	8.78
	Cs	0.42	1.91	0.48	2.00	0.59	4.92	1.25	4.03
Kidney	Na	80.00	0.56	60.89	0.47	98.56	0.65	68.31	0.45
	K	58.00	7.06	52.19	9.92	45.67	9.08	44.33	11.00
	Rb	1.22	2.19	3.36	11.20	8.46	28.20	8.98	13.40
	Cs	1.32	6.00	2.78	11.58	5.38	44.83	5.84	18.80
Liver	Na	38.25	0.27	30.63	0.24	62.22	0.41	43.99	0.29
	K	74.84	9.10	76.86	14.61	63.55	12.63	47.25	11.75
	Rb	3.14	5.61	5.62	18.73	8.90	29.83	12.32	18.40
	Cs	1.00	4.54	2.38	9.92	8.26	68.83	6.91	22.30
Stomach	Na	63.40	0.44	45.31	0.35	67.54	0.45	-	-
	K	65.21	7.93	45.31	8.61	24. 88	4.95	54.34	13.40
	Rb	2.28	4.07	3.36	11.20	6.74	22.47	16.17	24.10
	Cs	1.85	8.41	2.72	11.33	4.73	39.42	9.20	29.70
Duodenum	Na	66.66	0.67	53.19	0.41	86.79	0.57	67.26	0.45
	K	93.33	11.35	72.69	13.82	75.67	15.04	65.22	16.20
	Rb	2.60	4.64	4.89	16.30	10.42	34.74	11.86	28.40
	Cs	2.20	10.00	4.04	16.83	7.48	62.33	8.80	17.70
Large intestine	Na	54.32	0.38	45.63	0.35	44.94	0.30	58.14	0.39
	K	76.04	9.25	66.37	12.62	44.94	8.93	68.18	16.90
	Rb	3.30	5.89	3.48	11.60	5.39	17.97	10.29	15.40
	Cs	2.51	11.41	3.29	13.71	4.36	36.33	6.91	22.30
Adrenal gland	Na	66.16	0.46	-	-	78.09	0.52	63.83	0.42
	K	73.79	8.98	-	-	78.09	15.52	56.23	14.00
	Rb	-	-	-	-	9.37	31.23	6.66	9.90
	Cs	-	-	-	-	6.65	55.42	5.65	18.20
Testis	Na	-	-	-	-	-	-	51.41	0.34
	K	-	-	-	-	-	-	58.97	14.60
	Rb	-	-	-	-	-	-	6.77	10.10
	Cs	-	-	-	-	-	-	3.30	10.70

Data are given in µmoles per gram of fresh tissue or plasma. The tissue/plasma ratios are given under $[p]_{tissue}/[p]_{plasma}$. Note that in all cases, the $[p]_{tissue}/[p]_{plasma}$ for Na^+ are consistently below unity. A substantial fraction of the tissue Na^+ is in the extracellular space, which in this case was not subtracted. To obtain a rough idea how much of the tissue Na^+ is in the cells and how much in the extracellular space, see Table 7 following. (data from Ling 1962)

Table 7, in contrast, presents a more elaborate set of data on the K^+ and Na^+ distribution in 11 (or 12) types of frog tissues and cells beside Achilles tendon and skin. Based on data obtained by the Ling and Walton's *centrifugation method* for determining the amount of water (and solute) in the extracellular space, Table 7 presents both the weight percentage of extracellular-space water designated as *centrifugation-extractable water* and the K^+ and Na^+ content of unadulterated living cells. Without exception, all 11 (or 12) types of frog tissue cells demonstrate the same high intracellular/extracellular ratio for K^+ and low intracellular/extracellular ratio for Na^+ as seen in rabbit red blood cells. None of them, however, shows zero Na^+ content.

TABLE 7. The K^+ and Na^+ contents of 11 types of tissues and cells in addition to skin and Achilles tendon of normal North American leopard frogs (*Rana pipiens pipiens*, Schreber.)

Tissue	Total tissue water content (%)	Centrifugation extractable water (%)	Cell water content (%)	$[Na^+]_{in}$ µmoles/ gram wet wt	$[K^+]_{in}$ µmoles/ gram wet wt
Plasma				103.8 (mM)	2.5 (mM)
Achilles tendon	82.5 ± 0.40	18.4 ± 3.64	78.3 ± 1.31	65.8 ± 2.50	52.7 ± 2.43
egg	48.7 ± 0.48			40.3 ± 2.33	49.9 ± 1.94
heart (ventricle)	83.4 ± 0.35	15.7 ± 0.72	80.3 ± 0.32	33.4 ± 2.14	80.6 ± 2.32
intestine	81.4 ± 0.55	12.7 ± 1.31	78.7 ± 0.39	55.7 ± 2.20	71.2 ± 2.20
kidney	81.0 ± 0.50	17.6 ± .44	77.0 ± 0.33	43.7 ± 0.81	83.0 ± 0.72
lens	63.8 ± 0.61			61.8 ± 2.94	23.6 ± 2.81
liver	73.3 ± 0.46	15.9 ± 1.38	68.3 ± 0.36	24.0 ± 1.66	73.5 ± 0.43
muscle (sartorius)	79.3 ± 0.49	8.20 ± 0.32	77.4 ± 0.53	22.6 ± 3.17	106.3 ± 2.65
oviduct (with eggs)		10.8 ± 1.44	75.8 ± 0.46	14.9 ± 1.28	28.1 ± 3.16
oviduct (without eggs)	79.6 ± 0.67	24.0 ± 1.02	73.2 ± 3.65	47.3 ± 1.06	69.0 ± 7.47
skin	75.7 ± 1.10	15.1 ± 0.96	71.4 ± 1.02	73.0 ± 8.0	47.5 ± 2.18
spleen	77.1 ± 2.98	7.94 ± 1.60	75.1 ± 0.40	20.3 ± 0.87	107.9 ± 1.31
stomach	82.0 ± 0.69	11.2 ± 1.22	79.7 ± 0.53	65.7 ± 1.76	54.9 ± 1.77
testis	85.4 ± 1.14	18.5 ± 2.10	82.1 ± 1.10	30.5 ± 1.09	95.4 ± 0.81

To determine the percentage of water in cells and in the extracellular space, we used the centrifugation method of Ling and Walton (1975.) The method consists of weighing the tissue after following a standard procedure of blotting on wetted filter paper, followed by wrapping and hermetically sealing the tissue-semi wet filter paper stack in paraffin film (Parafilm) before centrifugation for 4 minutes at 1000 g. It is absolutely necessary to prepare the so-called semi-wet filter paper correctly and not allowing it to dry. To prepare semi-wet filter paper, a stack of Whatman No. 1 filter paper is soaked overnight in a regular frog Ringer' solution (Formula 731, see Ling and Bohr (1969) for detailed composition) and then centrifuged exactly the same way as the tissue (4 minutes at 1000 g) while the Parafilm wrapped package sits at the bottom of a 25 ml metal shield in an International Centrifuge and spun for 4 minutes at 1000 g. Once the extracellular water content, listed as centrifugation extractable water, is obtained, the K^+ and Na^+ contents of the tissue cells were then calculated from the total tissue K^+ and Na^+ contents and listed respectively as $[K^+]_{in}$ and $[Na^+]_{in}$ in µmoles / gram of fresh cell weight. (from Ling and Ochsenfeld, unpublished)

The failure of the atomic sieve theory is not limited to the asymmetric distribution of Na^+. Rather, it includes the intra-, extracellular distribution of all of the larger solutes that have been studied in adequate detail (Ling 1952 pp. 761–763; Ling 2006, Table 1 on p. 7.) Three technical advances have made it possible for us to say that we have so far not encountered a single water-soluble chemical substance that we can say without hesitation to be absolutely and permanently unable to go through a cell membrane or non-living model of the cell membrane. (That said, I must also admit that an elephant will not be able to enter a living cell. Anything less than an elephant but say almost as big as a living cell may be able to enter it, but only if we can verify that by waiting long enough.)

The three technical advances are: (1) a way of keeping isolated tissues *in vitro* in physiological condition for 9 days at 25° C and a month or more at 0° C (Ling and Bohr 1969); (2) the availability of a wide range of ions and chemical, big and small in the radioactively labeled form; and (3) the introduction of 5 independent methods for the accurate determination of the extracellular space of frog muscle and other tissues (for rough description and sources, see Ling 1997, p.136.)

Thus equipped, we were able to study in detail the permeation into, and accumulation in frog muscle cells, a wide variety of chemical substances. They include 21 sugars, sugar alcohols and other nonelectrolytes as listed in Table 8. The same table also shows that, without exception, everyone being able to penetrate and reach diffusion equilibrium within 48 hours — some in much shorter times — even though the study was conducted at the low temperature of 0° C; even though a solute like raffinose has a molar volume of almost half of a liter (499 cc.)

Next, we review another page of the history of cell physiology in the aftermath of the crisis produced by the collapse of the atomic sieve theory as applied to Na^+ distribution in living cells. To salvage the membrane theory, according to which a living cell is a membrane-enclosed solution of free water and free ions and other solutes, a hypothetical device called the sodium pump was installed to replace the atomic sieve now out of the picture. There is a striking difference, though, between the two models. A sieve performs its function without the steady energy expenditure; a pump cannot.

The sodium pump

In 1946, I came to the United States from China to study cell physiology at the world-famous Department of Physiology at the University of Chicago. It was a day in the second spring after my arrival in Chicago, on which I gave a Monday afternoon seminar at the Department. The subject of the talk was the Sodium Pump — based solely on a library research I made in the preceding weeks. At the outset of my talk, I told my audience that only thing I felt confident in sharing is that nobody seems to know what it is beyond the name.

To show that there was objective cause for my failure to find anything worth reporting, I can now cite from two scientists from the Physiological Laboratory of the Cambridge University of England. They apparently encountered a similar problem more than 25 years after me. Thus in the 1975 edition of the Annual Review of Physiology and under the title, *The Sodium Pump*, Glynn and Karlish wrote:

> "If the great mass of work that has been done led to the general acceptance, even provisionally and even in outline, of a hypothesis accounting for the working of the pump, we could

TABLE 8. Time for the 22 non-electrolytes (including labeled water) to reach diffusion equilibrium in frog muscle cells.

Solute	Equilibration Time (hours)
water	<< 1
methanol	<20
ethanol	<20
acetamide	<10
urea	<24
ethylene glycol	<10
1,2-propanediol	24
DMSO	< 1
1,2-butanediol	24
glycerol	<20
3-chloro-1,2-propanediol	24
erythritol	<20
D-arabinose	<45
L-arabinose	<45
L-xylose	<45
D-ribose	<24
xylitol	24
D-glucose	<15
D-sorbitol	<10
D-mannitol	<24
sucrose	< 8
raffinose	10

The sequential order in the list roughly follows the decreasing size or molecular volume of each compound, the first one being the smallest, the last one, the largest. The data as a whole shows that with the exception of the three pentoses, an incubation period of 24 hours at 0° C is adequate for all the other non-electrolytes listed. For other data presented in the same publication, the final *equilibrium distribution coefficients* or q-values for all solutes equal to or larger than those of erythritol (Molecular volume 130.27 cc), have q-values equal to, or smaller than 0.29. In other words, these larger non-electrolyes distribute themselves with an asymmetry quantitatively equal or very close to that of the Na^+ in the same frog muscle cells. (from Ling *et al* 1993)

have described the hypothesis and then consider the evidence for it. Unfortuinately, *no such hypothesis exists...*" (*Ital. mine*.)

However, what I did not expect occurred at the end of my 1948 talk. It was the extremely kindly but equally startling response of two of my much respected and beloved professors. Each took me aside and told me in private and in almost identical words that the sodium pump is a *sacred cow* and I should leave it alone. There is nothing gained by making yourself a martyr.

I sincerely thanked each of them for their kindness but asked myself, Why should anyone in power care about what a lowly graduate student thinks about a purely scientific theory? I could not just leave the sodium pump alone since it was directly in the path of my Ph.D. thesis on the electrical potential of single frog muscle cells.

So, the next thing you know, I was doing an elementary experiment that anyone in the same situation would have thought of immediately. That is, an experiment, which could allow me to find out if the K^+ and Na^+ in an isolated frog muscle would change dramatically when I cut off its energy supply by exposing it to metabolic poisons.

The very first experiment I did was mind absorbing. Nothing happened at all to either the K^+ content nor the Na^+ content — long after the cessation of all its active metabolism.

In the weeks and months following, I repeated this simple experiment again and again — without fail, each experiment reiterated to me the same story. As an illustration, the results of one of these repetitions was what I published in 1952 (Ling 1952, p. 765) and reproduced here as Table 9.

Disproof of the pump version of the membrane theory on the basis of energy insufficiency

As anyone who has pumped, say, water from a wet basement knows, pumping requires a constant supply of energy. The moment one turns off the electricity, pumping stops. This is, of course, an expression of the First Law of Thermodynamics, the Law of the Conservation of energy (Fermi 1936.).

Pumping water out of a basement performs work because water is lifted from a low place to a high place up a gravitational gradient. Pumping Na^+ out of the living cells also

TABLE 9. Effect of Na iodoacetate (IAA) and pure nitrogen and low temperature upon the K^+ concentration of frog muscle and nerves.

Type of Tissue	Muscle No.		Weight (gms.)	mM. K+/l. of intracellular water
Sartorius	1	Control	0.0870	60.7
	2	Expt'l	0.0750	69.8
Semitendinosus	1	Control	0.0710	72.6
	2	Expt'l	0.0795	81.8,
Tibialis anticus longus	1	Control	0.0938	71.1
	2	Expt'l	0.0900	79.2
N. ischiadicus +	1	Control	0.0300	38.1
N. tibialis + N. peroneus	2	Expt'l	0.0260	39.5
Sartorius	1	Control	0.0730	73.4
	2	Expt'l	0.0700	78.0
Semitendinosus	1	Control	0.0660	83.0
	2	Expt'l	0.0730	77.4
N. ischiadicus +	1	Control	0.0260	42.8
N. tibialis + N. peroneus	2	Expt'l	0.0242	40.0
			Muscles	Nerves
Average		Control	100.0%	100.0%
		Expt'l	105.2%	98.5%

All muscles and nerves were incubated for 5 hours at 0° C, the experimental series in a Ringer's solution containing 0.5 mM IAA in an atmosphere of pure nitrogen, the controls in a plain Ringer's solution in air. (from Ling 1952, by permission of the Johns Hopkins University Press, Baltimore, MD)

performs work. Only here it is done against two gradients, a concentration gradient and an electric gradient. The minimum energy that must be spent to pump one mole of Na^+ from inside a frog muscle cell to the outside can be calculated when one poisons isolated muscle cells with an atmosphere of pure nitrogen (plus 0.5 mM sodium cyanide) — , which suppresses aerobic respiration — and the poison, sodium iodoacetate (IAA), which suppress anaerobic metabolism, or glycolysis.

Of relevance here is the fact that in a frog muscle fully poisoned with pure nitrogen and IAA, the only *possible* energy source are the content of the so-called high energy phosphate bond compounds, creatine phosphate (CrP) and ATP present in the muscle at the moment the poisons applied terminated all active metabolism. The difference in the contents of CrP + ATP at this moment and at the conclusion of the experiment gives the maximally available energy (see Ling 1952, pp. 765–766, Ling *et al* 1973, pp. 11–12 for evidence against the existence of some as yet unknown energy source.)

Now, we need a Gerard-Graham-Ling (*alias* Ling-Gerard) microelectrode (Ling and Gerard 1948) to monitor the cellular resting potential (about 85 mV inside negative), a γ-scintillation counter to monitor the rate of outward flux of radioactively labeled Na^+ from the poisoned muscle cells and a cold room to accommodate the whole setup and keep it at 0° C. It needs be mentioned that given the membrane theory's doctrine of free water and free ions in the cell, virtually all the measured Na^+ coming out of the poisoned cells must be due to pumping (Ling 1997, p. 155.)

The first set of data comparing the maximally available energy and the minimum required energy was reported briefly in 1952 (Ling 1952.) Assuming that all the energy available has just one purpose, i.e., pumping Na^+, and that all processes involved in utilizing energy is 100% efficient, the minimum energy need was found to be 400% of the maximally available energy.

However, rather crude methods of analysis and measurements were employed. So in the course of the following five years, I spent much time improving the methods and making more and more, better and better experiments. Results of the last three sets of fully completed experiments in 1956 are presented in Figure 5. It shows that the minimally needed energy is at least from 15 to 30 times (or 1500% to 3000%) of the maximally available energy (Ling 1962, p. 211.) Thus from energy consideration alone, the sodium pump hypothesis was experimentally disproved.

One may add that the essence of the finding has been first confirmed by Jones in mammalian smooth muscle (1965) and then by Minkoff and Damadian (1973) in the bacteria, E. coli.

That said, I must add that this 15 to 30 times figure, overwhelming by any standard, is not an accurate estimate. It still grossly *under*estimates the energy disparity.

The causes for this underestimation are many and no effort will be made to count them all. Only two would suffice here. First, Na^+ is but only one among a countless number of solutes that are in the same position: *being able to cross the cell membrane and found in the cell at the concentration lower than that in the bathing medium.* In a by no means comprehensive search, Ling *et al* (1973) found a minimum of 18 pumps already postulated by the year 1968. Some of these postulated pumps are not single pumps but conglomerates of pumps, like the sugar pumps and free amino acid pumps (Table 10.) None of the scientists postulating these pumps paid attention to the already bankrupt state of energy supply from one sodium pump alone. The isolated living cells have nowhere to borrow energy.

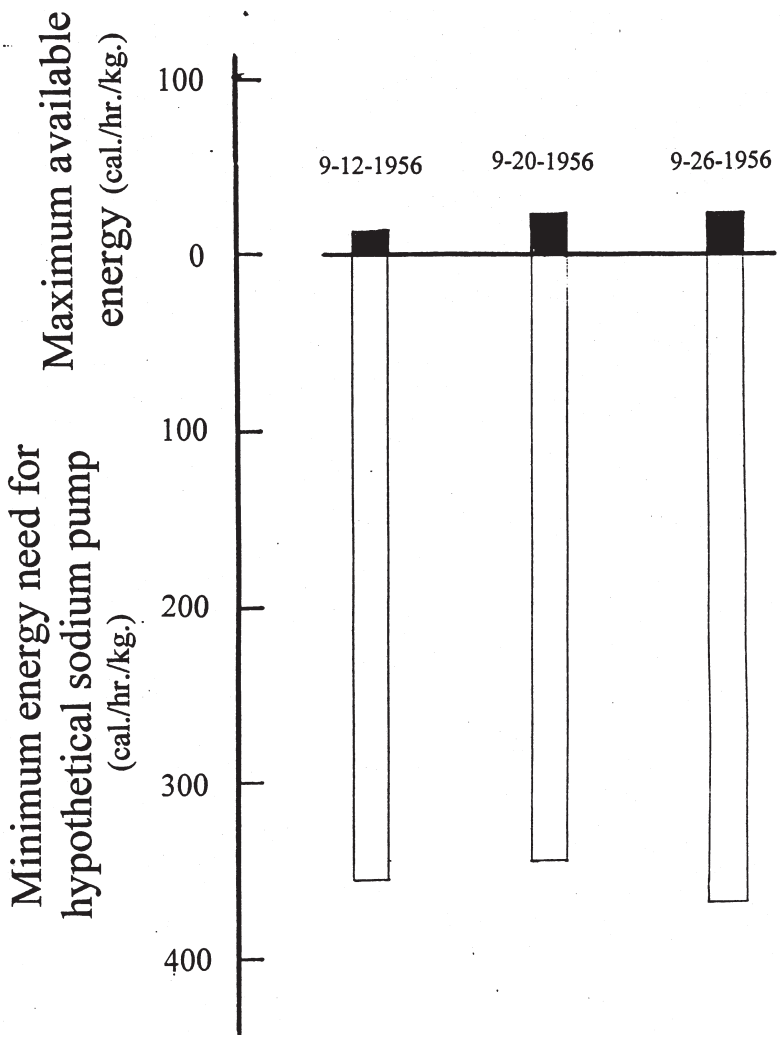

FIGURE 5. A comparison of the maximally available energy of (poisoned) frog sartorius muscle cells at 0°C (upward black bars) and the minimum energy need to pump Na^+ against both (measured) electric potential gradient and a concentration gradient. Duration of the experimental observation for Experiment (9-12-1956) lasted 10 hrs.; Experiment 9-20-1956, 4 hrs.; Experiment 9-26-1956, 4.5 hrs. Active oxidative metabolism was suppressed by exposure to pure nitrogen (99.99%, in addition to 0.001 M NaCN); glycolytic metabolism, by sodium iodoacetate and doubly insured by actual lactate analysis before and after the experiment. Other detailed studies reported in 1952 (Ling 1952, Table 5 on page 765) and in 1962 (Ling 1962, Table 8.4) showed respectively that under similar conditions of 0° C temperature and virtually complete inhibition of active energy metabolism, the K^+ and Na^+ concentrations in frog muscle, nerves and other tissues remain essentially unchanged for as long as the experiments lasted (5 hrs. for the 1952 reported experiment, and 7 hrs. and 45 min. in the 1962 reported findings. (For additional details, see Ling 1962, Chapter 8 and Ling 1997.) In the computations, it was assumed that the frog muscle cell does not use its metabolic energy for any other purpose(s) than pumping sodium ion and that all energy transformation and utilization are 100% efficient. (from Ling 2004)

TABLE 10. A partial list of pumps already postulated in 1968

Solute	Direction	System	Reference*
Na, K	coupled	many cells	169
Ca^{++}	outward	RBC, striated muscle	170, 171
Mg^{++}	outward	frog sartorius	172
$Choline^{+}$	inward	RBC	173
Amino acids	inward	RBC, muscle, tumor	174–176
D-xylose	inward	rat diaphragm	177
D-xylose	outward	rat diaphragm	178
Na^{+}	inward	frog sartorius -	179, 180
Noradrenaline	inward	vascular smooth muscle	181
Prostaglandins	inward	mammalian liver	182
Curarine	inward	mouse diaphragm	183
Br^{-}, I^{-}, ReO_4^{-}, WO_4^{-}	outward	Ascites	184
CU^{+2}	inward	Ascites	185
Aminopterin	inward	Yoshida sarcoma	186
Cl^{-}	inward	squid axon, motor neurons	187, 188
Mn^{++}	inward	*E. coli*	189
Cl^{-}	outward	*E. coli*	189
Sugars	inward	*E. coli*	189
Amino acids	inward	*E. coli*	189
Tetracycline	inward	*E. coli*	190

* For references to the sources of these publications see Ling *et al.* 1973. (Ling *et al.* 1973, by permission of the New York Academy of Sciences)

Second, the list of permeant solutes with below unity intra-, extracellular distribution ratios include compounds that had not existed on this planet until some chemists synthesized them for the first time in history. And, there is no limit to the number of these man-made chemicals that would require pumps. For that reason, the number of required pumps as a whole has no limit.

Since the full documentation of my energy study of frog muscle was first published in my 1962 book*, A Physical Theory of the Living State: the Association-Induction Hypothesis* (Ling 1962), and this book has been long out of print, I decided in 1997 to reproduce the entire section dealing with the subject as an appendix to a publication, entitled "*Debunking the Alleged Resurrection of the Sodium Pump Hypothesis*" (Ling 1997, Appendix 1.) (Other than directly going to the printed journal of the listed URL of the paper itself, you can also reach it by going to the website (www.gilbertling.org) and find Debunking as a link.)

The 41-page lone main text of the 75-page long Debunking was an in depth review of the disproof of the pump theory. It was written in response to a claim that there was enough energy for the sodium pump after all. The Debunking article shows how this alleged resurrection was based solely on a *non-existent* crucial experiment and on knowingly tellng half truths. Why did my once starry-eyed student sink so low just to earn a living, is what made me shed tears — not only for their loss but also for other would-be scientists in the world they find themselves. What is spelled out in Debunking is one

additional reason that had prompted me to take on the challenge of writing this document and its sequel.

I thank Dr. Raymond Damadian and all the members of his Fonar Corporation for their continued support, Margaret Ochsenfeld and Dr. Xhen-dong Chen for their dedicated and skilful help and valuable scientific contrituions.

Endnote 1.

The list of ten biology textbooks that Project 2061 has examined and found rich in details but short on "big ideas."

(1) *Biology* (Miller-Levine) Prentice Hall, 1998; (2) *Biology: A Community Context*, South-Western Educational Publishing, 1998; (3) *Biology: Principles and Explorations*, Holt, Rinehart & Weston, 1996; (4) *Biology: The Dynamics of Life*, Glencoe McGraw-Hill, 1996; (5) *Biology: Visualizing Life*, Holt, Rinehart & Weston, 1998; (6) *BSCS Biology*: A Human Approach, Kendall Hunt, 1998; (7) *BSCS Biology*: *An Ecological Approach*, Kendall Hunt, 1998; (8) *Health Biology*, D.C. Health & Co., 1991; (9) *Insights in Biology*, Kendall Hunt, 1998; (10) *Modern Biology*, Holt, Rinehart & Weston, 1999.

Four college biology textbooks examined by GL:

(1) *Molecular Biology of the Ce*ll, 3rd ed., Garland Publishing, Inc. 1994; (2) *Biology*, 5th ed., Addison, Wesley Longman, Inc. 1999; (3) *Essential Cell Biology*: *An Introduction to the Molecular Biology of the Cell*, Garland Publishing, Inc. 1998; (4) Molecular Cell Biology, W. H. Freeman and Co., 2000.

References

Abderhalden, E. (1898) *Z. physiol. Chem. 25:* 65 (p. 100).

Bayliss, W.M. (1927) *Principles of General Physiology* 4th edition, Longman,Green and Co., London.

Boyle, P.J. and Conway, E.J. (1941) *J. Physiol. 100:* 1.

Brooks, S.C. (1939) *J. Cell. Comp. Physiol.* 14: 383.

Cohn, W.E. and Cohn, E.T. (1939) *Proc. Soc. Exp. Biol. Med. 41:* 445.

Fermi, E. (1936) *Thermodynamics,* Dover Publications, Inc. New York, p. 11.

Findlay, A. (1919) *Osmotic Pressure* 2nd edition, Longmans, Green, Inc., London.

Glynn, I.M. and Karlish, S.J.D. (1975) *The Sodium Pump* in *Ann. Rev. Physiol. 37:* 13.

Gore, A. (1962) *An Inconvenient Truth; the Planetary Emergency of Global Warming and What We Can Do about It*, Rodale, Emmaus, PA.

Heppel, L. (1939) *Amer. J. Physiol. 127:* 385.

Heppel, L. (1940) *Amer. J. Physiol. 128:* 449.

Jones, A.W. (1965) Ph. D. Thesis, Appendix, University of Pennsylvania, Philadelphia.

Kaplanskii, S. Ya. and Boldyreva, N. (1933) *Fiziol. Zh. 16:* 219.

Kaplanskii, S. Ya. and Boldyreva, N. (1934) *Fiziol. Zh. 17:* 96.

Ling, G.N. (1952) In *Phosphorus Metabolism* (W.D. McElroy and B. Glass, eds.), Vol. II , p. 748, Johns Hopkins University Press, Baltimore, Maryland.

Ling, G.N. (1962) *A Physical Theory of the Living State: the Association-Induciton Hypothesis,* Blaisdell Publishing Co., Waltham, MA.

Ling, G.N. (1997) *Physiol. Chem. Phys & Med, NMR 29:* 123. Available via http://www.physiologicalchemistryandphysics.com/pdf/PCP29-2_ling.pdf

Ling, G.N. (2001) *Life at the Cell and Below-Cell Level: The Hidden History of a Fundamental Revolution in Biology,* Pacific Press, New York.

Ling, G.N. (2006) Chapter 1, A Convergence of Experimental and Theoretical Breakthroughs Affirms the PM Theory of Dynamically Structured Cell Water at the Theory's 40th Birthday in: *Water and the Cell* (Pollack, G.H., Cameron, I.L. and Wheatley, D.N., eds.) Springer Verlag, Berlin, New York.

Ling, G.N. and Bohr, G. (1969) *Physiol. Chem. Phys. 1*: 591.

Ling, G.N. and Gerard, R.W. (1948) *J. Cell. Comp. Physiol. 34:* 383.

Ling, G.N. and Walton, C. (1975) *Physiol. Chem. Phys. 7:* 215.

Ling, G.N., Miller, C. and Ochsenfeld, M.M. (1973) *Ann. N.Y. Acad. Sci. 204:* 6.

Ling, G.N., Niu, Z. and Ochsenfeld, M. (1993) *Physiol. Chem. Phys. & Med. NMR 25:* 177.

Ling, G.N., Walton, C. and Ling, M.R. (1979) *J. Cell. Comp. Physiol. 101:* 262.

Ling, G.N., Walton, C. and Ochsenfeld, M.M. (1983) *Physiol. Chem. Phys. 15:* 379.

Michaelis, L. (1926) *Naturwissenschften 14:* 33.

Miller (1936?) *Plant Physiology* McGraw Hill Publ. Co. New York

Minkoff, L. and Damadian, R. (1973) *Biophysical J. 13:* 167.

Mond, R. and Amson, K (1928) *Pflhgers Arch. ges. Physiol. 220:* 69, p. 78.

National Academy Press (1990) *Fulfilling the Promise: Biology Education in the Nation's Schools.*

National Commision on Excellence in Education (1983) *A Nation at Risk: the Imperative for Educational Reform.*

Nelson, G. (2000) *Big Biology Books Fail to Convey Big Ideas: Reports AAA's Project 2061*. http: project2061.aaas.org.newsinfo.press.r1000627.htm

Ostwald, W. (1890) *Z. phys. Chem. 6:* 71.

Pfeffer, M.F. (1877, 1st ed.) (1921, 2nd ed.) *Osmotische Untersuchungen: Studien zur Zell-Machanik,* Engelmann, Leipzig.

_____. (1985) *Osmotic Investigation Studies on Cell Mechanics* (English transl. by G. K. Kepner and Ed. J. Stadelmann, Leipzig), van Nostrand, Rheinhold, New York.

Ponder, E. (1948) *Hemolysis and Related Phenomena,* Grune and Stratton, New York .

Project 2061, AAAS (1990) *Science for All Americans*, Oxford University Press, Oxford, New York.

Project 2061, AAAS (1993) *Benchmarks for Science Literacy* Oxford University Press, Oxford, New York.

Steinbach, H.B. (1940) *J. Biol. Chem. 133:* 695.

Traube, M., (1867) *Arch. Anat. Physiol. u Wiss. Med.* 87–128; 129–165.

van't Hoff, J.H. (1887) *Z. phys. Chem. 1:* 481.

van't Hoff, J.H. (1888) *Phil. Mag. 26:* 81.

Wu, H. and Yang, E.F. (1931) *Proc. Soc. Exp. Biol. Med. 29:* 248.

Received November 10, 2006;
accepted December 19, 2006.